ISSN 1916-6117 (online)
ISBN 978-1-4868-7226-8 (PDF)

ISSN 0826-9580 (print)
ISBN 978-1-4868-7225-1 (print)

THESE TERMS GOVERN YOUR USE OF THIS DOCUMENT

Your use of this Ontario Geological Survey document (the "Content") is governed by the terms set out on this page ("Terms of Use"). By downloading this Content, you (the "User") have accepted, and have agreed to be bound by, the Terms of Use.

Content: This Content is offered by the Province of Ontario's *Ministry of Mines* (MINES, or the Ministry) as a public service, on an "as-is" basis. Recommendations and statements of opinion expressed in the Content are those of the author or authors and are not to be construed as statement of government policy. You are solely responsible for your use of the Content. You should not rely on the Content for legal advice nor as authoritative in your particular circumstances. Users should verify the accuracy and applicability of any Content before acting on it. The Ministry does not guarantee, or make any warranty express or implied, that the Content is current, accurate, complete or reliable. The Ministry is not responsible for any damage however caused, which results, directly or indirectly, from your use of the Content. The Ministry assumes no legal liability or responsibility for the Content whatsoever.

Links to Other Web Sites: This Content may contain links, to Web sites that are not operated by MINES. Linked Web sites may not be available in French. The Ministry neither endorses nor assumes any responsibility for the safety, accuracy or availability of linked Web sites or the information contained on them. The linked Web sites, their operation and content are the responsibility of the person or entity for which they were created or maintained (the "Owner"). Both your use of a linked Web site, and your right to use or reproduce information or materials from a linked Web site, are subject to the terms of use governing that particular Web site. Any comments or inquiries regarding a linked Web site must be directed to its Owner.

Copyright: Canadian and international intellectual property laws protect the Content. Unless otherwise indicated, copyright is held by the King's Printer for Ontario.

It is recommended that reference to the Content be made in the following form:

Gibson, H.L., Gemmell, T.P., Jørgensen, T.R.C., Hastie, E.C.G., Schofield, M.D., Haugaard, R., Smith, A.R., McKinley, B., Rees, M.I., Lafrance, B., Sherlock, R.L. and Chapon, B. 2023. Exploring differential metal endowment: A comparison of the western (Swayze) and eastern (Rouyn-Noranda) Abitibi greenstone belt: A geological guidebook; Geological Association of Canada–Mineralogical Association of Canada–Society for Geology Applied to Mineral Deposits, Joint Annual Meeting, Sudbury, Ontario, May 25–27, 2023, Field Trip FT07, Ontario Geological Survey, Open File Report 6395, 100p.

Use and Reproduction of Content: The Content may be used and reproduced only in accordance with applicable intellectual property laws. *Non-commercial* use of unsubstantial excerpts of the Content is permitted provided that appropriate credit is given and Crown copyright is acknowledged. Any substantial reproduction of the Content or any *commercial* use of all or part of the Content is prohibited without the prior written permission of MINES. Substantial reproduction includes the reproduction of any illustration or figure, such as, but not limited to graphs, charts and maps. Commercial use includes commercial distribution of the Content, the reproduction of multiple copies of the Content for any purpose whether or not commercial, use of the Content in commercial publications, and the creation of value-added products using the Content.

Contact:

FOR FURTHER INFORMATION ON	PLEASE CONTACT:	BY TELEPHONE:	BY E-MAIL:
The Reproduction of the EIP or Content	MINES Publication Services	Local: (705) 670-5691 Toll-Free: 1-888-415-9845, ext. 5691 (inside Canada, United States)	Pubsales.ndm@ontario.ca
The Purchase of MINES Publications	MINES Publication Sales	Local: (705) 670-5691 Toll-Free: 1-888-415-9845, ext. 5691 (inside Canada, United States)	Pubsales.ndm@ontario.ca
Crown Copyright	King's Printer	Local: (416) 326-2678 Toll-Free: 1-800-668-9938 (inside Canada, United States)	Copyright@ontario.ca

Ontario

Ontario Geological Survey
Open File Report 6395

Exploring Differential Metal Endowment: A Comparison of the Western (Swayze) and Eastern (Rouyn-Noranda) Abitibi Greenstone Belt: A Geological Guidebook

2023

Ontario

ONTARIO GEOLOGICAL SURVEY

Open File Report 6395

Exploring Differential Metal Endowment: A Comparison of the Western (Swayze) and Eastern (Rouyn-Noranda) Abitibi Greenstone Belt: A Geological Guidebook

by

H.L. Gibson, T.P. Gemmell, T.R.C. Jørgensen, E.C.G. Hastie, M.D. Schofield, R. Haugaard, A.R. Smith, B. McKinley, M.I. Rees, B. Lafrance, R.L. Sherlock and B. Chapon

2023

Gibson, H.L., Gemmell, T.P., Jørgensen, T.R.C., Hastie, E.C.G., Schofield, M.D., Haugaard, R., Smith, A.R., McKinley, B., Rees, M.I., Lafrance, B., Sherlock, R.L. and Chapon, B. 2023. Exploring differential metal endowment: A comparison of the western (Swayze) and eastern (Rouyn-Noranda) Abitibi greenstone belt: A geological guidebook; Geological Association of Canada–Mineralogical Association of Canada–Society for Geology Applied to Mineral Deposits, Joint Annual Meeting, Sudbury, Ontario, May 25–27, 2023, Field Trip FT07, Ontario Geological Survey, Open File Report 6395, 100p.

Users of OGS products should be aware that Indigenous communities may have Aboriginal or treaty rights or other interests that overlap with areas of mineral potential and exploration.

ISBN 978-1-4868-7225-1 (print)
ISBN 978-1-4868-7226-8 (PDF)

Open File Reports of the Ontario Geological Survey are available for viewing at the John B. Gammon Geoscience Library in Sudbury and at the regional Mines and Minerals office whose district includes the area covered by the report (see below).

Copies can be purchased at Publication Sales and the office whose district includes the area covered by the report. Although a particular report may not be in stock at locations other than the Publication Sales office in Sudbury, they can generally be obtained within 3 working days. All telephone, fax, mail and e-mail orders should be directed to the Publication Sales office in Sudbury. Purchases may be made using cash, debit card, VISA, MasterCard, cheque or money order. Cheques or money orders should be made payable to the *Minister of Finance*.

John B. Gammon Geoscience Library 933 Ramsey Lake Road, Level B2 Sudbury, Ontario P3E 6B5	Tel:	(705) 670-5614
Publication Sales 933 Ramsey Lake Rd., Level B2 Sudbury, Ontario P3E 6B5	Tel: Toll-free: Fax: E-mail:	(705) 670-5691 (local) 1-888-415-9845 ext. 5691 (705) 670-5770 pubsales.ndm@ontario.ca

Regional Mines and Minerals Offices:

Kenora – Suite 104, 810 Robertson St., Kenora P9N 4J2

Kirkland Lake – 1451 Hwy. 66, P.O. Box 40, Swastika P0K 1T0

Red Lake – 227 Howey Street, P.O. Box 324, Red Lake P0V 2M0

Sault Ste. Marie – 740 Great Northern Rd., Sault Ste. Marie P6A 5M1

Southern Ontario – 126 Old Troy Rd., Tweed K0K 3J0

Sudbury – 933 Ramsey Lake Rd., Level B2, Sudbury P3E 6B5

Thunder Bay – Suite B002, 435 James St. S., Thunder Bay P7E 6S7

Timmins – Ontario Government Complex, P.O. Bag 3060, 5520 Hwy. 101 East, South Porcupine P0N 1H0

Every possible effort has been made to ensure the accuracy of the information contained in this report; however, the Ontario Ministry of Mines does not assume liability for errors that may occur. Source references are included in the report and users are urged to verify critical information.

Cette publication est disponible en anglais seulement.

Parts of this report may be quoted if credit is given. It is recommended that reference be made in the following form:

Gibson, H.L., Gemmell, T.P., Jørgensen, T.R.C., Hastie, E.C.G., Schofield, M.D., Haugaard, R., Smith, A.R., McKinley, B., Rees, M.I., Lafrance, B., Sherlock, R.L. and Chapon, B. 2023. Exploring differential metal endowment: A comparison of the western (Swayze) and eastern (Rouyn-Noranda) Abitibi greenstone belt: A geological guidebook; Geological Association of Canada–Mineralogical Association of Canada–Society for Geology Applied to Mineral Deposits, Joint Annual Meeting, Sudbury, Ontario, May 25–27, 2023, Field Trip FT07, Ontario Geological Survey, Open File Report 6395, 100p.

Contents

FIGURES

PHOTOS

TABLE

Preface

This geological field trip guidebook was prepared initially for use with a field trip (trip number FT07) for the joint annual meeting of the Geological Association of Canada, the Mineralogical Association of Canada and the Society for Geology Applied to Mineral Deposits (GAC–MAC–SGA) held in Sudbury, Ontario, May 25–27, 2023.

Sudbury is one of the world's premier nickel-copper mining districts, a significant platinum group element (PGE) producer, and one of the oldest, largest, and best-exposed meteorite impact sites on Earth. As the world's largest integrated mining technology cluster, Sudbury has a vibrant mineral exploration and mining community that includes several major producers, numerous junior exploration companies, dozens of mining supply and service companies, 3 post-secondary educational institutions and associated exploration and mining centres, and several Ontario government mining and mineral ministry offices, making Sudbury one of the best places in the world to host a multidisciplinary meeting of this type. The City of Greater Sudbury, the largest city by landmass in Ontario, lies amidst glacially shaped ridges, green boreal forests, and contains 330 lakes over 10 hectares in size and 112 lakes over 100 hectares in size. The success of more than 40 continuous years of environmental reclamation efforts has led to numerous national and international awards, including a Government of Canada *Environmental Achievement Award*, a United States *Chevron Conservation Award*, and a United Nations *Local Government Honours Award*. And, as part of Sudbury's continuing regreening efforts, the milestone 10 millionth tree was planted in July 2022.

The theme of the GAC–MAC–SGA meeting—"Discovering Ancient to Modern Earth"—reflects the location of the meeting at the intersection of the Archean Superior Province and Proterozoic Southern and Grenville provinces, and Paleozoic–Quaternary cover sequences. The hybrid conference included a technical program of oral and poster presentations in Symposia, Special Sessions and Regular Sessions covering the complete spectrum of geoscience disciplines, which were complemented by 10 field trips, 6 workshops and 1 short course.

The meeting was hosted by the Harquail School of Earth Sciences and the Mineral Exploration Research Centre (MERC) at Laurentian University.

Abstract

Growing societal needs and the green economy depends on a secure source of critical metals. Canada's success in securing these metals is tied to our understanding of ore systems and the controls on differential metal endowment at district to craton scales. Only then can the metal potential of remote and underexplored areas of Canada and globally, most of which are under surface cover, be unlocked.

This field trip explores the processes responsible for the differential base and precious metal endowment of greenstone belts through a comparison of the geology and crustal architecture of the Swayze (Ontario) and Rouyn-Noranda (Quebec) areas in the western and eastern Abitibi greenstone belt, respectively. Crustal-scale processes and features affecting metal endowment, as defined through Metal Earth's seismic, magnetotelluric (MT) and gravity surveys, will be linked to surface geological features and crustal-scale faults. In the Swayze and Rouyn-Noranda areas, the trip focusses on key outcrops, tied to a new stratigraphy, that provides insights into the differences in the magmatic and structural evolution of the *circa* 2704–2695 Ma Blake River assemblage in both areas, their base and precious metal metallogeny, and evolution of crustal-scale faults. The trip includes a half-day visit to IAMGOLD's Côté Gold and Gosselin deposits (>19 million ounces gold) and will explore key differences in the setting and styles of ore deposits between the western and eastern Abitibi.

Exploring Differential Metal Endowment: A Comparison of the Western (Swayze) and Eastern (Rouyn-Noranda) Abitibi Greenstone Belt: A Geological Guidebook

H.L. Gibson[1], T.P. Gemmell[2], T.R.C. Jørgensen[3], E.C.G. Hastie[2], M.D. Schofield[3], R. Haugaard[3], A.R. Smith[4], B. McKinley[4], M.I. Rees[4], B. Lafrance[3], R.L. Sherlock[3] and B. Chapon[5]

Ontario Geological Survey
Open File Report 6395
2023

---

[1]**Professor Emeritus of Volcanology and Ore Deposits, Mineral Exploration Research Centre, Harquail School of Earth Sciences, Laurentian University, 935 Ramsey Lake Road, Sudbury, Ontario P3E 2C6** hgibson@laurentian.ca

[2]**Ontario Geological Survey, 933 Ramsey Lake Road, Sudbury, Ontario P3E 6B5**

[3]**Mineral Exploration Research Centre, Harquail School of Earth Sciences, Laurentian University**

[4]**IAMGOLD Corporation**

[5]**Cégep de l'Abitibi-Témiscamingue, 425 Blvd. du Collège, Rouyn-Noranda, Québec J9X 5E5**

Introduction

The non-uniform distribution of mineral deposits in and among cratons and provinces, subprovinces and terranes and belts, and districts and fields is well documented (e.g., Jaireth and Huston 2010; Jørgensen et al. 2022, and references herein). Using the quantity of metal contained in geological resources per unit surface area as a measure of endowment, the Archean Superior Province (~46 t/km^2 Cu+Zn+Pb) ranks high compared to its peers, e.g., the Yilgarn craton (~29 t/km^2 Cu+Zn+Pb) and the Slave Province (~33 t/km^2 Cu+Zn+Pb; Huston, Champion and Cassidy 2014). In the Superior Province, differential metal endowment is evident by the exceptional high endowment of the Abitibi Subprovince (Figure 1, ~171 t/km^2 Cu+Zn+Pb) relative to other subprovinces, e.g., the Uchi (~9 t/km^2 Cu+Zn+Pb) and Wabigoon (~20 t/km^2 Cu+Zn+Pb; Huston, Champion and Cassidy 2014). Within the Abitibi Subprovince (*see* Figure 1), the distribution of volcanogenic massive sulfide (VMS) deposits and tonnage of VMS ore produced indicates differential metal endowment among the 7 chronostratigraphic volcanic assemblages. The greatest base metal endowment is observed in the youngest 2704–2695 Ma Blake River assemblage (~5.4 deposits per 10^3 km^2 and ~65 Mt ore per 10^3 km^2) relative to the older assemblages, i.e., the 2710–2704 Ma Tisdale (~1.1 deposits per 10^3 km^2 and ~9 Mt ore per 10^3 km^2), 2719–2711 Ma Kidd–Munro (~0.4 deposits per 10^3 km^2 and ~27 Mt ore per 10^3 km^2), 2723–2720 Ma Stoughton–Roquemaure (~0.06 deposits per 10^3 km^2 and ~0.2 Mt ore per 10^3 km^2), 2734–2724 Ma Deloro (~3.2 deposits per 10^3 km^2 and ~14 Mt ore per 10^3 km^2), 2750–2735 Ma Pacaud (~2.7 deposits per 10^3 km^2 and ~6 Mt ore per 10^3 km^2), and the pre-2750 Ma assemblage with no known deposits (Monecke et al. 2017). Further illustrating the relative well-endowed nature of the Blake River assemblage is that it accounts for ~90% of the VMS-related gold in the Abitibi Subprovince, which corresponds to nearly 12% (1071 t) of the gold in the Abitibi belt as a whole (Mercier-Langevin et al. 2014; Dubé and Mercier-Langevin 2020). Orogenic quartz-carbonate hosted gold within the Superior Province also shows differential endowment with 14 of the 18 largest gold deposits located within the southeastern Abitibi Subprovince (Dubé and Mercier-Langevin 2020), where the majority of gold deposits are located along the Porcupine–Destor and Larder Lake–Cadillac faults. These major transcrustal structures and their associated deformation zones, have a long geological history; herein, these will be referred to as the Porcupine–Destor deformation zone (PDDZ) and Larder Lake–Cadillac deformation zone (LLCDZ)[*]. In the Rouyn-Noranda district, total production from 18 small orogenic gold deposits associated with the LLCDZ is eclipsed by the ≈14 million ounces (Moz) of gold produced from the Horne and Quemont VMS deposits (Gibson, Kerr and Cattalani 2000). In the Swayze area, the western extensions of the PDDZ and LLCDZ, the Deerfoot deformation zone (Vice and MacDonald 2019) and Ridout deformation zone (Heather 2001), respectively, have historically produced only 106 000 ounces of gold (van Hees et al. 2020), which is only approximately 0.05% of the total gold production in the rest of the Abitibi greenstone belt. The largest gold deposit in the Swayze area is the intrusion-related Côté Gold deposit (10 Moz: Cox et al. 2022), located immediately south (~3 km) of the Ridout deformation zone.

Lithospheric-scale crustal processes might exert a first-order control on base metal endowment, e.g., VMS deposits are preferentially localized in provinces with extensive juvenile crust (e.g., Stern et al. 1995; Syme et al. 1999; Huston, Champion and Cassidy 2014; Mole et al. 2022), possibly reflecting a setting with a negligible amount of evolved basement where rifting leads to highly attenuated crust that allows for enhanced heat flow and decompression melting of the lower crust and upper mantle (Syme et al. 1999; Hart, Gibson and Lesher 2004; Franklin et al. 2005; Huston, Champion and Cassidy 2014). At the belt and district scales, the pattern of differential metal endowment requires further evaluation of the geological features that promote clustering of deposits. Therefore, whole-of-crust analyses of both the Swayze area (Ontario) and the Rouyn-Noranda District (Quebec), based on the integration of geological and geophysical (seismic, gravity and magnetotelluric (MT)) data, were performed. The Rouyn-Noranda

[*] *Note, in Ontario, this area is generally referred to as the "Larder Lake–Cadillac deformation zone" (or the less preferred "Larder Lake–Cadillac break"). In the Province of Québec, it is known as the "Cadillac–Larder Lake deformation zone" (or "Cadillac–Larder Lake break"). For consistency, "Larder Lake–Cadillac deformation zone" is used herein.*

District data indicate an asymmetry in surface geology, structure and crustal architecture (Jørgensen et al. 2022). The southern part of the district, located adjacent to the ancestral transcrustal LLCDZ, contains ~104 Mt of the district's ~130 Mt VMS ore (15 of 18 VMS deposits) and has the greatest combined volume of synvolcanic trondhjemite-tonalite-granodiorite (TTG) plutons and felsic volcanic rocks, and the highest density of major synvolcanic structures (Jørgensen et al. 2022). This significant magmatic centre of the Rouyn-Noranda District is centred above a relative conductive lower crust that connects to surface by conductive subvertical pipe-like features interpreted to represent pathways for magmas and metalliferous fluids (Roots et al. 2022; Jørgensen et al. 2022). The 2 gold-rich VMS deposits of the Rouyn-Noranda District, the giant Horne (~325 t Au) and Quemont (~92 t Au) deposits, sit against a major synvolcanic structure that splays from the LLCDZ and coincides with a pipe-like conductive feature, highlighting the role of the transcrustal structure in localizing and allowing the magmatic system and ore-forming processes to be optimized, in turn explaining the clustering of deposits on the belt and district scales (Jørgensen et al. 2022).

The Swayze data indicate a symmetry in surface geology, structure and crustal architecture (T.P. Gemmell, OGS, unpublished data, 2023) where the older assemblages that crop out to the north and south continue below the Blake River assemblage, which occupies a central, "synclinal" portion of the belt. A large volume of lower conductivity in the mid to lower crust symmetrically underlies the Blake River assemblage with vertical conductive pipe-like features extending to surface. However, unlike the Rouyn-Noranda District, a significant magmatic centre with both synvolcanic and subvolcanic plutons has not been identified (T.P. Gemmell, OGS, unpublished data, 2023). The most prominent conductive pipe-like features correspond with the Deerfoot and Ridout deformation zones that extend downwards to a large mid-crustal conductive zone (T.P. Gemmell, OGS, unpublished data, 2023).

This field trip explores, in particular, the geological features that are indicative and important for the VMS endowment of Blake River assemblage volcanic rocks in the Swayze area, representing a relatively lower VMS endowment, and the Rouyn-Noranda area, representing a relatively higher VMS endowment. Many of these geological features can be related to geophysical signatures which will be addressed through discussions. The Abitibi greenstone belt is, of course, also renowned for its world-class orogenic gold deposits with quartz-carbonate vein–style deposits representing by far the most common and largest source of gold in the belt (>5925 t; Dubé and Mercier-Langevin 2020). Orogenic gold deposits have been shown to be spatially associated with the borders of magmatic centres and extensional faults (i.e., deformation zones) that also show a spatial connection to VMS deposits, despite the gold deposits forming millions of years later (e.g., Ramos et al. 2021). Similarly, orogenic gold deposits occur in the Rouyn-Noranda District, locally sharing a spatial relationship with VMS mineralization. Thus, the potential for a primary crustal architecture responsible for focussing both VMS and later gold mineralization makes the inspection of outcrops related to the orogenic gold mineralization important to the broader geological history.

Important to remember regarding the topic of endowment is the underlying economic value of what is being extracted from the ground, i.e., if a commodity increases in value or if a technological advance allows for a higher yield of a metal from its host, it is quite possible that additional mining of such a commodity will increase and our view of the endowment of an area would increase along with it since the perceived endowment is ultimately based on published production and resource numbers. For example, before the discovery and implementation of froth floatation in the last century, the average grade of copper deposits was >4% Cu, and the deposits were largely mined from underground operations. However, with the advent of froth floatation, the grades of mineable copper deposits steadily decreased to <1% Cu, and now most of the copper mined comes from giant, open-pit, porphyry copper mines. For gold, the story is somewhat different, because the driver since gold price fixation ended in 1974, was not technology, as much as metal price. The price of gold in 1990 was <US$400 per ounce and the current price hovers around US$1800 per ounce (International Monetary Fund 2023,

www.imf.org/en/Research/commodity-prices). In comparison, the price of base metals has not shown such a dramatic increase, for example, the price of copper in 1990 was US$1.14 per pound and the current price is around US$3.60 per pound (International Monetary Fund 2023, www.imf.org/en/Research/commodity-prices). The difference between the rise in value of gold versus base metals is not related primarily to an increase in demand by industrial use, but rather by social and economic factors that have allowed, over the past 10 years, the open-pit mining of very large low-grade gold deposits that were essentially the footprint of former higher grade orogenic vein deposits that were originally mined through underground operations, such as the Malartic and Detour deposits.

Preparation of this field guide builds on, and incorporates, descriptions from previous guidebooks, especially in established mining districts, such as Rouyn-Noranda, where there has been a century of mining, exploration and research. In recognition of this, we acknowledge the generous support of the Society of Economic Geologists in preparing this guidebook by allowing extensive use of figures and text contained within "Volcanogenic Massive Sulfide Deposits of the Noranda Camp" by Monecke, Gibson and Goutier (2017) and "The Larder Lake Cadillac Break and its Gold Districts" by Poulsen (2017a), both of which are chapters in the Society of Economic Geologists *Archean Base and Precious Metal Deposits, Southern Abitibi Greenstone Belt, Canada* (Reviews in Economic Geology v.19, edited by T. Monecke, P. Mercier-Langevin and B. Dubé).

SAFETY

For users of this guidebook, please bear in mind that some of the stops listed in this guidebook involve travel along gravel roads, some of which are used by logging operations, as well as semi-isolated work in the bush. Therefore, standard bush safety practices should be followed by users of this guidebook. Such practices include travelling in pairs; advising others of your starting time and location and your expected return time; carrying sufficient water for the trip; being prepared for sudden changes in the weather; and carrying the appropriate emergency and safety gear (e.g., proper footwear, rain gear, hat, sunscreen and safety glasses when hammering). Care should always be exercised when parking, exiting vehicles and crossing the roads. Use of safety vests and/or bright clothing is recommended to improve your visibility to motorists. Site-specific hazard information is provided at the beginning of each individual field trip stop, as needed. Many of the stops are at sites on private land or land controlled by companies, so permission is required.

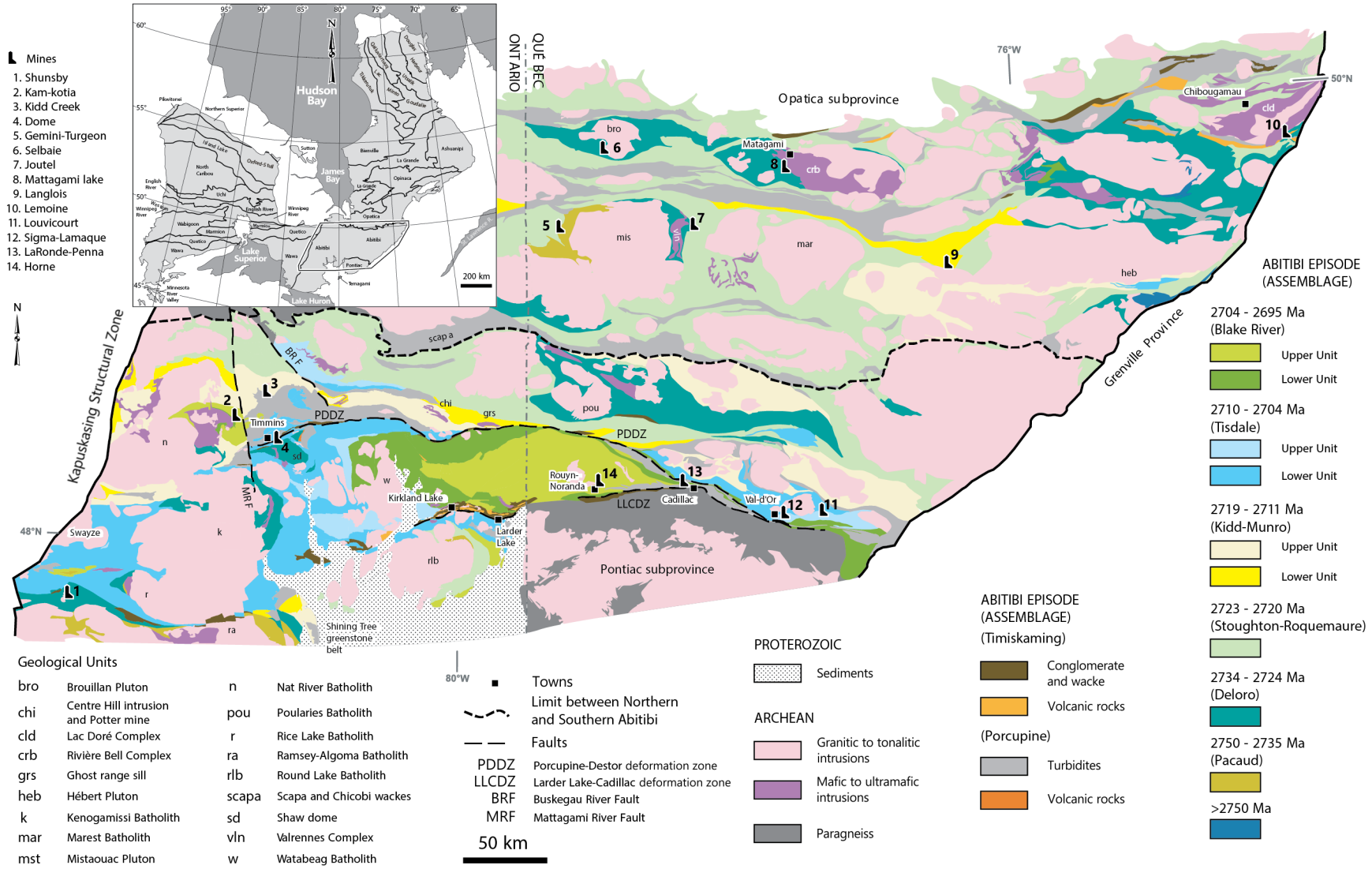

Figure 1. Chronostratigraphic map of the Abitibi greenstone belt, with inset indicating its location in the Superior Province (*modified from* Thurston et al. 2008).

Geological Settings

SWAYZE AREA: GEOLOGY, STRATIGRAPHY, VOLCANOGENIC MASSIVE SULFIDE AND GOLD DEPOSITS

The Swayze area (Figures 2 and 3) represents the southwestern extension of the Abitibi greenstone belt and hosts Ontario's newest large gold camp. Historically known as the "poor cousin to the Abitibi", it only produced ≈0.1 Moz of gold over the last century (Joburk and Jerome deposits; van Hees et al. 2020). However, with the discovery of the intrusion-related Côté Gold deposit (2740 Ma) (Katz et al. 2017, 2021), and other resources only now being fully realized (e.g., Gosselin and Jerome deposits), it has a growing resource of >20 Moz of gold (measured, indicated and inferred; Burt, Chance and Burns 2011; Cox et al. 2022).

Geology and Stratigraphy

The Swayze area (*see* Figure 2) of the western Abitibi greenstone belt contains the same chronostratigraphic metavolcanic assemblages as the metal-endowed eastern Abitibi greenstone belt and should, therefore, have the potential to host significant base metal deposits.

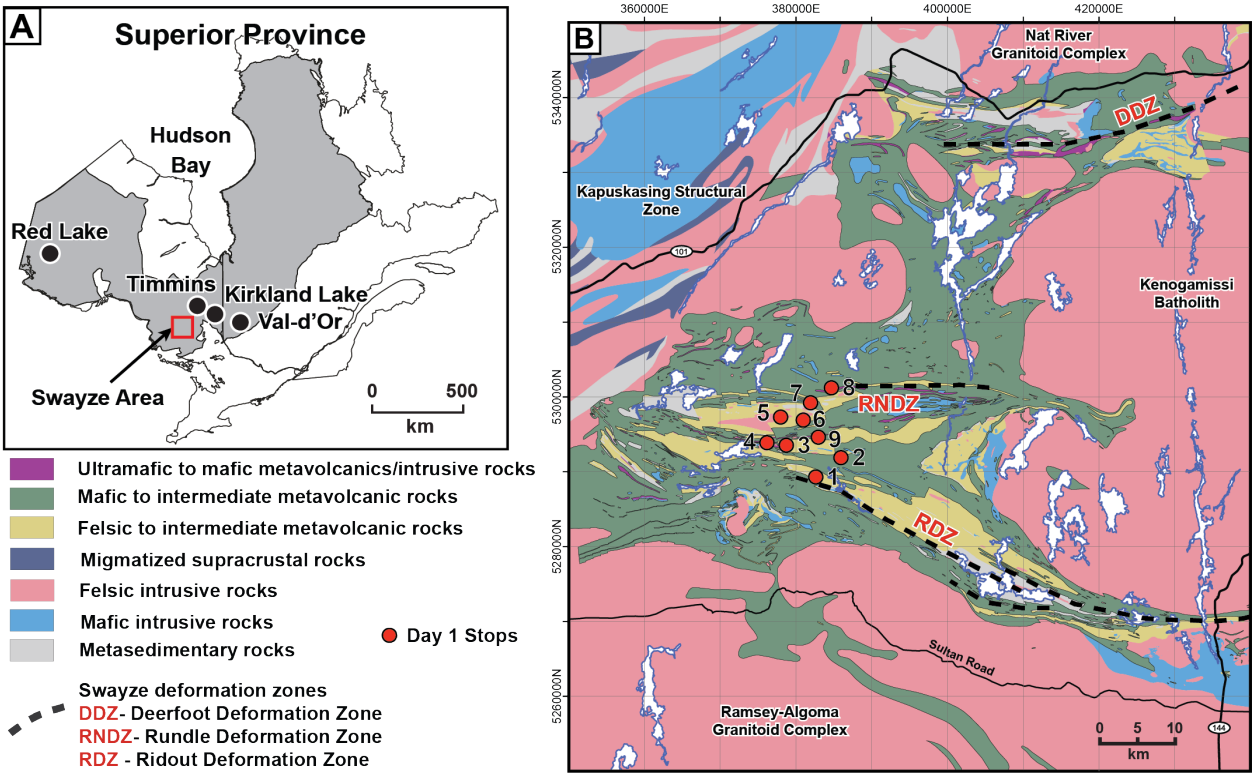

Figure 2. Geological map of the Swayze area, southwest Abitibi greenstone belt. **A**) Location of the Swayze area within the Superior Province. **B**) Simplified geologic map of the Swayze area showing Day 1 field trip stops. Location information provided as Universal Transverse Mercator (UTM) co-ordinates using North American Datum 1983 (NAD83) in Zone 17 (*modified from* Ontario Geological Survey 2011; MacDonald, Hastie and Davis 2017; Vice and MacDonald 2019; Hastie, Kontak and Lafrance 2020).

However, few deposits have been discovered and are atypical in character to those in the eastern Abitibi greenstone belt. The Swayze area is mainly composed of mafic to felsic metavolcanic rocks with localized ultramafic metavolcanic rocks, clastic and chemical metasedimentary rocks and synvolcanic to syntectonic felsic to ultramafic intrusive rocks (Heather 2001; Ayer, Ketchum and Trowell 2002; van Breemen, Heather and Ayer 2006; Gemmell and MacDonald 2016). The volcanic and sedimentary assemblages in the Abitibi greenstone belt are most recently defined by Thurston et al. (2008, and references therein), Monecke et al. (2017, and references therein) and Dubé and Mercier-Langevin (2020, and references therein): pre-2750 Ma, 2750–2735 Ma Pacaud assemblage, 2734–2724 Ma Deloro assemblage, 2723–2720 Ma Stoughton–Roquemaure assemblage, 2720–2710 Ma Kidd–Munro assemblage, 2710–2704 Ma Tisdale assemblage and the 2704–2695 Ma Blake River assemblage.

Overlying the volcanic assemblages are 2 dominantly sedimentary assemblages referred to as the Porcupine-type (2690–2685 Ma) and the Timiskaming-type (≤2679–2669 Ma) sedimentary basins. In the central and southern part, 2 regional deformation zones (Rundle and Ridout; *see* Figure 2) have a spatial association with gold occurrences and deposits in the Swayze area (*see* Figure 3).

The Blake River assemblage is the most base metal-endowed volcanic assemblage in the Abitibi greenstone belt because of the VMS deposits of the Rouyn-Noranda District (Gibson and Galley 2007; Monecke et al. 2017). New U/Pb zircon ages indicate that the Blake River assemblage is the most voluminous assemblage represented in the Swayze area. This field trip provides an important transect through a section of the lowermost to uppermost Blake River assemblage in the Swayze area, highlighting well-preserved volcanic facies and subeconomic base-metal mineralization. Discussions about the key differences between the Blake River assemblage in the Swayze and Rouyn-Noranda areas are planned during the field trip.

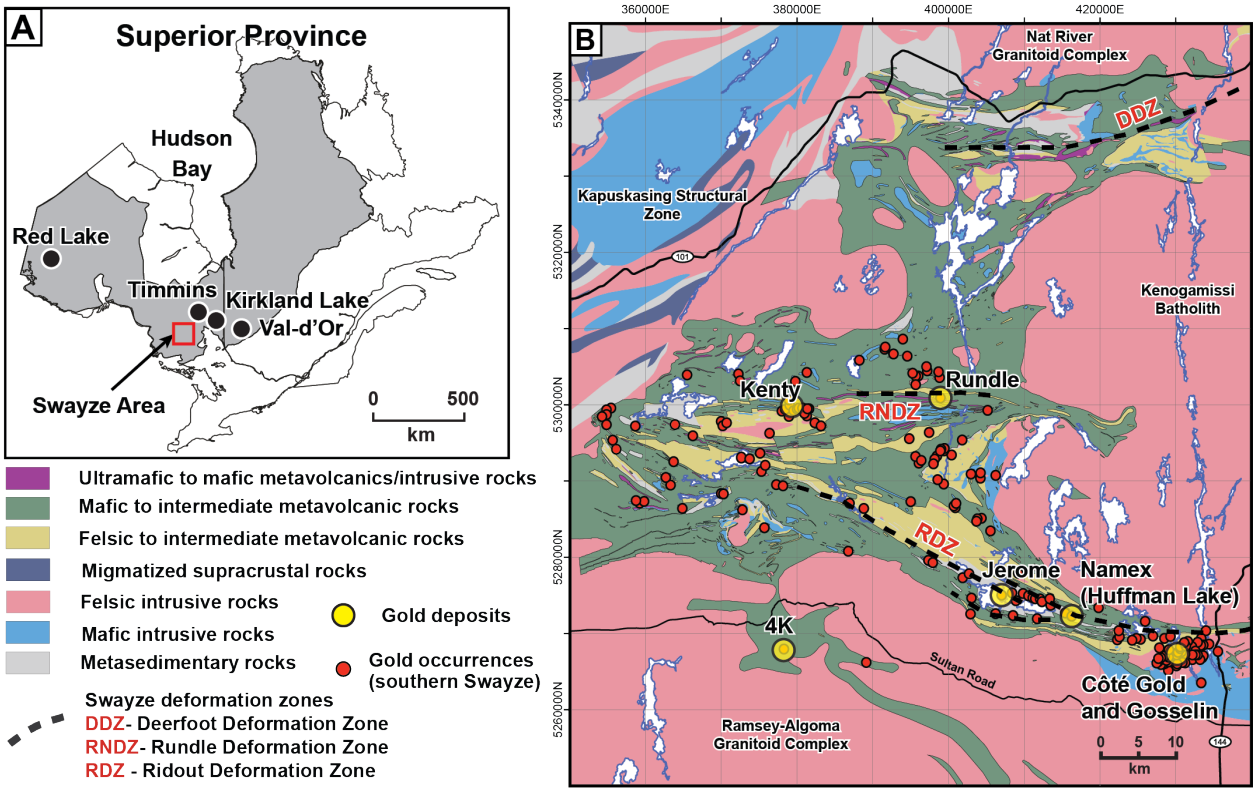

Figure 3. Geological map of the Swayze area, southwest Abitibi greenstone belt. **A**) Location of the Swayze area within the Superior Province. **B**) Simplified geological map of the Swayze area showing the locations of gold deposits and occurrences for the southern Swayze area. All UTM co-ordinates provided using NAD83 in Zone 17 (*modified from* Ontario Geological Survey 2011; MacDonald, Hastie and Davis 2017; Hastie, Kontak and Lafrance 2020).

GOLD DEPOSITS

Gold mineralization styles in the Swayze area are similar to those found in the Abitibi greenstone belt including greenstone-hosted orogenic (Kenty), banded iron formation (BIF)–hosted orogenic (4K), syn-Timiskaming intrusion-hosted gold deposits (Jerome and Namex; Hastie 2017; MacDonald, Hastie and Davis 2017; Ontario Geological Survey 2019; Hastie, Kontak and Lafrance 2020; Davis 2021). The Jerome and Namex deposits in the southern Swayze are associated with one of the largest Timiskaming-type basins in the Abitibi Subprovince. The basin is located along the Ridout deformation zone which can be viewed as the western extent of the gold endowed LLCDZ (*see* Figure 3). Despite this comparison, only the Jerome deposit has previously been mined for gold. This is surprising because this seemingly less-endowed clastic basin displays similar geometry, sedimentary character and dispersal patterns as other orogenic formed Timiskaming-type basins in the Abitibi greenstone belt (Haugaard et al. 2022, and references therein). The syn-Timiskaming intrusions at Jerome and Namex may have been genetically linked to the Ridout deformation zone, which can be seen as a crustal-scale fault that facilitated a flare-up of these syntectonic granitoids. In addition, the Côté Gold and Gosselin deposits represent an early (*ca*. 2741 Ma) gold mineralization style not seen elsewhere in the Abitibi greenstone belt (Katz et al. 2017, 2021). The Côté Gold (~10 Moz of gold at ~0.87 g/t Au: Cox et al. 2022) and Gosselin deposits, which are interpreted to be intrusion-related (porphyry-like) deposits (Katz et al. 2021), are located within the Chester intrusive complex, which is a low aluminum tonalitic and dioritic synvolcanic composite intrusion (Katz et al. 2017) that is bound to the north by felsic to intermediate metavolcanic rocks within the Ridout deformation zone and to the south by the Ramsey–Algoma granitoid complex (*see* Figures 2 and 3). Because of the presence of mafic volcanic xenoliths, its composition and the presence of miarolitic cavities and graphic-textured minerals (indicative of rapid cooling), it is suggested that the Chester intrusive complex intruded at a high crustal level into its own volcanic edifice (Berger 2012; Kontak, Creaser and Hamilton 2013; Gemmell 2015). The synvolcanic timing of the Côté Gold differs from the younger orogenic Malartic and Detour deposits and, along with the large tonnage low grade, it may represent a "new" deposit type or style that is becoming economically more important in part because of the high gold price and the possibility to mine at increasingly lower grades. Thus, a visit to the Côté Gold deposit serves to introduce this new type of gold deposit, and serves as a reminder how a change in metal price can result in a change in endowment designation.

ROUYN-NORANDA DISTRICT: GEOLOGY, STRATIGRAPHY, VOLCANOGENIC MASSIVE SULFIDE AND GOLD DEPOSITS

The Rouyn-Noranda District, Quebec, is one of Canada's premier base metal and gold camps and it is one of world's most thoroughly studied and documented volcanogenic massive sulfide (VMS) districts (e.g., Gibson and Galley 2007, and references therein; Figure 4). Since discovery of the Horne Mine in 1922, approximately 20 economic VMS deposits (Figure 5; Table 1) and 19 small orogenic quartz-carbonate vein deposits have been discovered (Gibson and Galley 2007). Cumulative, measured, indicated and inferred resources, including those undeveloped at the Horne Mine, total and in-ground metal endowment of 2.7 Mt Cu, 3.0 Mt Zn, 625 t Au (~20 Moz), and 4554 t Ag (~146 Moz) (Monecke, Gibson and Goutier 2017). Gold produced from the gold-rich Horne and Quemont deposits (Day 4 Stops 3 and 9) totals almost 440 t and eclipses the production from the District's orogenic gold deposits (Gibson, Kerr and Cattalani 2000). Other types of mineralization in the District include the intrusion-hosted and porphyry-like Don-Rouyn copper-molybdenum deposit, St. Jude copper-molybdenum deposit, Joliet Breccia (Day 4 Stop 8) and occurrences of quartz-sulfide copper-zinc-silver veins (Day 4 Stop 6) (Goldie, Kotila and Seward 1979; Gibson, Watkinson and Comba 1983; Gibson and Galley 2007; Schofield et al. 2021, in press; Schofield 2023).

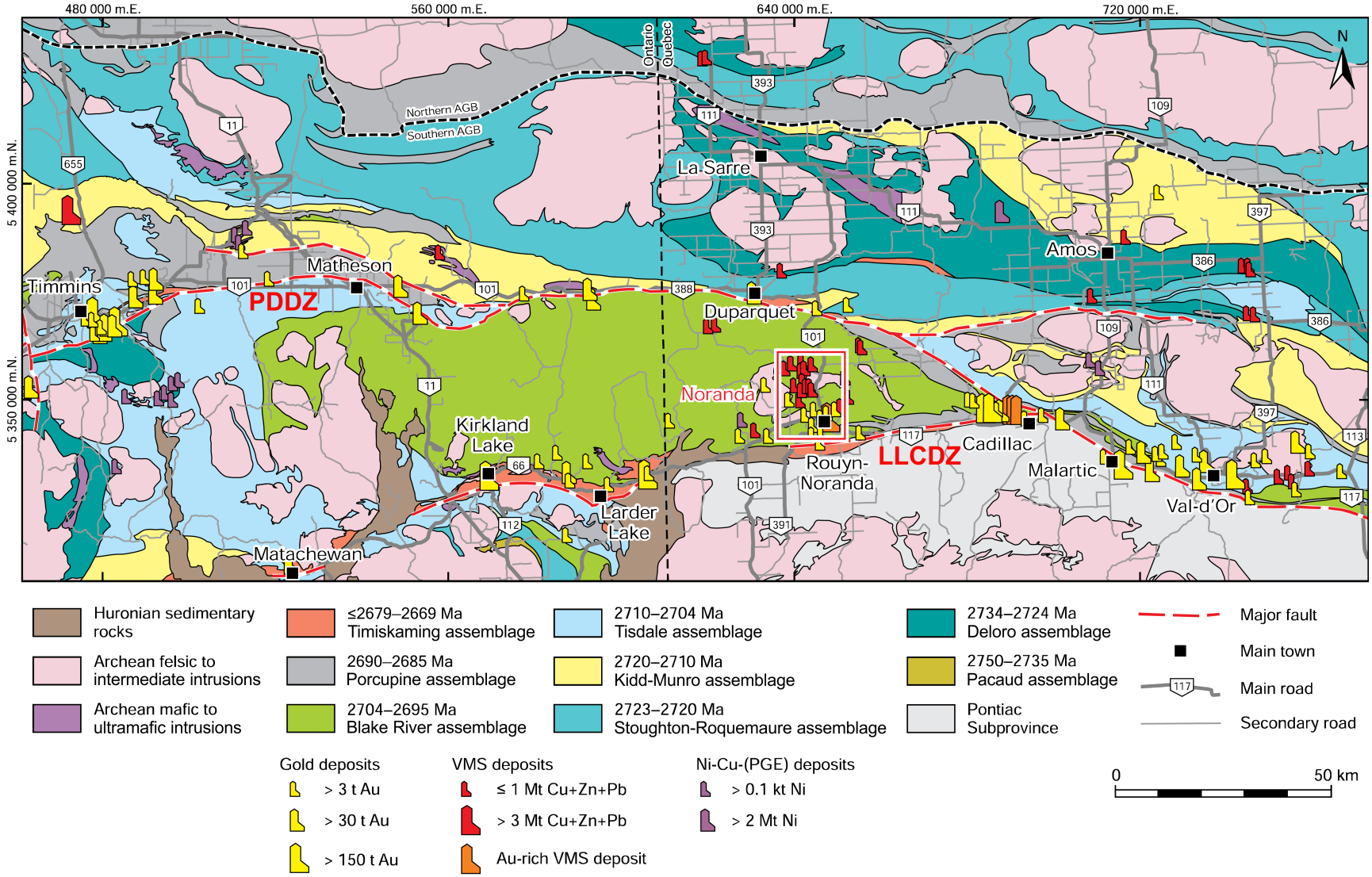

Figure 4. Chronostratigraphic map of the southern Abitibi Subprovince in the Kirkland Lake–Rouyn-Noranda area showing the Blake River assemblage and bounding PDDZ and LLCDZ. The most economically endowed part of the Rouyn-Noranda District is outlined by the red box (*from* Monecke, Gibson and Goutier 2017). The boundary between the northern Abitibi greenstone belt (AGB) and the southern AGB is shown by an east-to-west thick black dashed line. All UTM co-ordinates provided using NAD83 in Zone 17.

The abundant outcrop, low strain and low metamorphic grade in the District has resulted in the exceptional preservation of the VMS and orogenic gold deposits, and the remarkable exposures of superbly preserved submarine volcanic rocks. Early research at Noranda was instrumental in the development of the syngenetic VMS model and continued research over the decades has helped to shape the current VMS model and the development of exploration strategies (Gilmour 1965; Hutchinson 1965; Lickus 1965; Roscoe 1965; Boldy 1968; Fisher 1970; Sangster 1972; Spence 1967; Spence and de Rosen-Spence 1975; Boldy 1979; Riverin and Hodgson 1980; Franklin et al. 1981; Knuckey, Comba and Riverin 1982; Knuckey and Watkins 1982; Gibson, Watkinson and Comba 1983; Gibson 1990; Gibson and Watkinson 1990; Péloquin et al. 1990; Gibson, Morton and Hudak 1999; Franklin et al. 2005;

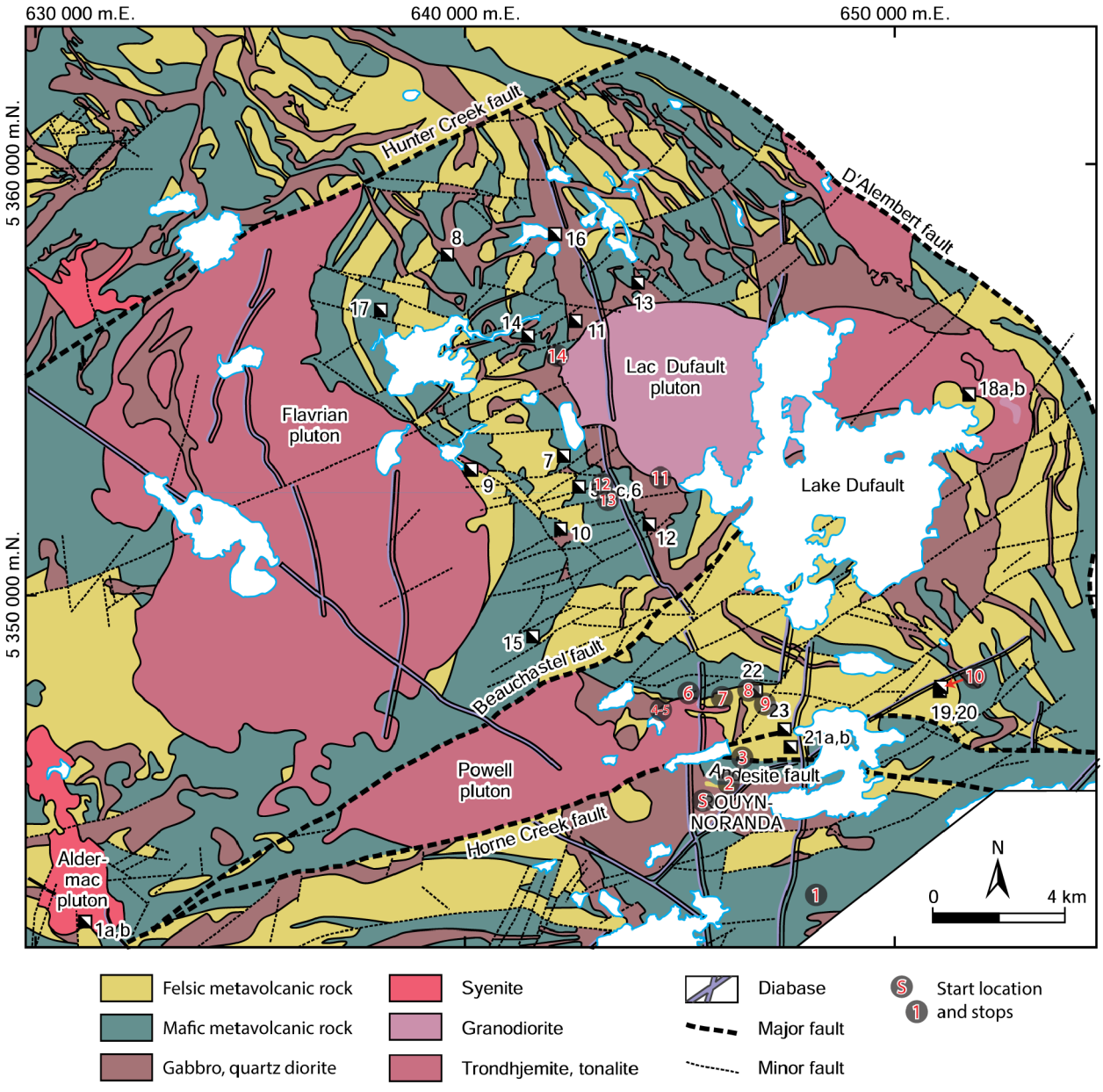

Figure 5. Geologic map showing felsic and mafic volcanic strata and intrusions of the Lower part of the Blake River Group (within the Blake River assemblage) that comprise the Noranda Volcanic Complex and Rouyn-Noranda District (*from* Monecke, Gibson and Goutier 2017). The VMS deposits are shown by numbered half-filled boxes, where the numbers refer to the tonnes and grade of deposits listed in Table 1. Day 4 stops are shown by red numbers in grey circles. All UTM co-ordinates provided using NAD83 in Zone 17.

Table 1. Grade and tonnage of VMS deposits of the Rouyn-Noranda District (data *from* Gibson and Watkinson (1990) and Gibson and Galley (2007); *modified from* Monecke, Gibson and Goutier 2017, p.176). Deposit numbers refer to deposit locations in Figure 5.

No.	Deposit	Tonnage (Mt)	Cu (%)	Zn (%)	Au (g/t)	Ag (g/t)	Years of Production
1a	Aldermac no.3-5	1.87	1.65	—	0.02	1.23	1933–1943
1b	Aldermac no.7, 8	1.04	1.50	4.13	0.30	31.20	—
2 [a]	Magusi	1.68	3.30	5.13	1.84	65.90	—
3 [a]	Fabie (New Insco)	0.46	2.53	—	0.02	1.23	1976–1977, 2008
4a [b]	Bouchard–Hébert	9.61	0.78	4.74	1.41	43.28	1995–2005
4b [b]	Mobrun	1.63	0.84	2.45	2.41	27.39	1986–1992
5a	Amulet Lower A	4.69	5.10	5.20	1.43	44.10	1937–1962
5b	Amulet Upper A	0.18	2.30	6.10	2.00	46.00	1937–1962
5c	Amulet 11 Shaft	0.44	3.60	2.40	0.70	22.00	1956–1962
6	Amulet C	0.56	2.20	8.50	0.60	86.70	1930–1953
7	Amulet F	0.27	3.40	8.60	0.30	46.30	1930–1937; 1944–1962
8	Ansil	1.60	7.06	1.77	2.21	26.30	1989–1993
9	Bedford	0.23	1.45	—	—	—	—
10	Corbet	2.65	2.92	1.57	0.84	17.48	1979–1986
11	East Waite	1.50	4.10	3.25	1.80	31.00	1952–1961
12	Millenbach	3.48	3.42	4.28	0.91	46.25	1971–1981
13	Norbec [c]	4.60	2.61	3.88	0.65	43.80	1964–1976
14	Old Waite	1.12	4.70	2.98	1.10	22.00	1928–1930; 1937–1948
15	Ribago	0.48	0.40	7.90	1.90	23.30	—
16	Vauze	0.36	3.10	2.20	0.69	30.78	1961–1965
17	West Ansil	1.13	3.35	0.29	0.82	7.45	—
18b	Gallen	2.60	0.12	4.94	1.12	33.57	1981–1985; 1997–2000
18b	West MacDonald	0.94	—	3.03	0.05	1.37	1955–1959
19	Delbridge	0.37	0.61	9.66	2.80	109.50	1969–1971
20	D'Eldona	0.08	0.20	5.27	4.10	27.36	1950–1952
21a [d]	Horne	53.70	2.22	—	6.06	13.00	1927–1976; 1985–1989; 1994
21b [d]	Horne No.5 [e]	112.70	0.18	0.85	1.53	16.44	1967–1976
22	Joliet [f]	2.08	1.00	—	—	—	1952–1959; 1961–1974
23	Quemont	13.82	1.32	2.44	5.49	30.90	1949–1971; 2001

***Abbreviations**: —, unknown; g/t, grams per tonne; Mt, million tonnes.*

[a] *Deposit numbers 2 and 3 are located outside of the area depicted in Figure 5, but are shown (not labelled) in Figure 4 near Duparquet (west-northwest of the red outlined box.*

[b] *Deposit numbers 4a and 4b are located outside of the area depicted in Figure 5, but are shown (not labelled) in Figure 4 to the northeast of the red outlined box.*

[c] *Includes D zone.*

[d] *The Horne #5 deposit (21b) is the same location (at depth) as the Horne deposit (21a).*

[e] *Measured, indicated and inferred resources as a Net Smelter Return CDN$55 cutoff (Falco Resources, news release, October 16, 2017).*

[f] *Falco Pacific Resource Group, news release, December 19, 2013.*

Gibson 2005; Gibson et al. 2007; Gibson and Galley 2007; McNicoll et al. 2014; Schofield et al. 2021, in press; Jørgensen et al. 2022). All volcanic and sedimentary rocks have been metamorphosed (subgreenschist to locally amphibolite facies), but the prefix "meta" has been omitted for ease of use and brevity (Monecke, Gibson and Goutier 2017).

Geology and Stratigraphy

The VMS deposits of the Rouyn-Noranda District occur within submarine volcanic rocks of the Blake River Group (Gunning 1937; Gunning and Ambrose 1940; Wilson 1948), which is part of the 2704–2695 Blake River assemblage, the youngest volcanic assemblage of the Abitibi Subprovince (*see* Figure 1; Ayer et al. 2005; Thurston et al. 2008; McNicol et al. 2014). The Rouyn-Noranda mining district and Blake River Group are bound to the south and north by the LLCDZ (e.g., Day 3 Stop 5) and PDDZ

faults, respectively (*see* Figure 4). These deformation zones are associated with turbiditic sediments of the 2690–2685 Ma Porcupine assemblage (Cadillac and Kewagama groups in Quebec; Goutier 1997; Davis 2002; Frieman et al. 2017) and ~2682 Ma Pontiac Group (Mortensen and Card 1993; Davis 2002; Frieman et al. 2017), and alluvial-fluvial successions of polymictic conglomeratic rocks, cross-bedded sandstone, alkali-shoshonitic volcanic rocks and syenitic-monzonitic intrusions of the ≤2679–2669 Ma Timiskaming assemblage (e.g., Day 3 Stops 1 and 6; Davis 2002; Ayer et al. 2005; Thurston et al. 2008; Frieman et al. 2017; Poulsen 2017a; Dubé and Mercier-Langevin 2020).

The Noranda Volcanic Complex (NVC) encompasses the entire Blake River Group and VMS deposits at Rouyn-Noranda and the terms Rouyn-Noranda District and NVC are interchangeable, although the NVC is commonly used when describing the geology, whereas as the Rouyn-Noranda District is commonly used when describing the ore deposits and metallogeny (*see* Figure 4). The NVC comprises a bimodal, tholeiitic to transitional basalt-dominated, central volcanic complex with subordinate transitional to calc-alkalic, FIII rhyolites and lesser dacites and rhyolites that is localized along the Larder Lake–Cadillac deformation zone to the south (de Rosen-Spence 1976; Lesher, Gibson and Campbell 1986; Gibson 1990; Hart, Gibson and Lesher 2004). It may consist of more than one overlapping volcanic edifices (Ludden, Gélinas and Trudel 1982; Gélinas, Trudel and Hubert 1984; Gibson and Watkinson 1990; Péloquin 2000, 2005). The NVC was subdivided into 5 fault-bounded blocks (*see* Figures 4 and 5; de Rosen-Spence 1976, Dimroth et al. 1982). From north to south, these blocks include the Hunter block between the PDDZ and Hunter Creek faults, the Flavrian block, between the Hunter Creek and Beauchastel faults, the Powell block between the Beauchastel and Horne Creek faults, the Horne block between the Horne Creek and Andesite faults, and the Rouyn-Pelletier block between the Andesite fault and LLCDZ (*see* Figure 5; de Rosen-Spence 1976). The Hunter Creek, Beauchastel, Horne Creek and Andesite faults are second-order splays of the LLCDZ (Robert 1989; Jackson et al. 1995; Verpaelst et al. 1995; Carrier et al. 2000; Poulsen 2017a) and have been interpreted as reactivated synvolcanic faults (Spence and de Rosen-Spence 1975; de Rosen-Spence 1976; Lichtblau and Dimroth 1980; Dimroth et al. 1982; Gibson 1990; Gibson and Watkinson 1990; Kerr and Gibson, 1993; Gibson and Galley 2007; McNicol et al. 2014; Jørgensen et al. 2022).The 2 largest and gold-rich deposits, the Horne and Quemont (~440 t Au; Kerr and Mason 1990; Gibson and Kerr 1993; Gibson, Kerr and Cattalani 2000), occur juxtaposed across the Horne Creek fault, within the Horne and adjacent Powell blocks, respectively, and are hosted by thick monolithic successions of coherent rhyolite flows, domes and volcaniclastic rocks (Day 4 Stops 3 and 9; Kerr and Mason 1990; Kerr and Gibson 1993; Mercier-Langevin et al. 2011; Schofield 2023). The more numerous, but smaller "conventional Cu-Zn-Pb-Ag-Au" VMS deposits of the Flavrian and Hunter blocks are hosted by a basalt-dominated, bimodal succession of mafic and felsic coherent flows and lesser volcaniclastic rocks (Day 4 Stops 12 and 13; Kerr and Gibson 1993; Gibson and Kerr 1993; Gibson and Galley 2007). Uncertainty remains as to the relative stratigraphic position of the age-equivalent Horne and Quemont deposits (*ca*. 2702 Ma; McNicoll et al. 2014) and their stratigraphic position and temporal relationship to VMS deposits of the Flavrian and Hunter blocks (Spence and de Rosen-Spence 1975; Gibson and Watkinson 1990; Barrett et al. 1991; Gibson, Kerr and Cattalani 2000; Monecke et al. 2008; Monecke, Gibson and Goutier 2017; Moore et al. 2016).

The synvolcanic, trondhjemite-tonalite-gabbro Flavrian–Powell intrusive complex (FPIC) intrudes the NVC within the Flavrian, and Powell blocks along the southern portion of the complex where its north and south limits are structural, constrained by the Hunter and Horne Creek faults, respectively (*see* Figure 5; Day 4 Stops 4 and 5). The FPIC, similar to the Chester intrusive complex, is a low aluminum tonalitic and dioritic synvolcanic composite intrusion that is host to base metal and gold mineralization (Galley 2003). Several ages have been determined for the trondhjemite phases of the Flavrian and Powell plutons: 2700.8 $^{+2.6}/_{-1.0}$ Ma by Mortensen (1993), 2700.7±0.6 Ma and 2700.1±1.0 Ma by McNicoll et al. (2014) and 2701±0.80 by Schofield et al. (2021). The FPIC defines the principal magmatic centre for the NVC. It is interpreted to be the subvolcanic heat source that drove a high-temperature, seawater-dominated hydrothermal convective system responsible for the formation of VMS deposits within the

District (Goldie 1976; Campbell et al. 1981; Kennedy 1985; Galley 2003; Gibson and Galley 2007) and/or provided a metal source that contributed metals via magmatic fluids to a modified seawater-dominated hydrothermal fluid (Gibson and Watkinson 1990; Galley 2003; Gibson and Galley 2007; Franklin et al. 2005; Sharman et al. 2015). The smaller Fabie, emplaced from 2701.5 to 2699.6 Ma (Sutton 2020), and Dufault East intrusions in the Hunter and Flavrian blocks, respectively, are interpreted to have played a similar, but proportionally smaller role (*see* Figure 5; Kerr and Gibson 1993; Sutton 2020). The younger Lac Dufault pluton (west body) is a granodiorite intrusion associated with a pronounced contact metamorphic aureole (*see* Figure 5; de Rosen-Spence 1969; Riverin and Hodgson 1980; Beaty and Taylor 1982). A U/Pb zircon age of 2690.3±1 Ma by Mortensen (1993) indicates that emplacement of this intrusion postdates submarine volcanism and formation of the NVC and its VMS deposits.

Numerous mafic and felsic dikes and sills occur throughout the NVC where they are often altered and overprinted by the Lac Dufault pluton contact metamorphism. Ages for these intrusions are limited but ages of 2697±0.8 Ma for the Dufresnoy gabbro in the Flavrian block (Day 4 Stop 11) and of 2702±0.8 Ma and 2698±0.9 Ma for felsic dikes in the Powell block (Day 4 Stops 6 and 8; McNicoll et al. 2014; Schofield et al. 2021) support field evidence of a synvolcanic timing. The most pervasive post-Timiskaming age deformation event is characterized by a regional east-trending cleavage axial planar to large-scale antiforms and synforms, and faults or deformation zones, including the LLCDZ and PDDZ (e.g., Dimroth et al. 1983; Wilkinson, Cruden and Krogh 1999; Daigneault, Mueller and Chown 2002; Bleeker 2012; Poulsen 2017a; Bedeaux et al. 2017). This north-trending deformation (shortening) event occurred between *circa* 2670 and 2660 Ma and coincides with peak metamorphism in the southern Abitibi greenstone belt, which occurred between ~2669 and 2653 Ma (Powell, Carmichael and Hodgson 1995; Piette-Lauzière et al. 2019; Dubé and Mercier-Langevin 2020). This was followed by northwest-directed shortening and later dextral transcurrent reactivation of the LLCDZ and PDDZ (Dimroth et al. 1983; Hubert, Trudel and Gélinas 1984; Wilkinson, Cruden and Krogh 1999; Daigneault, Mueller and Chown 2002; Ispolatov et al. 2008; Bleeker 2012; Poulsen 2017a; Bedeaux et al. 2017). In accordance with most previous work in the Rouyn-Noranda District, the main post-Timiskaming age deformation event is referred to as "D_2" and the dextral transcurrent event as "D_3" (Goulet 1978; Dimroth et al. 1983; Hubert, Trudel and Gélinas 1984).

VOLCANIC STRATIGRAPHY

The stratigraphic nomenclature for volcanic rocks of the NVC and Rouyn-Noranda District has evolved over decades of mapping and geochronological research (Monecke et al. 2017; Monecke, Gibson and Goutier 2017). Historically, stratigraphic subdivisions within the NVC have been lithostratigraphic and in compliance with the North American Stratigraphic Code (e.g., Wilson 1941; de Rosen-Spence 1976; Gibson 1990). Spence (1967) and Spence and de Rosen-Spence (1975) grouped the informal lithostratigraphic units into "cycles"; de Rosen-Spence (1976) proposed the first informal regional lithostratigraphic subdivision for the District, which she interpreted to comprise a large, 7–9 km thick, subaqueous, shield-like, volcanic edifice, with an unfolded diameter of ~40–50 km known as the Noranda Volcanic Complex (NVC). The NVC was interpreted to contain a large subsidence structure, postulated to be an ancient caldera (de Rosen-Spence 1976; Lichtblau and Dimroth 1980). Gibson (1990) and Gibson and Watkinson (1990) re-grouped the lithostratigraphic formations and "cycles" into larger informal pre-cauldron, cauldron and post-cauldron units in accordance with limited U/Pb zircon ages available at that time (Mortensen 1987, 1993). The term cauldron was proposed by Gibson and Watkinson (1990) because, unlike a caldera, a cauldron is not constrained by shape or connection with surface volcanism and commonly involves passive, piecemeal and asymmetric collapse above a static or rising body of magma (Smith and Bailey 1968; Williams and McBirney 1979). The limits of the Noranda cauldron were interpreted to be the Hunter Creek and Horne Creek faults to the north and south, respectively, and the Flavrian pluton and the Dalembert shear zone, to the west and east, respectively (*see* Figure 5; Gibson and Watkinson 1990). More recently, it has been proposed that the NVC represents a large, nested caldera

complex comprising at least 3 calderas of different sizes, with the Noranda cauldron being the smallest and youngest (Pearson 2005; Daigneault and Pearson 2006; Pearson and Daigneault 2009; Mueller 2006; Mueller et al. 2009, 2012; Moore, Mueller and Daigneault 2012; Moore et al. 2016). The FPIC floors the Noranda cauldron, and the voluminous tonalite-trondhjemite phases were largely emplaced into the NVC during a period of resurgent magmatism following subsidence (Gibson 1990; Gibson and Watkinson 1990).

In order to facilitate temporal correlation of volcanic units within the NVC, McNicoll et al. (2014) used existing and numerous new U/Pb zircon ages and regrouped the established informal lithostratigraphic formations into 8 informal "formations" based on age. This resulted in hybrid "lithostratigraphic and chronostratigraphic" units and previous lithostratigraphic formations of the Flavrian, Powell and Horne blocks were grouped into the new Noranda, Camac, Horne, Dupuis and Reneault–Dufresnoy "formations" (McNicoll et al. 2014). However, the limits and extent of these "formations" are not mappable in the field, and the use of the lithostratigraphic term "formation" in a "time" context as applied by McNicoll et al. (2014) does not meet the criteria for "formation" as defined in the North American Stratigraphic Code (2005, 2021). Furthermore, the hybrid formations comprise lithostratigraphic formations with various ages, compositions, features and aerial extent. For example, their "Noranda formation" encompasses 28 informal lithostratigraphic formations previously defined through high-resolution mapping (de Rosen-Spence 1976; Gibson 1990; Monecke, Gibson and Goutier 2017).

At a larger scale, Ayer et al. (2005) and Thurston et al. (2008), divided the Blake River assemblage of the Abitibi greenstone belt into Lower and Upper Blake River parts, separated by a break in volcanism spanning *circa* 2701–2700 Ma. However, McNicoll et al. (2014), using a much more extensive geochronological database for Blake River volcanic and intrusive rocks in Ontario and Quebec, recognized the gap in volcanism at 2700–2698.5 Ma. As the gap in volcanism defined by McNicoll et al. (2014) is a better constrained subdivision of the entire Blake River assemblage, we will follow Schofield et al. (2021) and Schofield (2023), and subdivide the NVC into Upper and Lower Blake River groups. Thus, in this field guide, we retain usage of the historical lithostratigraphic formations and nomenclature and group these into Upper and Lower Blake River groups to facilitate discussion and comparison with the Blake River assemblage outside of Rouyn-Noranda and, in particular, with the Blake River assemblage in the Swayze area of the western Abitibi greenstone belt.

VOLCANOGENIC MASSIVE SULFIDE DEPOSITS

The VMS deposits of the Rouyn-Noranda District are associated with a bimodal succession of predominantly tholeiitic to transitional basaltic to basaltic andesitic lavas, with lesser volumes of FIII and FII rhyolitic domes, lavas and lesser volumes of FIII–FII rhyolitic to dacitic volcaniclastic rocks (Ludden, Gélinas and Trudel 1982; Lesher, Gibson and Campbell 1986; Barrie, Ludden and Green 1993; Kerr and Gibson 1993; Gibson and Kerr 1993; Hart, Gibson and Lesher 2004). Based on this lithological association and geochemical affinity, the VMS deposits fall within the bimodal mafic type of Franklin et al. (2005) and can be further subdivided into 2 predominant lithofacies types, flow and volcaniclastic, where the latter includes primary pyroclastic, and resedimented syneruptive deposits (Gibson, Morton and Hudak 1999; Gibson 2005; Franklin et al. 2005).

Of the 20 economic VMS deposits in the District, 18 of the deposits are hosted primarily by rhyolitic and basaltic-andesitic flows with lesser pyroclastic rocks (e.g., Corbet and Ansil; Gibson and Watkinson 1990; Gibson and Galley 2007). These deposits are characterized by well-defined, vertically extensive, pipe-like chlorite (inner) and lesser sericite (outer) alteration halos, and mound-shaped massive sulfide lenses that formed on the seafloor through successive processes of chimney collapse, brecciation and internal sulfide replacement during zone refining (Day 4 Stop 13; Lydon 1988; Franklin et al. 2005). Only the Horne and Bouchard–Hébert deposits fall within the volcaniclastic type, as they are hosted by primary and syneruptive pyroclastic rocks and lesser lava flows, domes (cryptodomes) and their associated

breccias (Kerr and Gibson 1993). They are characterized by broad zones of footwall alteration that appear semiconformable locally, but are discordant and composed principally of sericite and quartz (with intense silicification) with local, inner zones of discordant chlorite alteration (Day 4 Stop 3). The massive sulfide has a stratabound lens morphology and grew primarily in the subseafloor through processes of sulfide replacement and open-space filling (Kerr and Gibson 1993; Gibson and Kerr 1993; Krushnisky et al. 2020). Both the flow- and volcaniclastic-hosted deposits have a pronounced metal zonation characterized by a copper-rich core to the stringer zone and sulfide lens with a more zinc-rich fringe (Knuckey, Comba and Riverin 1982; Gibson and Watkinson 1990; Gibson 2005). Gold and silver are preferentially associated with either the copper-rich core or the zinc-rich fringe (Knuckey, Comba and Riverin 1982). For more detailed descriptions of the Rouyn-Noranda VMS deposits, their alteration and host rocks, the reader is referred to the extensive literature that exists on these deposits (Spence and de Rosen-Spence 1975; Boldy 1979; Riverin and Hodgson 1980; Franklin, Lydon and Sangster 1981; Knuckey, Comba and Riverin 1982; Gibson, Watkinson and Comba 1983; Gibson and Watkinson 1990; Gibson, Morton and Hudak 1999; Franklin et al. 2005; Gibson et al. 2007; McNicoll et al. 2014). Herein, we are most interested in the distribution of conventional and gold-rich VMS deposits within the NVC.

The distribution of VMS deposits, including those currently not economic, within the NVC is not uniform (Gibson and Kerr 1993; Gibson and Galley 2007; Jørgensen et al. 2022). From a temporal perspective, we argue that all of the VMS deposits formed during different stages of Lower part of the Blake River Group volcanism, which constructed the NVC and its subsidence structure(s). This is controversial, as McNicoll et al. (2014) placed all the VMS deposits in the Flavrian block (15 of 20 economic deposits in the NVC) within a new, Upper part of the Blake River, hybrid and informal "Noranda formation". This age assignment stems from a U/Pb zircon age of 2698.5±2 Ma for a coherent quartz-feldspar porphyritic rhyolite unit interpreted to be part of the lithostratigraphic Millenbach rhyolite formation of the Flavrian block (David et al. 2010). The contacts of this rhyolite are not exposed and it is uncertain if it represents an extrusive unit or an intrusion. This uncertainty in field relations for the age of *circa* 2698.5 Ma, its similarity in age to a quartz-feldspar porphyritic rhyolite intrusion in the Powell block (2698±0.9 Ma: Schofield et al. 2021) and the Dufresnoy gabbro in the Powell block (2697.9±0.8 Ma: McNicoll et al. 2014), and incongruency with previous lithostratigraphic correlations between the Flavrian and Powel blocks established by "walking formations" across the Beauchastel fault (e.g., de Rosen-Spence 1976; Lichtblau and Dimroth 1980; Dimroth et al. 1982; Gibson 1990), prompted Metal Earth to undertake 3 additional age determinations. These preliminary ages are provided by M.A. Hamilton, at the Jack Satterley Laboratory, University of Toronto, and include the first from drill core that intersected the mineralized and altered Millenbach quartz and feldspar porphyritic rhyolite that hosts to VMS ore at the Millenbach mine; a second of the Nuinsco rhyolite that conformably overlies the Amulet Andesite formation that, in turn, conformably overlies the Millenbach rhyolite formation; and a third from the Lower member of the Amulet Rhyolite formation that underlies the Millenbach Andesite and Millenbach rhyolite formations. Preliminary U/Pb zircon ages obtained for the Nuinsco, Millenbach and Lower Amulet rhyolites are Lower part of the Blake River group, with the Nuinsco rhyolite younger (*ca.* 2699 Ma) and, therefore, are consistent with its stratigraphic position above the Millenbach rhyolite (*ca.* 2701 Ma) and Amulet Lower member (2702 Ma) (M.A. Hamilton, University of Toronto, written communication, 2023). These new ages essentially negate an Upper part of the Blake River age and the "Noranda formation" and place volcanic strata of the Flavrian block firmly within the Lower part of the Blake River Group. The only Upper part of the Blake River Group strata traditionally placed within Rouyn-Noranda District occurs east of the Dalembert fault, which was interpreted to mark the east margin of the Noranda cauldron (Gibson 1990; Gibson and Watkinson 1990; Kerr and Gibson 1993; Gibson and Galley 2007). The Bouchard–Hébert VMS deposit (2698±1 Ma: Mortensen 1993) occurs within this Upper part of the Blake River Group succession, which extends southeastward to include the Upper part of the Blake River Group Doyon–Bousquet–LaRonde District. Consequently, the Bouchard–Hébert deposit and host strata may be more correctly assigned to the Upper part of the Blake River Group volcanic centre that hosts the Doyon–Bousquet–LaRonde District and, as such, is not discussed herein.

The pronounced south-to-north asymmetry in the variation in the number, grade, tonnage and gold content of VMS deposits within the NVC had been recognized (Gibson and Watkinson 1990; Kerr and Gibson 1993; Gibson and Kerr 1993). However, the quantification of these spatial variations, as well as spatial variations in host rock composition and intrusion density, has only recently been addressed and related to variations in district-scale crustal structures (Jørgensen et al. 2022; Figure 6). Using the distinct crustal blocks, Jørgensen et al. (2022) demonstrated that the Flavrian, Powell, and Horne blocks are characterized by higher metal content, density of structures, and proportion of felsic volcanic rocks and synvolcanic TTG intrusions. Furthermore, the Powell and Horne blocks contains the largest deposits, highest gold grade, and number of ounces (14 Moz of gold; *see* Figure 6). The geological observations were then integrated with a new ~50 km regional, deep seismic reflection profile centred on the Rouyn-Noranda District, a density cross-section and 3-D isosurface model produced from new and existing gravity data on a regional gravity grid, and a resistivity cross-section and 3-D isosurface resistivity model from new and existing broadband magnetotelluric (MT) data, all of which allowed for a whole-of-crust analysis and insights into the crustal architecture (Jørgensen et al. 2022). In cross-section along the seismic profile, the integration reveals an asymmetry in the geophysical features that corresponds to that observed in the surface geology (Figures 7A and 7B). Low seismic reflectivity extends from the surface to ~14–16 km depth across the southern part of the profile (S1 on Figure 7B), compared to ~6–8 km depth in the north (S2 on Figure 7B). Distinct density lows in the upper crust are more abundant in the southern part of the profile, compared to in the north (Figure 8). Low-resistivity areas (~10–100 Ω·m) in the upper ~1–2 km of the crust, are more prevalent in the southern part of the District compared to a relatively resistive north at similar depths (≥1000 Ω·m; Figure 9). These low-resistivity features in the south are connected by subvertical low-resistivity (≤50 Ω·m) features that transects an otherwise relatively uniform high-resistivity upper crustal signature across the District that extends down to ~14 km (Jørgensen et al. 2022). The transition to a lower resistivity regime (<1000 Ω·m), therefore, corresponds to the brittle-ductile transition zone (~10–15 km), but the mid- to lower crustal signature is not uniform across the District. In the southern part of the District, the mid- to lower crust is characterized by a ~35 km wide, low-resistivity feature (~50–100 Ω·m), whereas the same area in the north is relatively resistive (~500–1000 Ω·m; *see* Figure 9). The connectivity of the low-resistivity features in the southern part of the District is highlighted in a longitudinal section along the Horne Creek fault, where a subvertical low-resistivity feature transects ~20 km of crust and connects a low-resistivity zone near the surface with another in the mid- to lower crust (Figure 10). In the 3-D MT model of the District, low-resistivity isosurfaces define subvertical pipe-like features that, at depth, connect to a broad subhorizontal low-resistivity volume, itself possibly extending into the upper mantle (Jørgensen et al. 2022; Figure 11). On average, VMS deposits are within ~6 km to the nearest 100 Ω·m contour when calculating the shortest horizontal distance at several depth slices in the resistivity model to a depth of ~40 km. Notably, the 2 gold-rich VMS deposits are the only deposits that are consistently located within a 100 Ω·m contour at the ~1–2 km depth interval (Jørgensen et al. 2022). The coinciding location of deposits, synvolcanic structures and subvertical low-resistivity MT features promotes an interpretation where magmas and metalliferous fluids located in deeper crustal to mantle sources were brought to upper crustal sinks via transcrustal synvolcanic structures (Jørgensen et al. 2022). The magmatic centre is localized to these major structures as indicated by the greater volume of synvolcanic intrusions observed at surface and corroborated by the seismic and gravity data. Thus, the clustering of deposits in the District is controlled by this crustal architecture where a transcrustal structure and its splays localized and optimized magmatic and ore forming processes (Jørgensen et al. 2022). Furthermore, it indicates that the VMS mineralization is a near-surface expression of a much larger vertically extensive but areally localized, deep crustal to mantle, magmatic-hydrothermal system, rather than a shallow, subseafloor (~<5 km) convective, modified seawater-dominated hydrothermal system which is often the context given for VMS formation. The Horne Creek fault, defining the southern limit of the magmatic centre, represents the optimal location for a magmatic input of metals to the VMS system and may explain why the only 2 gold-rich deposits in the Rouyn-Noranda District are juxtaposed with this structure.

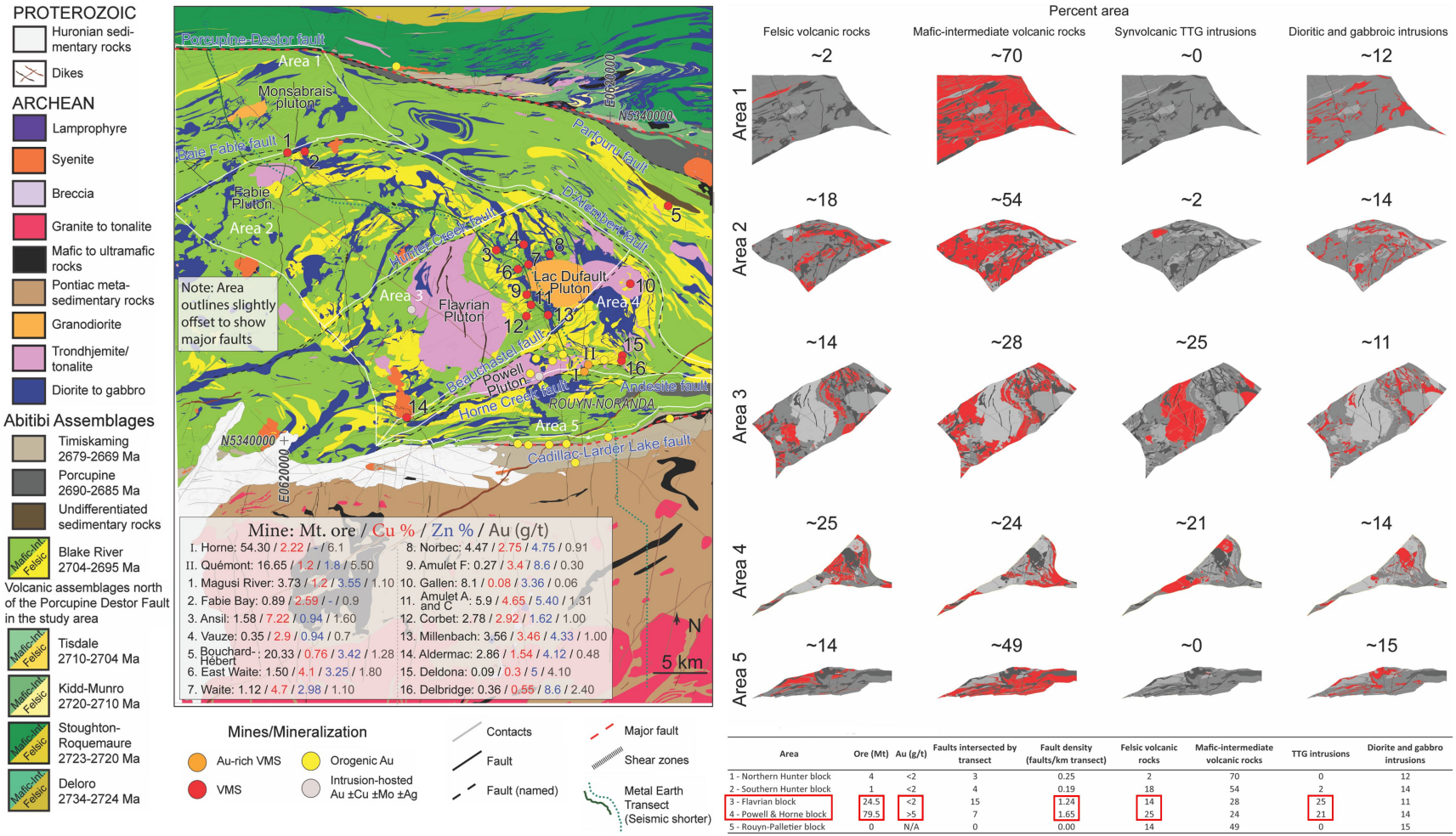

Area	Ore (Mt)	Au (g/t)	Faults intersected by transect	Fault density (faults/km transect)	Felsic volcanic rocks	Mafic-intermediate volcanic rocks	TTG intrusions	Dioritic and gabbro intrusions
1 - Northern Hunter block	4	<2	3	0.25	2	70	0	12
2 - Southern Hunter block	1	<2	4	0.19	18	54	2	14
3 - Flavrian block	24.5	<2	15	1.24	14	28	25	11
4 - Powell & Horne block	79.5	>5	7	1.65	25	24	21	14
5 - Rouyn-Pelletier block	0	N/A	0	0.00	14	49	0	15

Figure 6. Surface area analyses performed in 5 different areas along the Metal Earth Rouyn-Noranda Transect to compare relative areas of felsic metavolcanic rocks, mafic-intermediate metavolcanic rocks, synvolcanic trondhjemite-tonalite-granodiorite (TTG) intrusions and diorite-gabbro intrusions (*modified from* Jørgensen et al. 2022). Areas 1 and 2 are the Hunter block divided by the Baie Fabie fault into northern and southern portions; Area 3 is equivalent to the Flavrian block; Area 4 is the Powell and Horne blocks combined; and Area 5 is the Rouyn-Pelletier block. Figure © 2022 T.R.C. Jørgensen, H.L. Gibson, E.A. Roots, R. Vayavur, G.J. Hill, D.B. Snyder and M. Naghizadeh. Published by Springer Nature Limited. doi.org/10.1038/s41598-022-18836-y. An open access article distributed under the terms of the Creative Commons CC-BY 4.0 license. This figure is an excerpt *from* Jørgensen et al. (2022, Figure 1) and has been modified as follows: the geological legend has been re-arranged, and the surface analyses and table have been added.

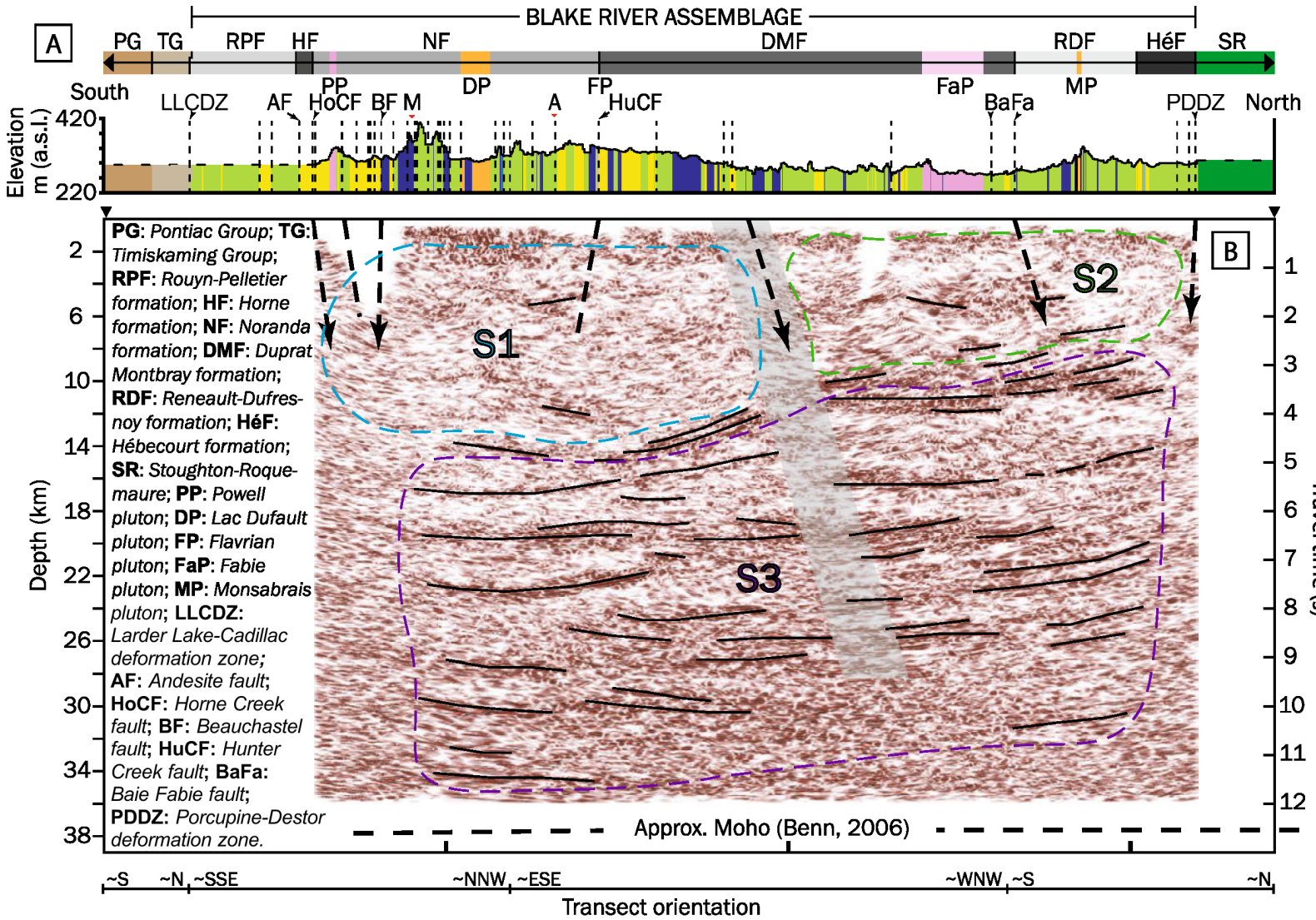

Figure 7. A) Geological and **B)** seismic cross sections along the Metal Earth Rouyn-Noranda Transect with interpreted subhorizontal reflectors (solid black lines) and subvertical faults (dashed black lines) (*from* Jørgensen et al. 2022); *see* Figure 6 for surface geology legend. Figure © 2022 T.R.C. Jørgensen, H.L. Gibson, E.A. Roots, R. Vayavur, G.J. Hill, D.B. Snyder and M. Naghizadeh. Published by Springer Nature Limited. doi.org/10.1038/s41598-022-18836-y. An open access article distributed under the terms of the Creative Commons CC-BY 4.0 license. This figure is an excerpt *from* Jørgensen et al. (2022, Figure 2): panels C, D and E were removed from the original figure, and 2 abbreviations and definitions were changed.

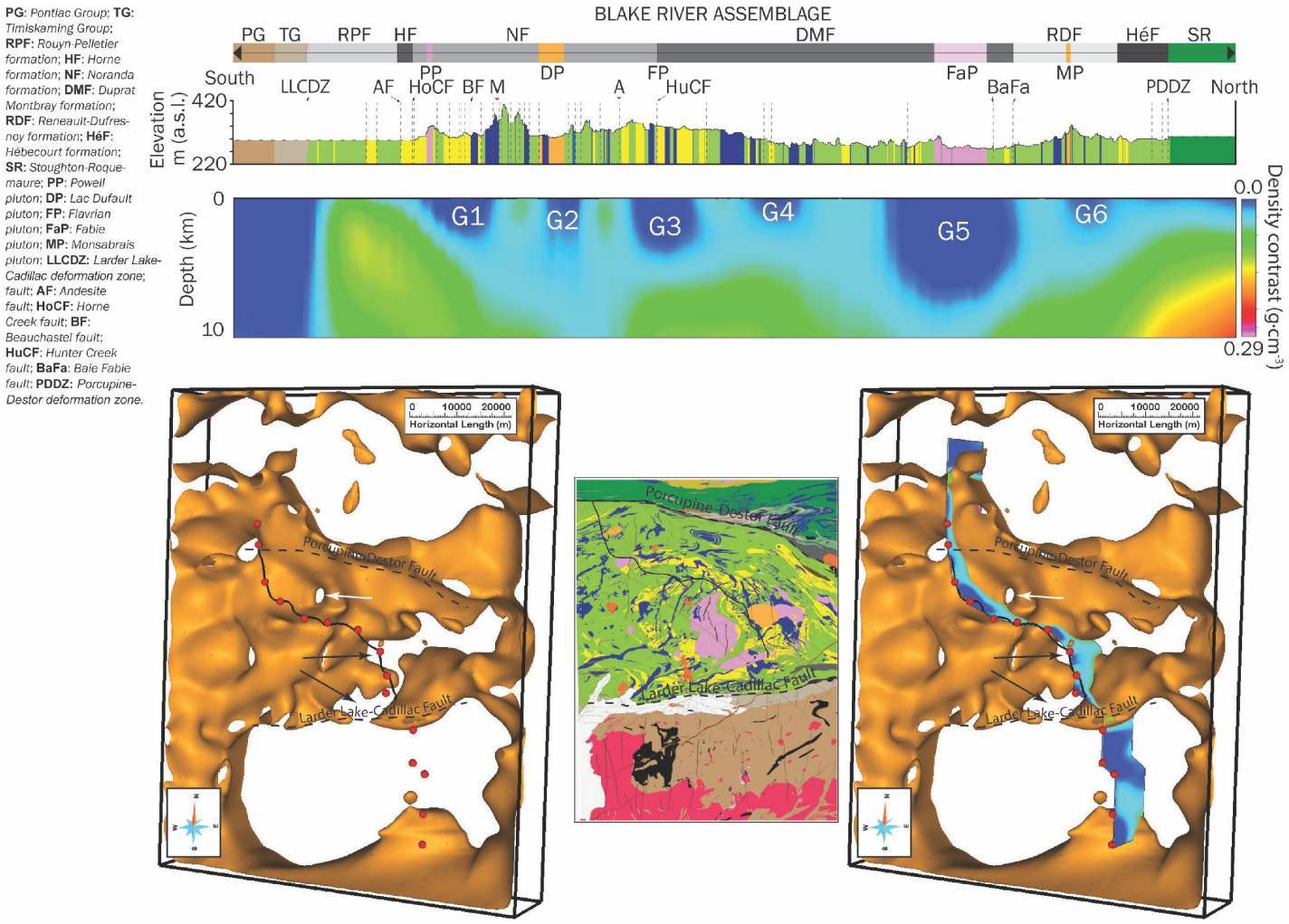

Figure 8. Surface geology cross section (*see* Figure 6 for legend) shown above a density cross section along the Metal Earth Rouyn-Noranda Transect; simplified geological map shown in centre below density section (*from* Jørgensen et al. 2022). Note that the relatively low-density contrast features G1 to G6, with the exception of G4, coincide with the location of outcropping synvolcanic intrusions. Lower left is a 3-D isosurface of high density (>0.1 density value) region overlain with MT survey locations and seismic survey line. Lower right is a 3-D isosurface of high density (>0.1 density value) region overlain with the density cross section. Black and white arrows indicate low density regions along the Rouyn-Noranda transect between the major faults. Figure © 2022 T.R.C. Jørgensen, H.L. Gibson, E.A. Roots, R. Vayavur, G.J. Hill, D.B. Snyder and M. Naghizadeh. Published by Springer Nature Limited. doi.org/10.1038/s41598-022-18836-y. An open access article distributed under the terms of the Creative Commons CC-BY 4.0 license. This figure is excerpted *from* Jørgensen et al. (2022, Figures 1 and 2) and has been modified as follows: from Figure 1, a simplified base geology map was used; and from Figure 2, panels B, D and E were removed from the original figure; the list of geological abbreviations from panel B was retained, with changes to 2 abbreviations and definitions.

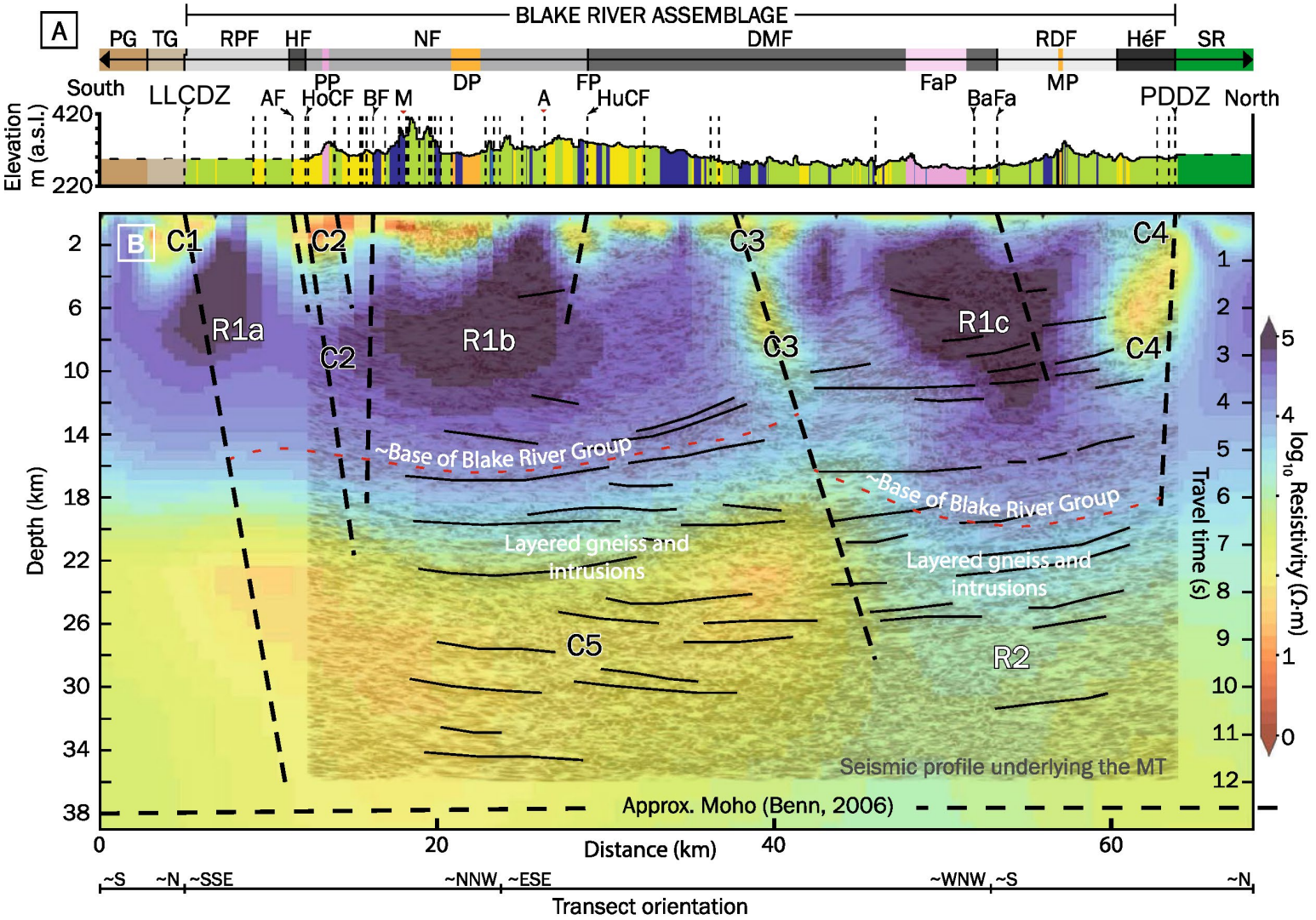

Figure 9. **A)** Geological and **B)** magnetotelluric (MT) cross sections along the Metal Earth Rouyn-Noranda Transect with interpreted subhorizontal reflectors (solid black lines) and subvertical faults (dashed black lines) (*from* Jørgensen et al. 2022); *see* Figures 6 and 7 for surface geology and abbreviation legends. Relatively low-resistivity features are indicated by C1 to C5; high-resistivity features are indicated by R1. This figure is an excerpt *from* Jørgensen et al. (2022, Figure 2) and was modified as follows: panels B, C and E were removed from the original figure, and 2 labels were changed.

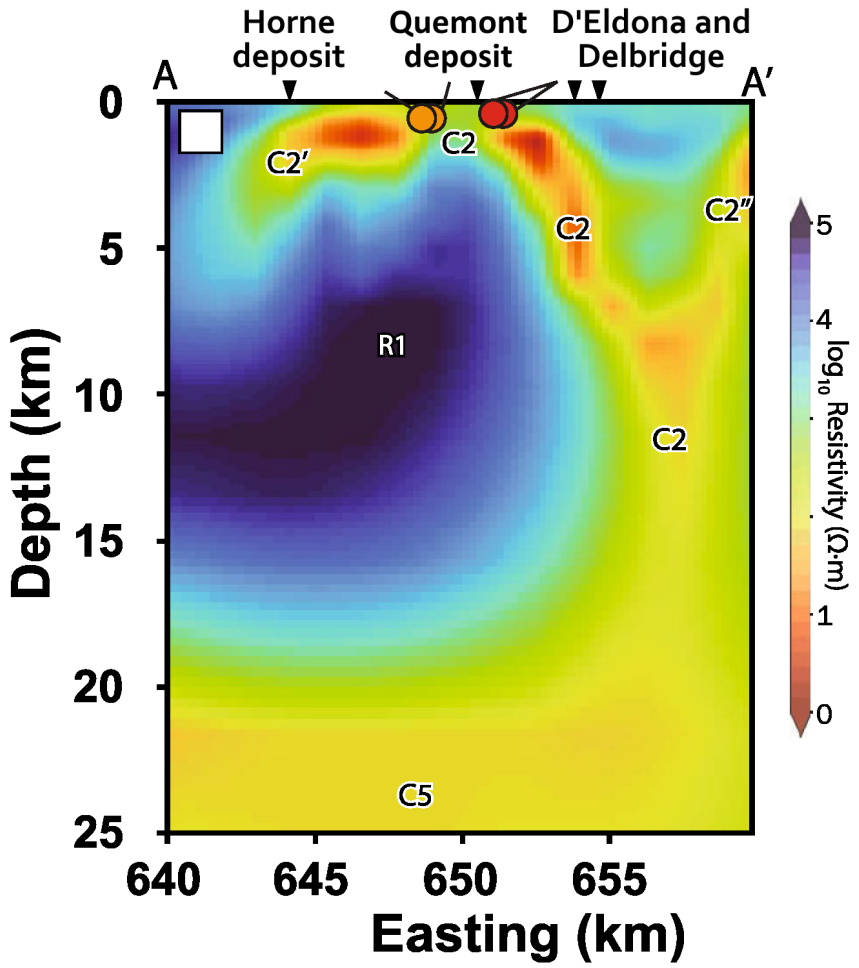

Figure 10. A magnetotelluric (MT) longitudinal section along the Horne Creek fault (*from* Jørgensen et al. 2022). Relatively low-resistivity features are indicated by C2, C2′, C2″ and C5; an area of high-resistivity is indicated by R1. Figure © 2022 T.R.C. Jørgensen, H.L. Gibson, E.A. Roots, R. Vayavur, G.J. Hill, D.B. Snyder and M. Naghizadeh. Published by Springer Nature Limited. doi.org/10.1038/s41598-022-18836-y. An open access article distributed under the terms of the Creative Commons CC-BY 4.0 license. This figure is an excerpt *from* Jørgensen et al. (2022, Figure 3) and has been modified as follows: panels A, B, C and D were removed from the original figure, as was the log resistivity colour scale, and labels modified.

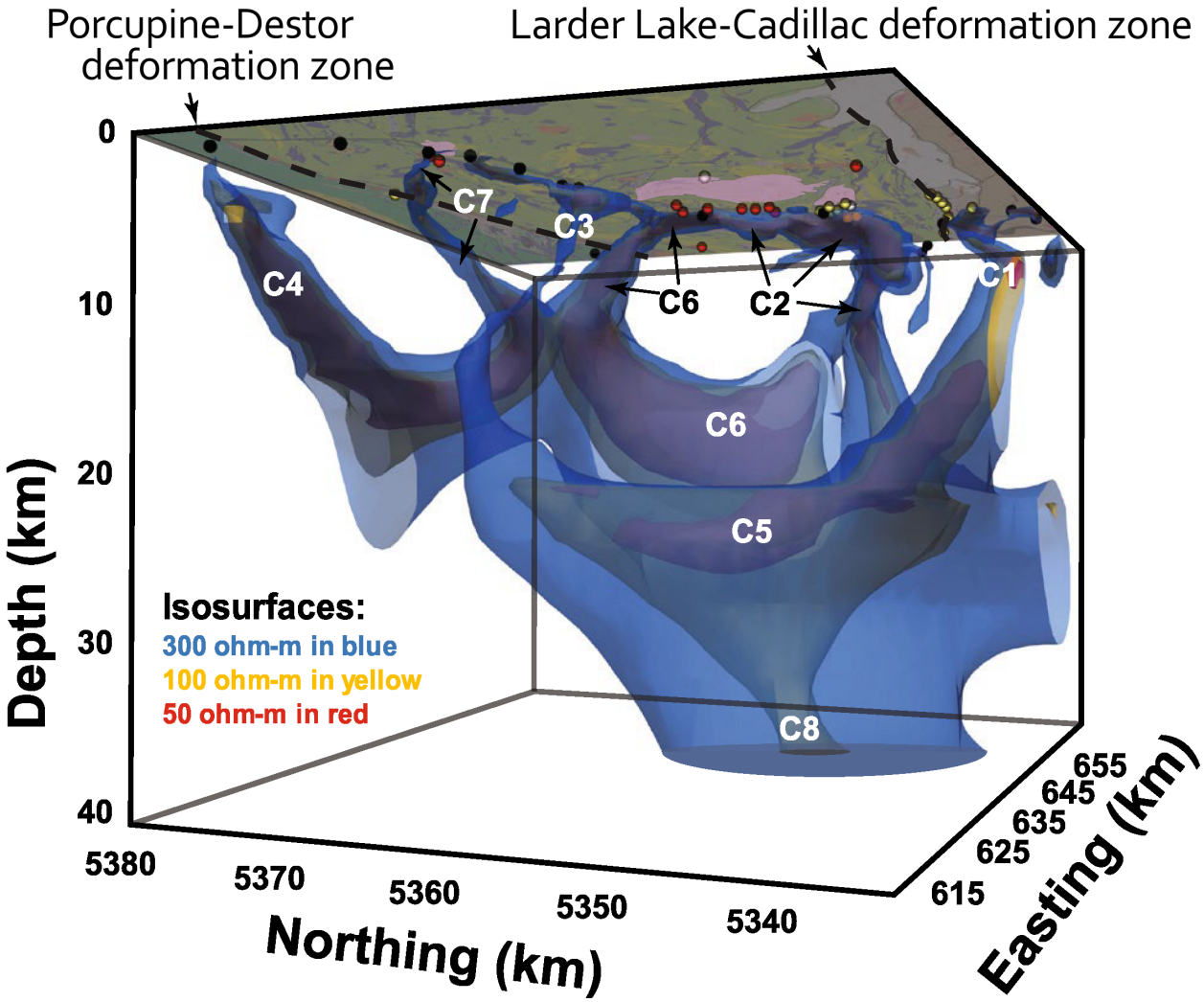

Figure 11. A 3-D magnetotelluric (MT) model with surface geology (*see* Figure 6) (*from* Jørgensen et al. 2022). Labels C1 to C8 indicate significant low-resistivity features; view up is toward the northeast. Figure © 2022 T.R.C. Jørgensen, H.L. Gibson, E.A. Roots, R. Vayavur, G.J. Hill, D.B. Snyder and M. Naghizadeh. Published by Springer Nature Limited. doi.org/10.1038/s41598-022-18836-y. An open access article distributed under the terms of the Creative Commons CC-BY 4.0 license. This figure is an excerpt *from* Jørgensen et al. (2022, Figure 4) and has been modified as follows: labels were changed or removed.

GOLD DEPOSITS

Volcanogenic massive sulfide deposits account for ~13% (~1190 t) of the gold in the Abitibi greenstone belt (AGB). Because gold often represents the primary commodity in these deposits (Dubé and Mercier-Langevin 2020), the AGB VMS deposits were featured in a recent book on the world's major gold deposits published by the Society of Economic Geologists. The Blake River Group is responsible for ~90% of the VMS-related gold in the AGB to which the Horne and Quemont deposits (~440 t Au) of the Rouyn-Noranda District make a considerable contribution (Mercier-Langevin et al. 2014). As such, the gold endowment in the Rouyn-Noranda District is predominantly VMS related, in contrast to the AGB as a whole where orogenic quartz-carbonate vein deposits represent the largest source of gold (>5925 t Au; Dubé and Mercier-Langevin 2020). Nonetheless, the Rouyn-Noranda District hosts 19 small, orogenic gold deposits, all of which are orogenic quartz-carbonate vein deposits (e.g., Day 3 Stop 5), except for the Chadbourne deposit (Day 4 Stop 2). The orogenic vein deposits have been subdivided into 3 types based

on their spatial relationship to the LLCDZ and morphology. The first type (14 deposits) includes structurally controlled, disseminated and quartz-vein lode deposits associated with the LLCDZ and its parallel to subparallel splays (e.g., Day 3 Stop 6; Robert 1990; Gauthier et al. 1990). In the Rouyn-Noranda District, the LLCDZ is steeply dipping toward the north along a narrow interval of komatiitic volcanic rocks of the Piché Group (Kidd–Munro assemblage) bounded on the sides by clastic sedimentary rocks of the Timiskaming Group (Poulsen 2017a). In the hanging wall, the Timiskaming Group is dominantly facing toward the south and unconformably overlies volcanic rocks of the Blake River Group (Poulsen 2017a). The Timiskaming Group south of the deformation zone are believed to be broadly correlative with its northern counterpart and overlie graywacke of Pontiac Group (Poulsen 2017a). The gold-hosting quartz-carbonate veins occur within metavolcanic rocks of the Lower part of the Blake River Group, ultramafic rocks of the Piché Group, and metasedimentary rocks of the Timiskaming Group, where they are spatially related to either megascopic Z-folds that refold earlier east-trending shears or to areas of intersection between east-trending shears and later northeast-striking faults (Gauthier et al. 1990). The second type (5 deposits) is hosted by northeast-trending, shear zone-hosted quartz veins within phases of the subvolcanic FPIC (Day 4 Stops 4 and 5; Robert 1990; Riverin, Bernard and Boily 1990; Carrier et al. 2000). The third type (Chadbourne deposit) is hosted by a vertical, diatreme breccia pipe where the gold occurs, along with quartz, pyrite and siderite, within the breccia matrix (Day 4 Stop 2; Walker and Cregheur 1982). The breccia pipe is proximal to late syenite dikes and a plug (Poulsen 2017a).

INTRUSION-RELATED DEPOSITS

Two types of intrusion-related mineralization occur within the Rouyn-Noranda District. The Don-Rouyn copper-molybdenum deposit is hosted within an early trondhjemite phase of the FPIC, where it is crosscut by a late phase tonalitic dike swarm. The deposit is interpreted to be an Archean porphyry deposit, and consists of a bornite-pyrite-rich strongly silicified core moving outward to a chalcopyrite-pyrite vein stockwork with biotite alteration, which collectively constitutes a mineral resource of approximately 36 Mt with an average grade of 0.15% Cu, with anomalous molybdenum and gold (Kotila 1975; Goldie, Kotila and Seward 1979; Jébrak et al. 1997; Pelletier and Jébrak 1994).

Along the western margin of the FPIC, a swarm of quartz diorite and rhyolite dikes in Lower Blake River strata hosts numerous pyrite-galena-gold and pyrite-magnetite vein occurrences (Kennedy 1985; Richard 1998). This vein-dike system terminates at its northern end at the St. Jude copper-molybdenum-enriched, magmatic hydrothermal breccia pipe (Kennedy 1985; Carrier et al. 2000). An intra-mineralization aplite dike associated with this mineralizing phase has a U/Pb zircon age of 2697±2 Ma (Galley and van Breemen 2002). This Upper Blake River age is similar to that of the youngest trondhjemite phase in the core of the FPIC, and to the Joliet Breccia (Day 4 Stop 8; Schofield et al. 2021), indicating superimposition of Upper part of the Blake River magmatism on Lower part of the Blake River intrusions and strata.

QUARTZ-SULFIDE COPPER-ZINC-SILVER VEINS

Quartz-sulfide copper-zinc-silver veins have been recognized in Lower part of the Blake River strata of the Flavrian (Day 4 Stop 6; e.g., C-Shaft and McDougall veins: Gibson, Watkinson and Comba 1983; Zubowski 2011) and Powell blocks (e.g., F-Shaft vein: Schofield et al., in press). None of the veins have been mined. The veins are symmetrically altered, with vein proximal chlorite (iron-chlorite) alteration grading outward into thin zones of sericite alteration that display compositional variations identical to that observed in discordant VMS footwall chlorite-sericite alteration zones (Gibson, Watkinson and Comba 1983; Zubowski 2011; Schofield et al. in press). Schofield et al. (in press) have shown that quartz-sulfide

copper-zinc-silver veins in the Powell block are characterized by $\delta^{18}O_{quartz}$ values of 8.5±0.8‰, reflecting $\delta^{18}O_{fluid}$ compositions of −0.4‰ to 3.1‰ (250–350°C), typical of Archean seawater, with a proximal iron-rich chlorite alteration and marginal spotted sericite-chlorite alteration having whole rock $\delta^{18}O$ values of 2.9–5.9‰, which are similar values to those documented by Cathles (1993) for VMS chlorite and sericite footwall alteration zones. The quartz-sulfide copper-zinc-silver veins are interpreted to represent deeper crustal level VMS up-flow zones, which may have produced VMS deposits located at a higher stratigraphic level (Gibson, Watkinson and Comba 1983; Zubowski 2011; Schofield et al. in press). Schofield et al. (in press) have shown that quartz-sulfide copper-zinc-silver veins in the Powell block are Upper part of the Blake River in age (*ca.* 2697 Ma) and indicate the local superposition of an Upper part of the Blake River VMS system on older Lower part of the Blake River Group strata; there are no age constraints for identical veins of the Flavrian block.

Road Logs: Swayze Area

Note: Caution should be taken when parking vehicles on the shoulders of the road or highways and when examining outcrops located along the field trip route. All UTM co-ordinates are provided using NAD83 in Zone 17.

DAY 1. SWAYZE AREA, BLAKE RIVER ASSEMBLAGE: BASE METAL DAY

Start location

The start of the Swayze area trip is the front parking lot of Watershed Den. The camp is situated about 1 km west of Highway 144 on the Sultan Industrial Road located approximately halfway between Timmins and Sudbury (*see* Figures 1 and 2). Turn west from the Watershed gas station, then turn left at the Watershed Den sign and continue 0.5 km south.

Stop 1. Mortimer Magnan jasper banded iron formation

UTM 382255E 5289496N

Potential hazards:

- Steep and/or slippery slopes; loose rocks
- Stay on marked trail

The banded iron formation (BIF) is well exposed on the Mortimer Magnan jasper property about 2 km along Dore Road from site #2 and 4-5 km west off the Dore Road. It is ~50 m in thickness and can be traced ~80–100 m along strike (Photo 1). It is composed of alternating micro- and meso-bands of jasper, chert and magnetite. Many small brittle thrust faults are evident throughout. The BIF represents an important stratigraphic marker horizon in the Swayze area (and the western extension of the Abitibi greenstone belt in general). It has been mapped by Heather (2001) as the Woman River formation overlying the Marion Group (2735–2725 Ma, equivalent to the Deloro assemblage), but no age determination supports that inference. However, the Jasper BIF is interbedded with a lapilli-tuff unit: a recent age determination reveals a slightly younger depositional age of *circa* 2722 Ma (preliminary age; J.H. Marsh, Laurentian University, personal communication, 2018) for the BIF–volcanic sequence (correlative to the Stoughton–Roquemaure assemblage). As the deposition of BIF represents a long period of submarine hydrothermal activity, the BIF represents an important gap in the volcanic stratigraphy increasing the potential for syngenetic mineralization. This BIF can possibly be correlated with other similar BIFs in the Swayze area and in the Abitibi greenstone belt, helping constrain the overall stratigraphy in the Abitibi greenstone belt. The younging direction for the sequence is likely to the south as a result of younging indicators in the volcanic rocks found both north and south of the BIF. Beside the lapilli-tuff, the adjacent volcanic rocks also contain tuff and tuff-breccia.

Photo 1. Overhead drone image of the Mortimer Magnan jasper BIF in sharp contact with volcanic tuff (dashed line) (Day 1 Stop 1). Looking down. Top of photograph toward the southwest. Photo by T.P. Gemmell.

Stop 2. Pillow breccia of the Lower part of the Blake River assemblage

UTM 385730E 5291668N

Potential hazards:

- Steep and/or slippery slopes; loose rocks
- Busy road with high speed traffic; stay off road shoulder and remain away from parked vehicles if possible; high-visibility vests required

The Pillow breccia outcrop is only ~550 m off the Dore Road. Turn east at the second right at UTM 385223E 5291405N. Drive to the end where there is a good area to turn around.

These pillow breccias represent the lower, more mafic part, of the Lower part of the Blake River assemblage (Photo 2). The breccias are sparsely observed; the majority of the metavolcanic rocks are pillowed or massive flows.

Photo 2. Pillow breccia fragments in the Lower part of the Blake River assemblage (Day 1 Stop 2). Photo by T.P. Gemmell.

Stop 3. Massive sulfide lens within felsic metavolcanic rocks near the top of the Lower part of the Blake River assemblage

UTM 378634E 5293484N

Potential hazards:

- Steep and/or slippery slopes; loose rocks
- Busy road with high speed traffic; stay off road shoulder and remain away from parked vehicles if possible; high-visibility vests required
- Stay on marked trail

The outcrop is within ~50 m of an old sandy road with a turnaround area at the end of the road. Turn left (west) off the Dore Road at UTM 379782E 5294109N, drive ~1.2 km, then turn left again (south, UTM 378629E 5293719N). Stop alongside the road ~220 m (UTM 378674E 5293503N) from the last turn and then walk ~50 m into the bush on the west side of the road to the outcrop.

The outcrop (Photo 3) represents the only known inter-assemblage massive sulfide occurrence in the Swayze area. The mineralization is mostly pyrrhotite and pyrite with trace amounts of copper and zinc and appears to overprint a felsic to intermediate volcaniclastic rock. A massive feldspar-phyric dacite, located ~80 m to the north, was sampled; an age determination of 2700.3±1.9 Ma (Kamo 2018) places this unit near the top of the Lower part of the Blake River assemblage.

Photo 3. Massive sulfide lens in a felsic volcaniclastic rock in the upper section of the Lower part of the Blake River assemblage (Day 1 Stop 3). Photo by T.P. Gemmell.

Stop 4. Komatiite and felsic metavolcanic rocks on “Spinifelsic” road

UTM 375931E 5293484N

Potential hazards:

- Steep and/or slippery slopes; loose rocks
- Busy road with high speed traffic; stay off road shoulder and remain away from parked vehicles if possible; high-visibility vests required
- Stay on marked trail

The outcrops are located along a new logging road branching off the Swayze Road. Drive along the Dore Road; at UTM 379784E 5294249N, keep to the left onto the Swayze Road (no sign). After approximately 4 km, at UTM 375934E 5295224N, turn left onto a new logging road (locally named “Spinifelsic” road). Remain on this main road and, after approximately 1 km, at a fork at UTM 375917E 5294170N, keep to the right. The first substop is ~130 m past the turn and the second substop is at the end of the road.

The komatiites have been recently exposed and exhibit classic “elephant-skin” appearance with abundant spinifex textures both in the extrusive rocks and the sills that cut the extrusive rocks (Photo 4). At the end of the road, felsic tuffs (Photo 5) to tuff-breccias occur in contact with quartz-phyric tuffs or porphyries. A distinct quartz-phyric felsic unit is also in contact with ultramafic rocks, although the exact nature of the contact relationship is currently unknown. These rocks are presumably the lower section of the Upper part of the Blake River assemblage, continuing down from the east-northeast.

Photo 4. Komatiite exhibiting spinifex texture (Day 1 Stop 4) (Brunton compass for scale is 22 cm long). Photo by T.P. Gemmell.

Photo 5. Felsic tuff with alternating light and dark beds (Day 1 Stop 4) (Brunton compass for scale is 22 cm long). Photo by T.P. Gemmell.

Stop 5. Mega-breccia at Kenty Lake

UTM 378199E 5297357N

Potential hazards:

- Steep and/or slippery slopes; loose rocks
- Busy road with high speed traffic; stay off road shoulder and remain away from parked vehicles if possible; high-visibility vests required
- Stay on marked trail

The outcrop is along a side road off the old Dore Road, but access is better by driving along Dore Road and turning left at UTM 381521 5298721. After 1.3 km, park the vehicles at a large area where the road splits into 2 roads. Then walk approximately 1 km to the outcrop that can found along the left side of the road.

The mega-breccia outcrop is located in the central part of a large (~10 by 3 km) east-striking domain dominated by metavolcanic rock, volcaniclastic rock and likely synvolcanic porphyries (correlative to the Porcupine assemblage and, more specifically, the formation metavolcanic rocks around the Timmins gold camp). These Porcupine assemblage-age (*ca.* 2690 Ma) igneous rocks are deposited on top of the Blake River metavolcanic rocks where they now comprise the inner part of the Blake River syncline. The outcrop represents an extraordinary breccia containing chaotically distributed fragments of up to 1 m in size (Photo 6). Some of these fragments have fabric developed that indicates deformation prior to rip-up and deposition. Whether this breccia is sedimentary or volcanic in origin is currently unknown. An age determination of an adjacent volcaniclastic unit yielded an age of *circa* 2690 Ma (preliminary age: M.A. Hamilton, University of Toronto, personal communication, 2019). The breccia only consists of few types of fragments that could indicate a very local source. The unit is partly traceable for at least 1.5 km toward the east-southeast.

Photo 6. The Porcupine-age mega-breccia at Kenty Lake showing multiple sized fragments (Day 1 Stop 5) (pen for scale is 14 cm long). Photo by T.P. Gemmell.

Stop 6. Felsic to intermediate volcaniclastic rocks from the upper section of the Upper part of the Blake River assemblage

UTM 382255E 5289496N

Potential hazards:

- Steep and/or slippery slopes; loose rocks
- Busy road with high-speed traffic; stay off road shoulder and remain away from parked vehicles if possible; high-visibility vests required
- Stay on marked trail

The outcrop is along a discontinued side road off the Dore Road. Stop and park at UTM 381826E 5297343N on the left side of the road. It is an ~600 m easy walk (~10 minutes) to the stripped outcrop along the old side road (UTM 381362E 5296876N).

The outcrop is a large stripped area that shows both tuffaceous and volcaniclastic facies of the upper section of the Upper part of the Blake River assemblage (Photo 7). It is also important to note the presence of massive sulfide fragments within the volcaniclastic rocks (*see* Photo 7). The metavolcanic rocks are also in contact with a quartz-feldspar porphyry intrusion along a small deformation zone.

Photo 7. Upper portion of the Upper part of the Blake River assemblage felsic to intermediate volcaniclastic rocks with massive sulfide fragments (Day 1 Stop 6) (hammer for scale is 22 cm long). Photo by T.P. Gemmell.

Stop 7. Felsic to intermediate tuffaceous rocks overlying Blake River assemblage

UTM 381532E 5298713N

Potential hazards:

- Steep and/or slippery slopes; loose rocks
- Busy road with high-speed traffic; stay off road shoulder and remain away from parked vehicles if possible; high-visibility vests required

Drive along Dore Road, park on the left (west) side of the road at UTM 381532E 5298713N; walk carefully across the road to the small outcrop.

The outcrop, located on the southeastern side of Dore Road, represents what is inferred to be the youngest observed felsic volcanism in the Swayze area. The outcrop exhibits episodic felsic tuffs with sparse lapillis, as well as more low-energy muddy millimetre-scale laminations (Photo 8).

Photo 8. Felsic tuff unit interpreted to be younger than the Blake River assemblage (Day 1 Stop 7) (Brunton compass for scale is 22 cm long). Photo by T.P. Gemmell.

Stop 8. Intermediate to mafic pillowed flows of the lower section of the Upper part of the Blake River assemblage

UTM 384227E 5300959N

Potential hazards:

- Steep and/or slippery slopes; loose rocks
- Busy road with high-speed traffic; stay off road shoulder and remain away from parked vehicles if possible; high-visibility vests required

Drive along Dore Road. Turn right (east) at UTM 382062E 5300664N onto a secondary logging road. Continue approximately 2.2 km along this road, keep left at the fork at UTM 384263E 5300874N. The outcrop is just past the fork on the left.

This outcrop is a magnificent exposure of amoeboid to almost mattress pillowed flows that are interpreted to belong to the lower section of the Upper part of the Blake River assemblage (Photo 9). They exhibit vesicles and alteration around the edges of the pillow and have 1–3 cm selvages. Pillows on this outcrop young to the south and represent the northern limb of the central Swayze Blake River assemblage volcanic rocks.

Photo 9. South-younging intermediate to mafic pillowed flow from the lower section of the Upper part of the Blake River assemblage (Day 1 Stop 8) (Brunton compass for scale is 22 cm long). Photo by T.P. Gemmell.

Stop 9 (alternative). Komatiites

UTM 380951E 5294995N

Potential hazards:

- Steep and/or slippery slopes; loose rocks
- Busy road with high-speed traffic; stay off road shoulder and remain away from parked vehicles if possible; high-visibility vests required
- Vertical outcrops with loose debris; rockfall hazard, hard hats must be worn
- Stay on marked trail

Along the Dore Road, black komatiites stand out as a 2–3 m high and 10 m wide exposures on each side of the road. They exhibit well-developed spinifex texture throughout with only minor alteration, such as serpentinization. On the northern side, pillowed komatiitic basalts are observed, with a north-younging direction. Furthermore, hyaloclastites can be seen in the south portion of the outcrop; this, in addition to the pillows, indicates a submarine emplacement for these ultramafic volcanic flows. This is important because, in other parts of the Metal Earth Abitibi (Swayze) Transect, it is still uncertain whether the komatiites are sills or part of the extrusive stratigraphy (e.g., the komatiites within the Pontiac group turbidite sediments in the Noranda area). The komatiites here are equivalent to the *circa* 2700 Ma Blake River assemblage (or belong to the Swayze group Newton formation using Heather (2001) nomenclature) and are interpreted as being part of the volcanic stratigraphy. As for BIF, komatiites are very important stratigraphic markers and their emplacement history and depositional environment are crucial in understanding the stratigraphy in the Swayze area and, more broadly, in the regional correlation in the Abitibi greenstone belt.

DAY 2. SWAYZE AREA, BLAKE RIVER ASSEMBLAGE: GOLD DAY

Start location

The start of the Swayze area Day 2 is the front parking lot of Watershed Den. The camp is situated about 1 km west of Highway 144 on the Sultan Industrial Road (*see* Figure 3) located approximately halfway between Timmins and Sudbury. Turn west from the Watershed gas station, then turn left at the Watershed Den sign and continue 0.5 km south.

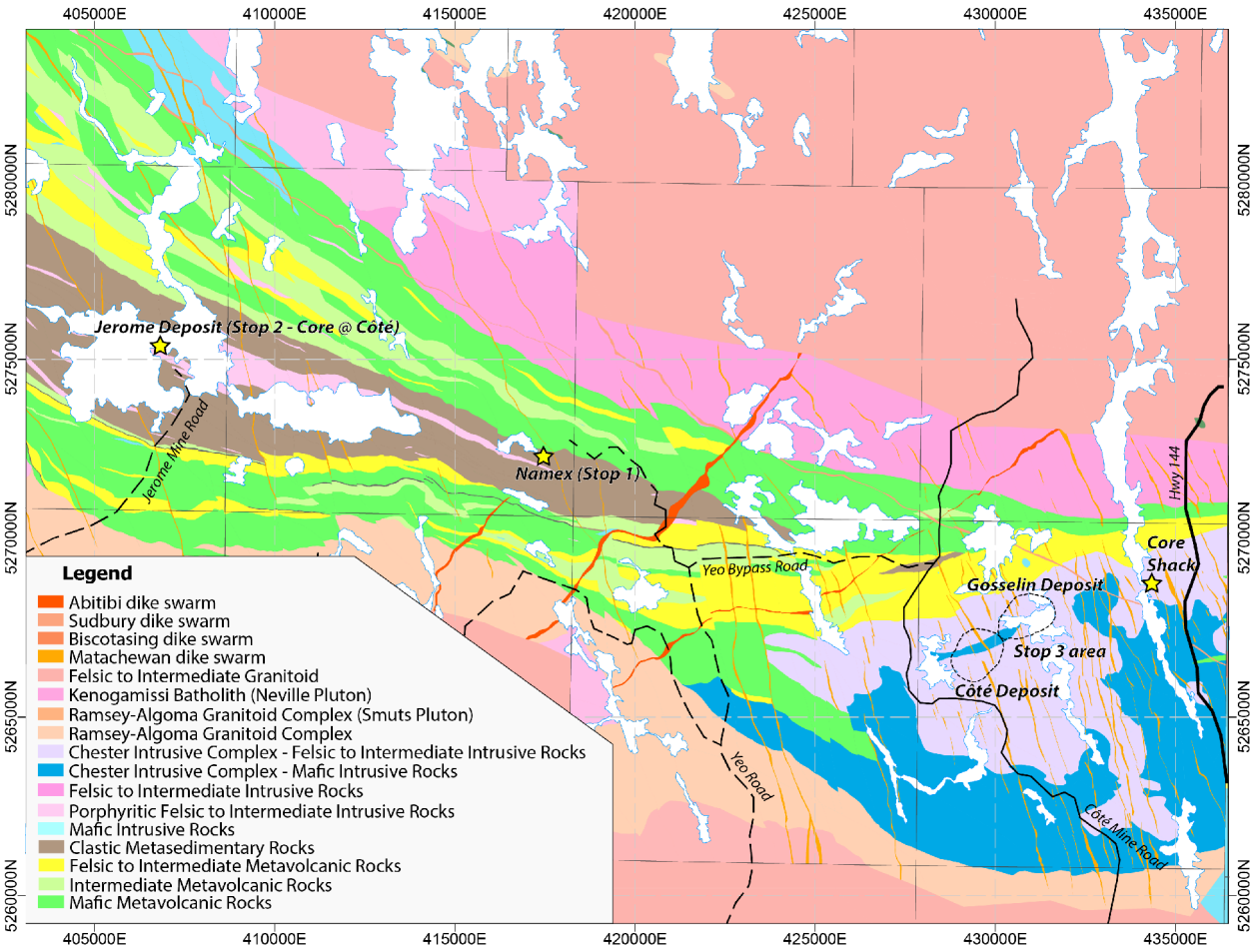

Figure 12. Geological setting and location of Swayze area Day 2 field trip stops (geology *from* Gemmell and MacDonald (2017) and *from* MacDonald, Bisaillon and Gemmell (2018)). All UTM co-ordinates provided using NAD83 in Zone 17.

Stop 1. Namex deposit (also referred to as Huffman Lake property)

UTM 416226E 5272334N

Potential hazards:

- Some of these outcrops are near old mining equipment and buildings. Please refrain from going in buildings or going near old equipment.
- The outcrops can become quite slippery when wet or damp and having small vegetation that may be a tripping hazard. Care should be taken at all times on the outcrops to avoid slips and trips.
- The Namex deposit outcrops, particularly in the western area, are near trails containing holes and long grass. These are also particularly dangerous tripping hazards.

The Namex gold-silver deposit, or Huffman Lake property, (Figures 3 and 12) is located just south of Huffman Lake in the southeast corner of Huffman Township (Hastie 2017; Hastie et al. 2023). It can be accessed from the Yeo Road and, at the time of writing this field trip guidebook, is owned by IAMGOLD Corporation. Surface exposure represents approximately 340 by 140 m of outcrop located within the Ridout deformation zone. The best field relationships and majority of gold mineralization exists on the eastern portion of the outcrop (Figure 13A). In this eastern portion, polymictic conglomerate has been intruded by a monzogranite body (Figures 13A and 13B). The conglomerate contains deformed and elongate clasts of volcanic rocks, iron formation, gabbro, breccia and monzogranite within a matrix composed of quartz, chlorite, feldspar, ankerite and muscovite (Figure 13C). The monzogranite is composed of potassium feldspar, quartz, plagioclase, muscovite and ankerite, and has potassium feldspar phenocrysts that range in size from 0.5 to 2 cm (Figures 13D and 13E). Overlapping U/Pb zircon ages of 2680±4 Ma for the monzogranite and <2684±3 Ma for the youngest detrital zircons in the conglomerate (*see* Figure 13A; Ontario Geological Survey 2019; Davis 2021) suggests that the monzogranite and conglomerate are broadly synchronous.

There are 2 types of gold mineralization within the host monzogranite: 1) early, disseminated pyrite throughout the monzogranite that is relatively low grade (0.1–1 ppm Au; Hastie et al. 2023); and 2) late gold-silver tellurides associated with galena and tetrahedrite-(Zn) (Figure 13F; Hastie et al. 2023). It is worth noting that the Namex deposit represents the type locality for this zinc end-member of tetrahedrite (Biagioni et al. 2020).

Based on overprinting relationships, 3 generations of structural features that postdate basin formation can be identified at the Namex deposit. The oldest generation (G_1) is represented by east- and west-striking isoclinal F_1 folds that are defined by transposed and folded clast-rich conglomerate beds (Hastie 2017). Chlorite, sericite and the long axis of flattened clasts define an S_1 fabric that is axial planar to the F_1 folds (Hastie 2017). Early, east- and west-striking quartz veins (V_1) that are steeply dipping and barren have been boudinaged parallel to S_1. The conglomerate and monzogranite also display boudinaged contacts (*see* Figure 13B) and the boudin necks along with the early barren veins are cut by a second generation of extensional quartz veins (V_2) that are north- and south-striking and steeply dipping, and consistent with north-to-south compression (Hastie 2017).

Tight to isoclinal F_2 folds with S-shaped asymmetry overprint S_1 fabrics and represent a second generation of structures (G_2). A third generation of quartz-ankerite extension veins (V_3) with tetrahedrite-(Zn) mineralization cut the S_1 fabric. These veins strike both northeast and southwest, are steeply dipping, show F_2 S-shaped asymmetry (Figure 13G) and indicate sinistral shearing consistent with northeast-to-southwest bulk shortening (Hastie et al. 2023).

A strong S_3 foliation that overprints the S_1 fabrics and the axial plane of S-shaped F_2 folds represents a third generation of structures (G_3). This foliation, which is closely spaced and defined by chlorite and muscovite, is anticlockwise to S_1 and host rock contacts. Folding of this S_3 foliation occurs along the margin of extensional veins (V_3) and has produced asymmetrical flanking structures, indicating dextral movement (*see* Figure 13G). Along the S_3 foliation is a mineral stretching lineation (L_3) that plunges 15° toward the east. A fourth generation of quartz-ankerite extension veins (V_4) with tetrahedrite mineralization strike both northwest and southeast, are steeply dipping, and display Z-shaped asymmetry. In addition, a fourth generation of extensional quartz + ankerite + tetrahedrite veins have been observed, which are steeply dipping, strike both northwest and southeast, and display Z-shaped asymmetry. Collectively, G_3 structures suggest dextral shearing consistent with northwest-to-southeast bulk shortening (Hastie 2017).

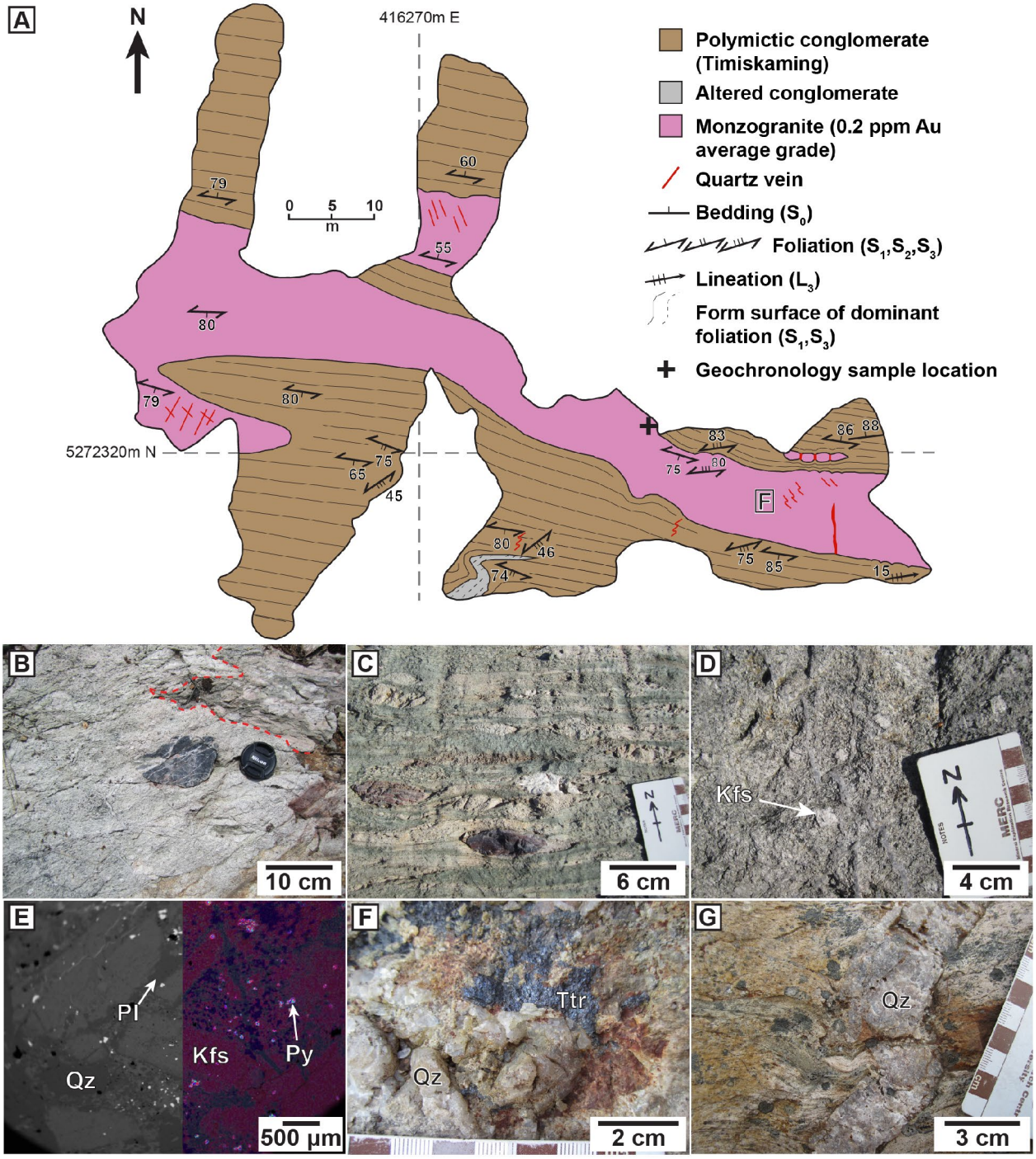

Figure 13. Geology of the Namex deposit and photographs of representative host rocks (Day 2 Stop 1) (*modified from* Hastie et al. 2023). **A)** Geologic map of the Namex deposit. **B)** Monzogranite with a conglomerate clast. Red dotted line represents the contact with conglomerate. **C)** Polymictic conglomerate that has been deformed (flattened clasts). **D)** Potassium feldspar porphyry. **E)** Backscattered electron image and scanning electron microscope energy dispersive spectrometry (SEM-EDS) analyses of quartz and potassium feldspar grains. **F)** Monzogranite (gold bearing) with tetrahedrite in associated quartz vein (location indicated by letter in Figure 13A). **G)** Quartz extensional vein in conglomerate showing sinistral movement with overprinting dextral fringe structures (*from* Hastie et al. 2023). Lens cap is 5 cm in diameter. Abbreviations: Kfs, potassium feldspar; Pl, plagioclase; Py, pyrite; Qz, quartz; Ttr, tetrahedrite. All UTM co-ordinates provided using NAD83 in Zone 17.

Stop 2. Jerome deposit
(Note: Drill core viewed at IAMGOLD Mine Site)

UTM 406900E 5275123N

Potential hazards:

- Drill cores examined from the Jerome deposit are stored by IAMGOLD Corp. at the Côté Gold site. In 2023, the Côté Gold site is an area of active mining and day-to-day traffic. Please avoid any buildings unless IAMGOLD representatives have granted express permission to enter. IAMGOLD personnel will be present to ensure we adhere to their own safety protocols while on the Côté Gold property.
- There may be traffic on the road through the Côté Gold site. Please be careful when crossing the road and look for traffic before doing so.
- Please avoid lifting the core boxes or shifting the stands on which they rest. Improper lifting techniques and falling core boxes can cause serious injury.

The Jerome deposit is located within the Ridout deformation zone (*see* Figure 3), approximately 20 km east-northeast from the Côté Gold and Gosselin deposits and centred on Opeepeesway Lake (*see* Figure 12). The historic Jerome Mine produced 56 878 ounces of gold and 15 104 ounces of silver from 1941 to 1943 and has an inferred resource of 1 Moz of gold using a 0.3 g/t Au cut-off grade (Burt et al. 2011). The Jerome Mine Road branches north from the Sultan Industrial Road near the kilometre 40 road marker and allows access to the peninsula where the Jerome deposit is located. The peninsula lacks significant outcrop, thus requiring diamond-drill cores to view the host rocks to mineralization.

The host rocks at the Jerome deposit are highly altered and deformed monzonites and polymictic conglomerates (Figures 14A to 14D). The monzonite is composed of potassium feldspar, quartz, plagioclase, muscovite and ankerite and has potassium feldspar phenocrysts that range in size from 1 to 5 mm (Figures 14B and 14E). The U/Pb zircon age of the monzonite (2684±3 Ma: Ontario Geological Survey 2019) is similar to the age of the monzogranite from the Namex deposit discussed as part of Day 1 Stop 1. Also similar to the Namex deposit, the conglomerate contains deformed and elongate clasts of volcanic rocks, iron formation, gabbro, breccia and monzogranite within a matrix composed of quartz, chlorite, feldspar, ankerite and muscovite (*see* Figure 14C). Zones of gold mineralization contain stockworks of quartz-ankerite veins (*see* Figure 14D) and hydrothermal breccias the gold grades of which can exceed 100 ppm Au locally. Ore mineralogy is composed mainly of arsenian pyrite and free gold that was remobilized from pyrite (Hastie, Kontak and Lafrance 2020).

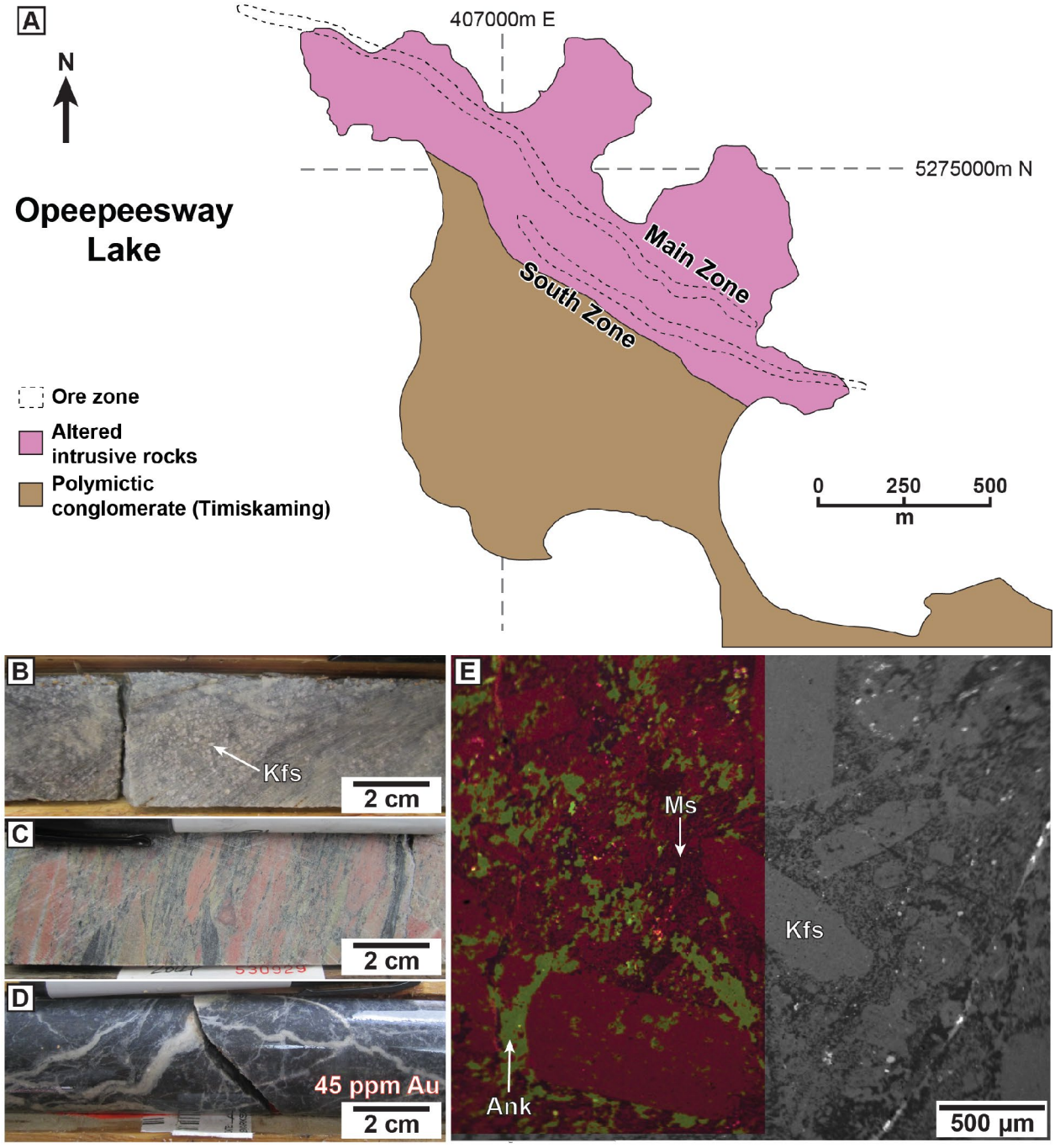

Figure 14. Geology of the Jerome deposit and photographs of representative host rocks (Day 2 Stop 2) (*from* Hastie et al. 2023). **A)** Geologic map of the Jerome deposit. **B)** Least altered monzonite with ankerite and sericite alteration. **C)** Deformed polymictic conglomerate with felsic and mafic volcanic rock and iron formation clasts that are sericite altered. **D)** Heavily altered monzonite with 45 ppm Au exhibiting quartz-ankerite stockwork. **E)** Composite SEM-EDS and backscattered electron image of least altered monzonite. Abbreviations: Ank, ankerite; Kfs, potassium feldspar; Ms, muscovite. All UTM co-ordinates provided using NAD83 in Zone 17.

Stop 3. IAMGOLD Côté Gold Mine site (and Gosselin outcrops)

UTM 434239E 5268862N

Côté Gold Mine site (and Core Shack) safety information and potential local hazards:

- IAMGOLD Corp. Côté project safety department will provide 15-minute visitors orientation and sign-in. Hazards will be reviewed, including those related to construction activity and those locally at each stop location. A review will include the travel stops and schedule.
- Please remember to bring your Personal Protective Equipment (PPE) to the core shack. Core shack PPE requirements include steel-toed boots and an orange safety vest. Other PPE including hard hats, safety glasses and gloves will be required when in the field and on the mine site.
- The Côté Gold project is an active mine construction site with heavy construction-related day-to-day traffic. Vehicle assignments will be made for Côté Exploration and Production Geology vehicles and participants will remain with the lead drivers of these vehicles.
- IAMGOLD personnel will be present to ensure field trip participants adhere to the company's own safety protocols while on the Côté Gold mine site. Please avoid any buildings unless IAMGOLD representatives have granted express permission to enter.
- Emergency Muster Point at the Mesomikenda Exploration camp will be reviewed.
- Please note that cell phones and cameras must not be used at the Côté Mine site stops.

The Côté Gold and Gosselin deposits (Figures 15 and 16) represent early gold mineralization (*ca.* 2741 Ma) in the Abitibi greenstone belt (Katz et al. 2017, 2021). These are located within the Chester intrusive complex, which is a low aluminum tonalitic and dioritic synvolcanic composite intrusion (Katz et al. 2017) that is bounded to the north by felsic to intermediate metavolcanic rocks within the Ridout deformation zone and to the south by the Ramsey–Algoma granitoid complex (*see* Figures 2 and 3). With a growing combined resource estimate (measured, indicated and inferred) that exceeds 19 Moz (Cox et al. 2022), these deposits represent Ontario's newest large gold camp, and the recognition of early, synvolcanic, low-grade large tonnage deposits is important as it highlights the possibility for similar deposit styles and timing elsewhere in the Superior Craton.

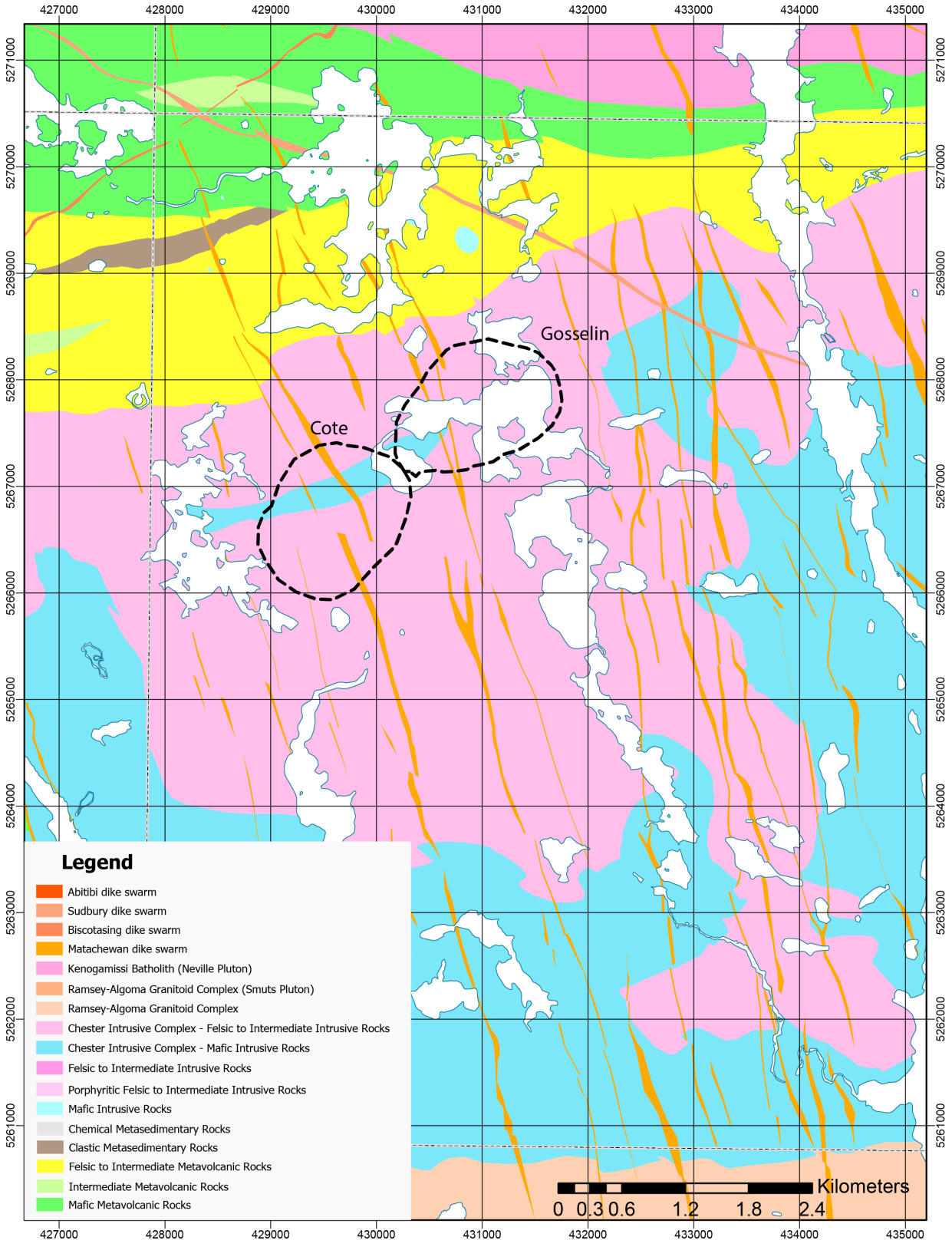

Figure 15. Simplified geological map of the Chester intrusive complex indicating the locations of the Côté Gold and Gosselin pits (Day 2 Stop 3) (*modified from* Gemmell and MacDonald 2017; black dashed pit outlines *from* Cox et al. 2022). All UTM co-ordinates provided using NAD83 in Zone 17.

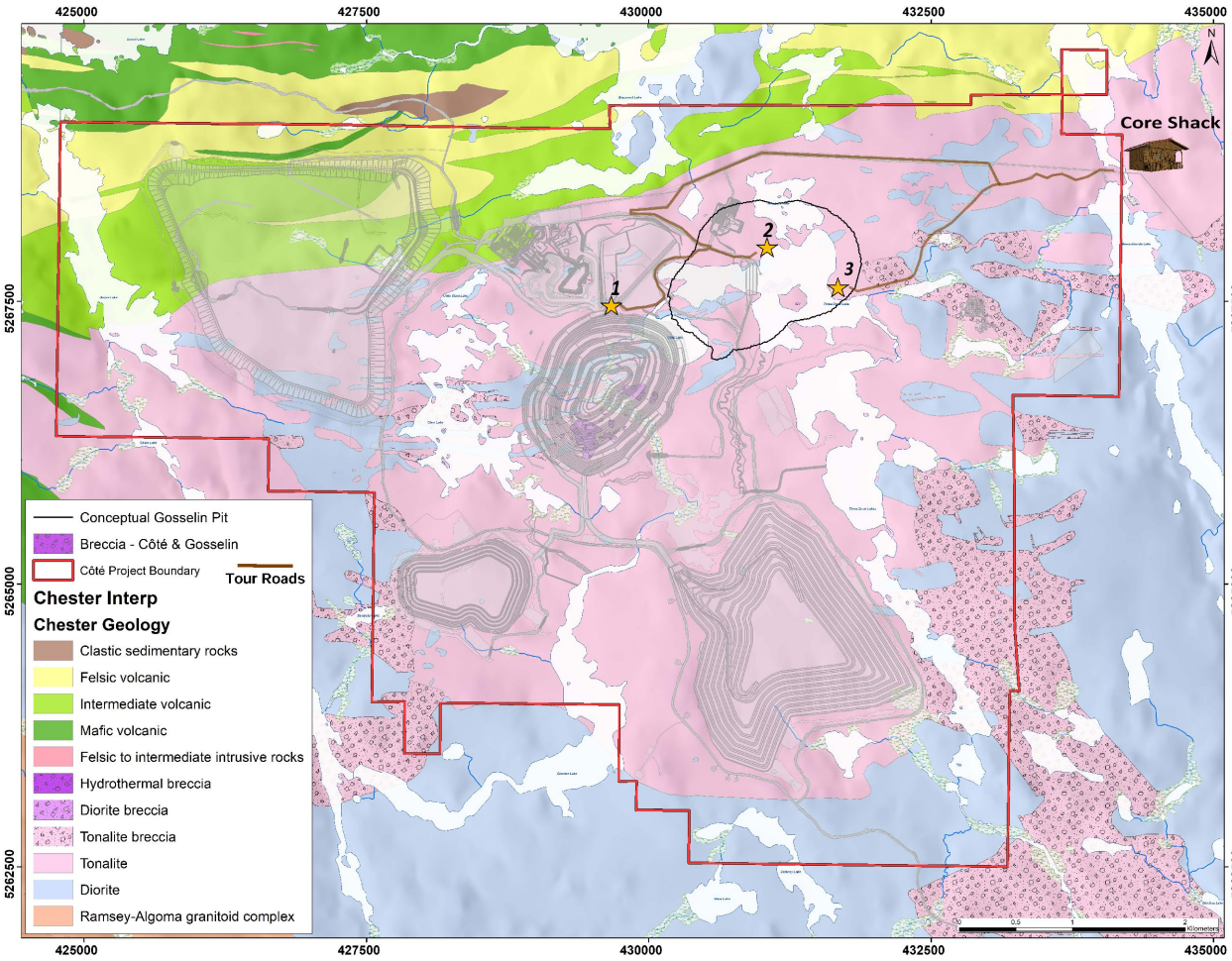

Figure 16. Geology of the Côté Gold mine site with field stop locations (Day 1 Stops 3-1, 3-2, 3-3 and 3-4 (core shack)). Figure courtesy of IAMGOLD Corp. All UTM co-ordinates provided using NAD83 in Zone 17.

Stop 3-1. Côté open pit overlook and geological overview

UTM 429470E 5267311N

A presentation overlooking the open pit by Irikefe Eruero (Chief Mine Geologist, Côté Gold, IAMGOLD Corp.) including geology overview (Photo 10), breccia samples, and production information is planned. A presentation board at the overlook is included.

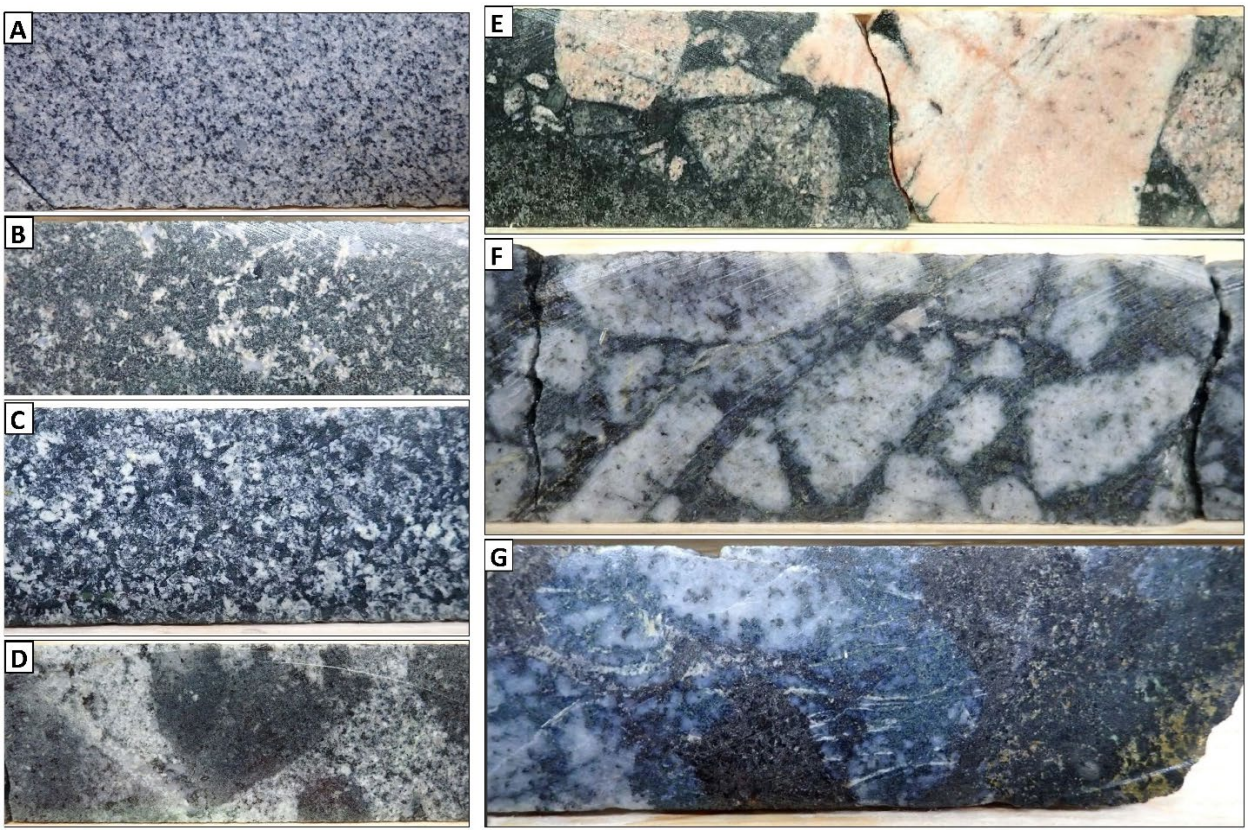

Photo 10. Photos of primary rock units at the Côté Gold deposit: **A)** tonalite, **B)** quartz diorite, **C)** diorite, **D)** tonalite breccia, **E)** diorite breccia, **F)** hydrothermal breccia, and **G)** hydrothermal breccia with biotite-chlorite-sulfide matrix (all photos are of NQ-sized core that is approximately 4.8 cm in diameter; photos courtesy of IAMGOLD Corp).

Stop 3-2. Candy Cane outcrop

UTM 431062E 5267992N

The Candy Cane outcrop is located ~1.4 km northeast of the Côté Gold open pit and shows subparallel fractures filled with sulfides ± quartz that cut tonalite host rock (Photo 11). These fractures are spaced 0.3 to 1.5 m apart, strike toward the northwest (approximately 300°), and dip moderately (50°–55°). Sericite ± pyrite alteration halos that are 1 to 10 cm with chlorite-rich selvages border the subparallel fractures (Smith 2016). The name of the outcrop is derived from the pronounced visual striping that results from the alteration halos and oxidized pyrite (Figure 17; *see also* Photo 11). One of the most important structural features of the outcrop is a foliation that strikes 290° and dips 60°. This foliation overprints the northwest-striking veins and subordinate north-striking veins along with their alteration halos. The veins underwent a clockwise rotation during the formation of this foliation. This suggest that this deformation

even occurred during dextral shearing (Smith 2016). Molybdenite within similar veins at the North Breccia outcrop (now part of the open pit) yielded a Re/Os age of 2746.8±11.4 Ma (Katz et al. 2021), similar to the age of the host tonalite and diorite of the Chester intrusive complex.

Results from a total of 50 channel samples taken across the Candy Cane outcrop indicate that samples, which included vein and alteration halos, yielded higher grades (0.009–2.11 g/t Au) compared to the surrounding less altered tonalite host rock (<0.001–0.49 g/t Au), and the less deformed samples (0.018–0.276 g/t Au) on average returned higher grades than the more deformed samples (0.005–0.063 g/t Au). The sample breakdown includes the following rock types: 21 vein material + phyllic alteration halo; 19 less altered tonalite; 5 strongly deformed veins with alteration halos; and 5 relatively undeformed veins with alteration halos.

Photo 11. Candy Cane outcrop consisting of tonalite transected by numerous, sheeted sulfide ± quartz-filled fractures (Day 2 Stop 3-2) (*see also* Figure 17) (photo faces northeast; width of outcrop at the base of the photo is approximately 2 m). Photo by T.P. Gemmell.

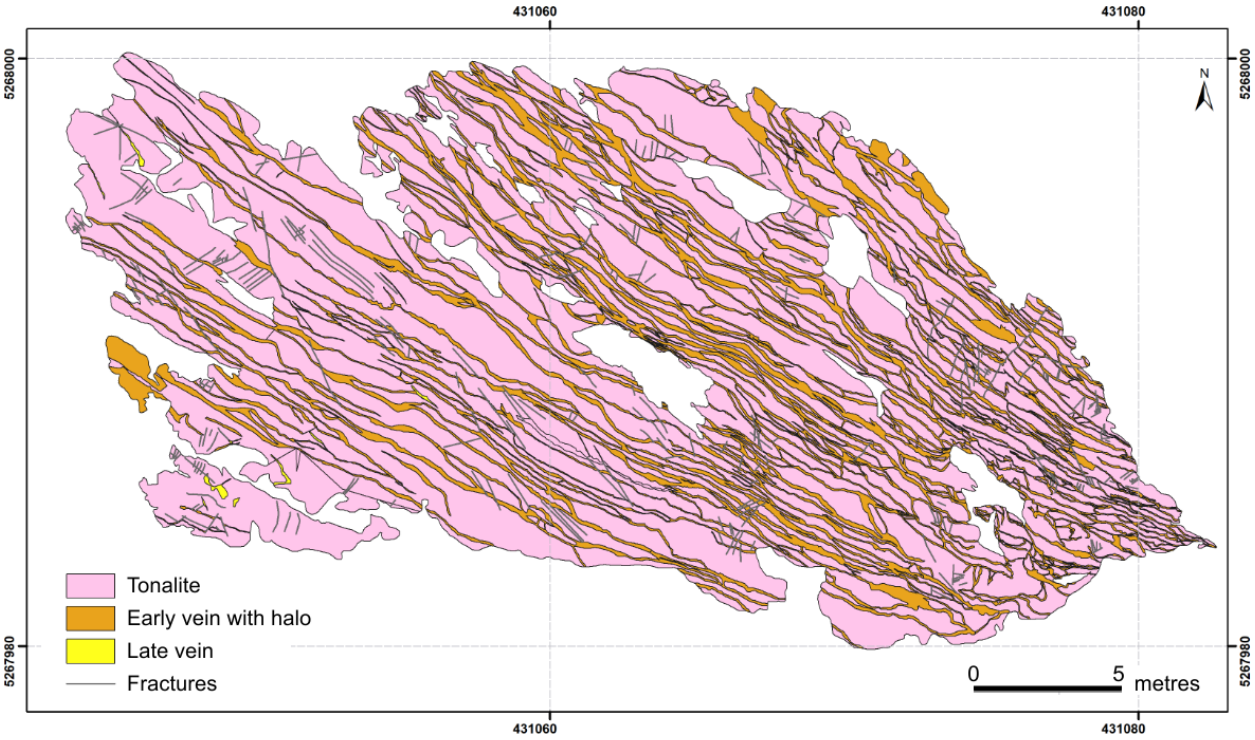

Figure 17. Simplified geological map of the Candy Cane outcrop (Day 1 Stop 3-2) (figure courtesy of IAMGOLD Corp). All UTM co-ordinates provided using NAD83 in Zone 17.

Stop 3-3. Gosselin discovery outcrop

UTM 431638E 5267690N

This stop is at the site of an outcrop that was exposed by stripping and washing in 2016 by IAMGOLD Exploration in preparation for geological mapping. The outcrop lies immediately east of the original Gosselin showing described as a "spectacular showing of native gold on the east shore of Three Ducks Lake" discovered by prospector Alfred Gosselin in 1930. Mechanical stripping, outcrop washing and channel sampling revealed favorable gold-bearing structures (veins, fractures and local shears) within altered tonalite. Although the gold values were not continuous, the alteration noted throughout both east and west outcrops was significant enough to justify diamond drilling to determine the geographic extent. Following initial drill-testing, the gold-bearing structures and alteration envelopes were modelled and led to the discovery of hydrothermal breccia that cores the Gosselin deposit.

Gosselin West (Figure 18; Photo 12): This outcrop is composed of medium-grained tonalite that contains moderate pervasive sericite alteration and disseminated (1–2%) and fracture-controlled biotite–chlorite alteration. Trace to <2% pyrite occurs disseminated in tonalite and along biotite fractures.

Two main east-oriented shear zones (<2 m wide) occur and incorporate quartz-sulfide veins. In the shear zones, there is strong, pervasive sericite alteration. In addition, a weak, patchy carbonate alteration occurs proximal to the shear zones. The quartz-sulfide veins are boudinaged and typically contain <2% pyrite. However, the strong sericite alteration halo around the veins can be variably mineralized ranging from 1–3% pyrite and 1–6% chalcopyrite.

Gosselin East (*see* Figure 18): This outcrop is composed of medium-grained tonalite that is variably altered. Outside of the shear zone, the host rock contains disseminated (3–5%) biotite–chlorite alteration and sericite alteration ranges from weak to strong. Trace to 2% pyrite ± chalcopyrite is present in the host rock with an increase of sulfide mineralization proximal to the shear zone.

In the middle of the outcrop, there is a <6 m wide shear zone that includes several roughly east-trending quartz-sulfide veins. This zone contains intense sericite alteration and moderate chlorite alteration. Fracture-controlled silica and/or albite alteration (<2 cm wide) occurs in the shear zone and is localized along 2 fracture sets (280/81 and 263/83). Directly south of the deformation zone, the tonalite is strongly fractured with repeating fracture sets at 251/58 and 233/58.

The quartz-sulfide veins are millimetres to centimetres in width and contain up to 5% pyrite + chalcopyrite + pyrrhotite and trace malachite. Several unmineralized quartz-chlorite veins (<10 cm wide) also cut through this outcrop at several orientations (e.g., 139/41, 141/15, 175/45 and 021/77).

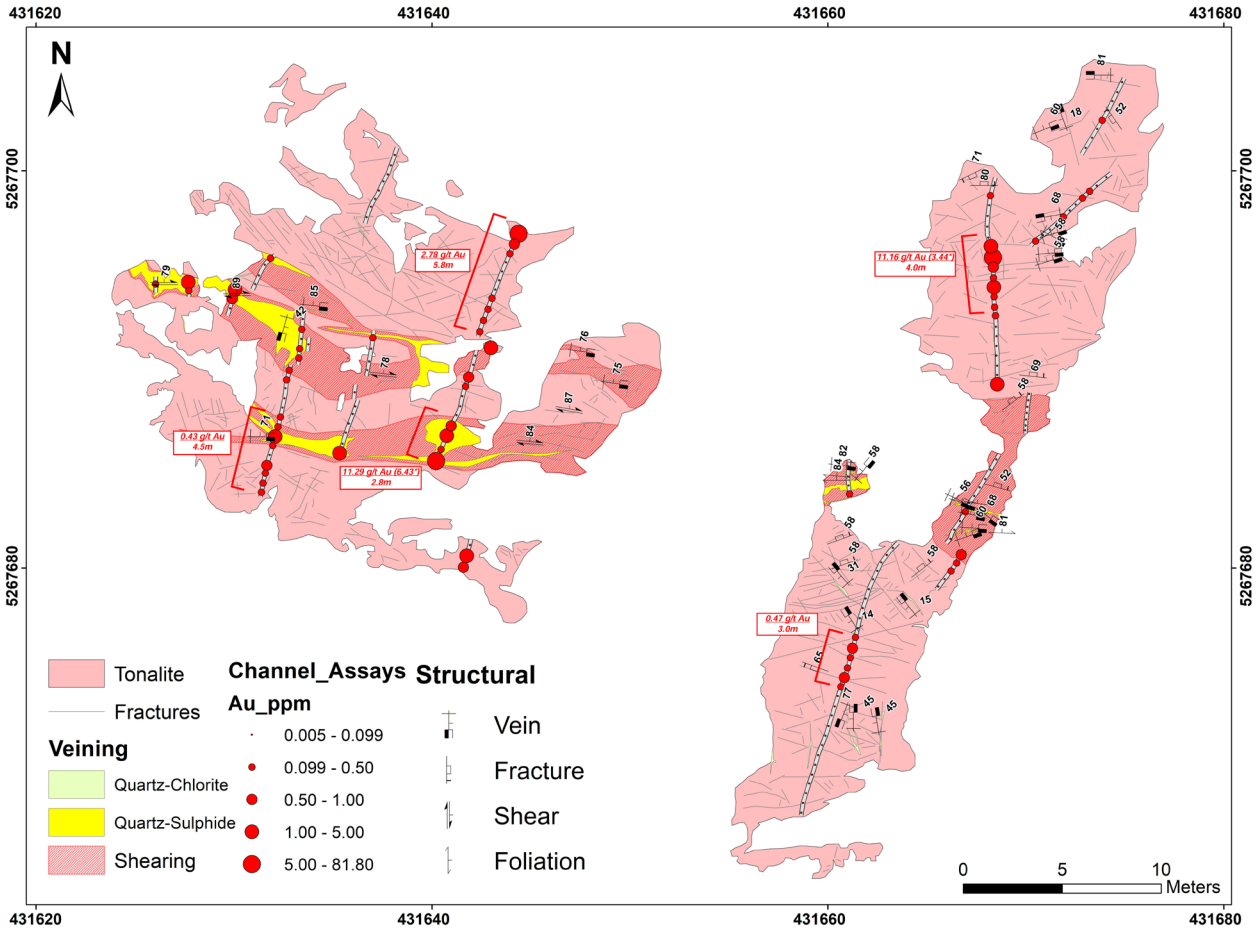

Figure 18. Simplified geological map with structural measurements and composite gold channel sample values on the Gosselin East and West outcrops (Day 2 Stop 3-3) (figure courtesy of IAMGOLD Corp.). All UTM co-ordinates provided using NAD83 in Zone 17.

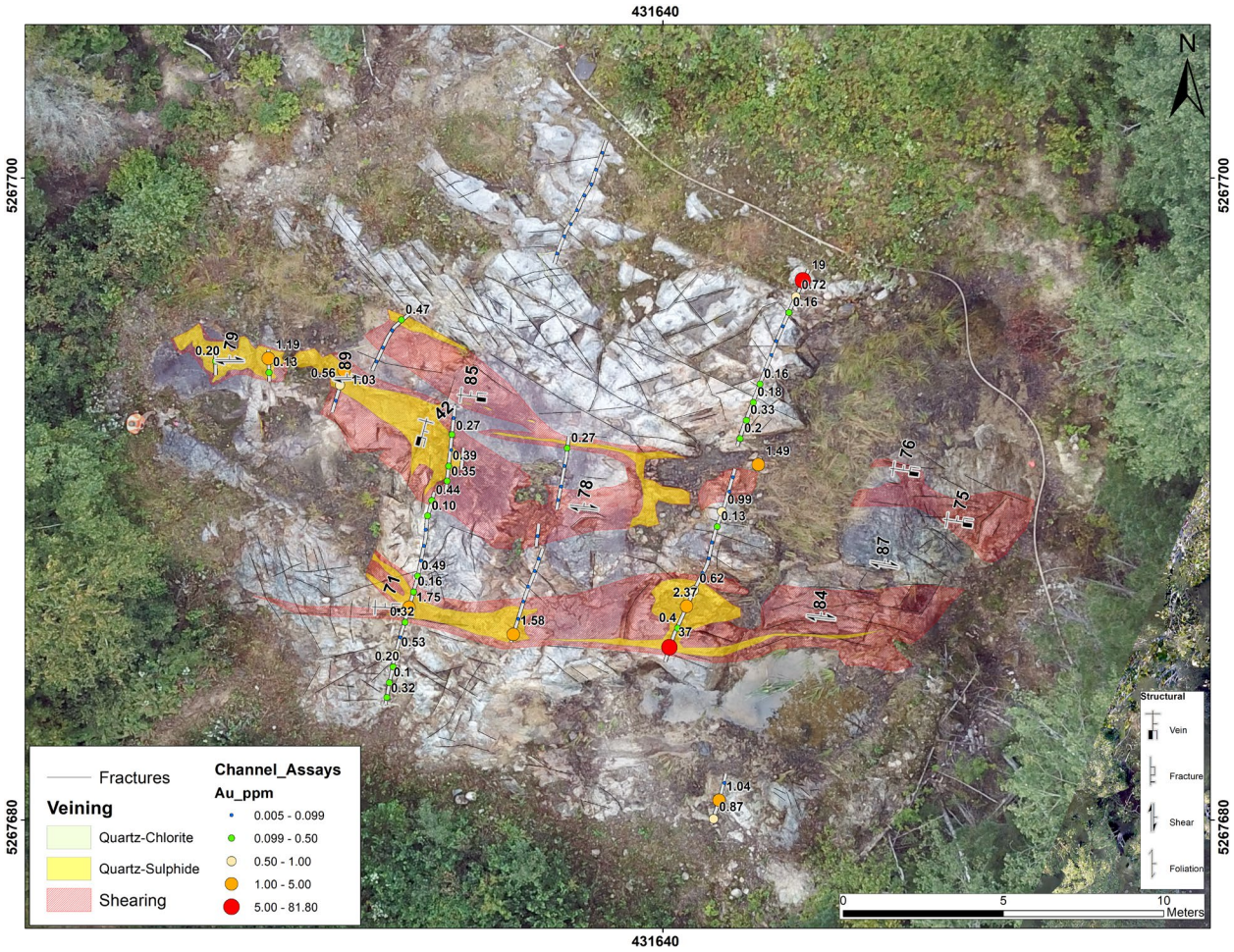

Photo 12. Overhead drone image of the Gosselin West discovery outcrop, annotated to show the structures, locations of channel samples, and gold grades across the outcrop (Day 2 Stop 3-3) (image courtesy of IAMGOLD Corp.). Channel sample intervals range from 0.2 to 1.5 m.

Stop 3-4. Core Shack (Côté–Gosselin–Jerome drill core)

UTM 434239E 5268862N

Potential hazards:

- Drill cores examined from the Côté, Gosselin and Jerome deposits are stored by IAMGOLD Corp. at the Côté Gold site. In 2023, the Côté Gold site is an area of active mining and day-to-day traffic. Please avoid any buildings unless IAMGOLD representatives have granted express permission to enter. IAMGOLD personnel will be present to ensure field trip participants adhere to the company's own safety protocols while on the Côté Gold property.
- There may be traffic on the road through the Côté Gold site. Please be careful when crossing the road and look for traffic before doing so.
- Please avoid lifting the core boxes or shifting the stands on which they rest. Improper lifting techniques and falling core boxes can cause serious injury.

Gosselin Drill Core Viewing: Diamond-drill core from 4 Gosselin deposit drill holes have been selected for viewing (Figures 19 and 20). Drill holes include GOS21-81, GOS22-105, GOS22-126 and GOS22-129.

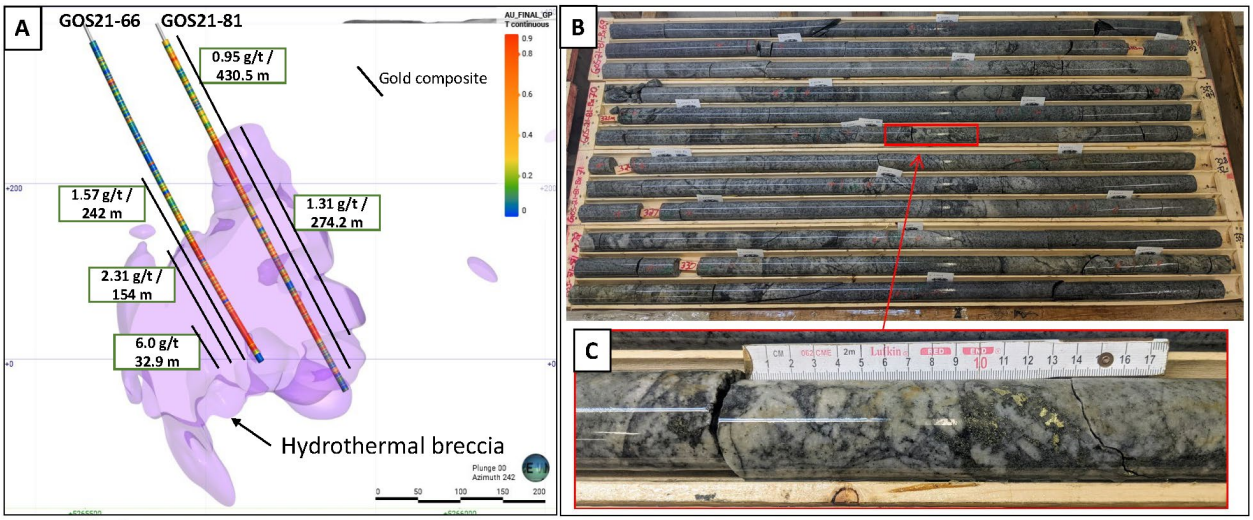

A – Drill-hole GOS21-81 cross-section

B – GOS21-81 interval of hydrothermal breccia 315.1 to 332.7m

C – Hydrothermal breccia – zoomed in core photo at 323.4m

Figure 19. Cross-section and drill-core photos from Gosselin deposit drill-hole GOS21-81 (Day 2 Stop 3-4) (images courtesy of IAMGOLD Corp.). **A)** Cross-section view showing position of drill-hole GOS21-81 with down-hole gold grades. Modelled hydrothermal breccia is represented by solid purple. **B)**, **C)** Photos of hydrothermal breccia in GOS21-81 drill core: **B)** shows core from 315.1 to 332.7 m; and **C)** shows the drill core at 323.4 m. The hydrothermal breccia appears to be less well developed than at the Côté Gold deposit, and is manifested as an *in situ*, "crackle-style" breccia, featuring a high fracture density. The fractures commonly contain sulfides (pyrite ± chalcopyrite ± pyrrhotite). The hydrothermal breccia at the Gosselin deposit is predominantly fragment supported, containing up to 95% tightly packed fragments.

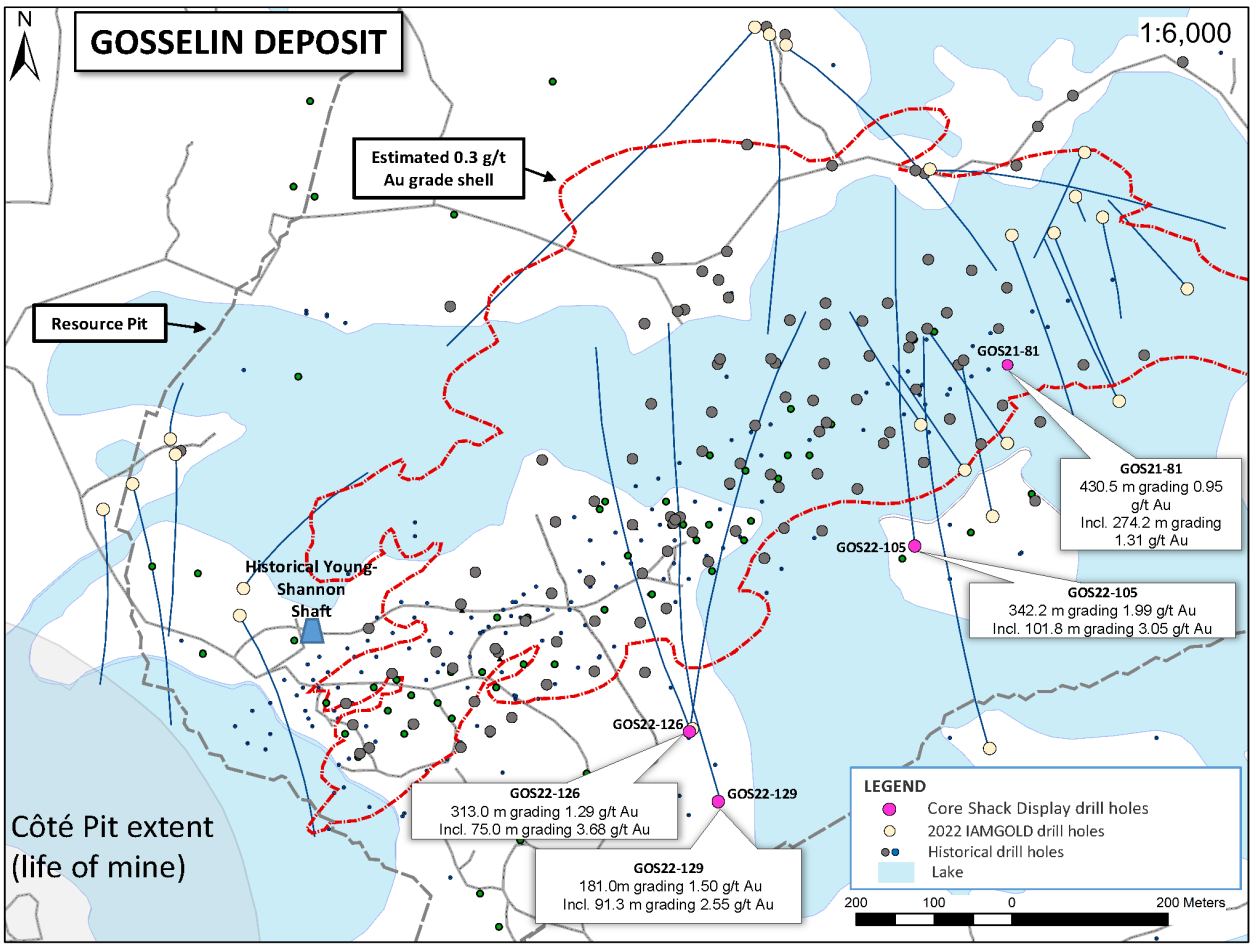

Figure 20. Location map of Gosselin deposit drill holes (Day 2 Stop 3-4) (figure courtesy of IAMGOLD Corp.). Core viewed at the core shack are from drill-hole locations (denoted by pink circles) labelled with large boxes with drill-hole number and assay results.

End of Swayze area road logs.

Road Logs: Noranda Area

Note: Caution should be taken when parking vehicles on the shoulders of the road or highways and when examining outcrops located along the field trip route. All UTM co-ordinates are provided using NAD83 in Zone 17U in the Rouyn-Noranda area.

The outcrops examined during the Rouyn-Noranda segment are classic "Noranda Field Trip Stops" and are located on the properties of Falco Resources Ltd., Glencore Ltd. and Yorbeau Resources Inc., and their permission is required prior to access. Please do not hammer or sample the outcrops so they can be preserved for training the next generation of students and professional geologists.

DAY 3. ROUYN-NORANDA AREA: GOLD DAY

The day trip departs from the Quality Inn in Rouyn-Noranda with the first stop at the Wilson outcrop in the McWatters area. From the McWatters area, the trip continues southwest to look at Timiskaming Group conglomerate on Route des Pionniers. From there, the drive will continue west along Rang Ducharme and Rang Hull with stops along the LLCDZ and end at the Yorbeau property.

Stop 1. Unconformity between volcanic rocks of the Blake River Group and conglomerate of the Timiskaming Group

UTM 654704E 5342651N

Potential hazards:

- Slippery slopes; loose rocks
- Busy road with high-speed traffic; stay off road shoulder and remain away from parked vehicles if possible; high-visibility vests required
- Stay on trail as much as possible

In the Rouyn-Noranda area, the contact between sedimentary rocks of the Timiskaming Group and the volcanic rocks of the Blake River Group locally defines an angular unconformity (Figures 21 and 22; Wilson 1956, 1962). The outcrop at this Stop is situated on the northern contact of the Timiskaming Group, which is overturned to the south and truncated by the LLCDZ that juxtaposes it against carbonate-altered ultramafic to mafic volcanic rocks of the Piché Group (*see* Figure 21). The outcrop exposes a relatively undeformed erosional contact at the base of the Timiskaming Group where conglomerate was deposited on pillowed and lobate basalt of the Blake River Group (Figure 22; Wilson 1956, 1962). The conglomerate is composed of angular to subrounded clasts including basalt, rhyolite, gabbro and granitoid. According to mapping in the area by Wilson (1948) and Coté (1975), facing directions of the basalts are mainly southward, which produce a stratigraphic discordance explained by large pre-Timiskaming folds in the Blake River Group (e.g., Hubert 1990; *see* Figure 21). The tectonic significance and depositional environment for the Timiskaming Group conglomeratic rocks are topics of continued debate with extensional, strike-slip and contractional settings proposed (e.g., Holubec 1972; Kerrich and Wyman 1990; Cameron 1993; Mueller, Donaldson and Doucet 1994; Corcoran and Mueller 2007; Poulsen 2010; Bleeker 2015).

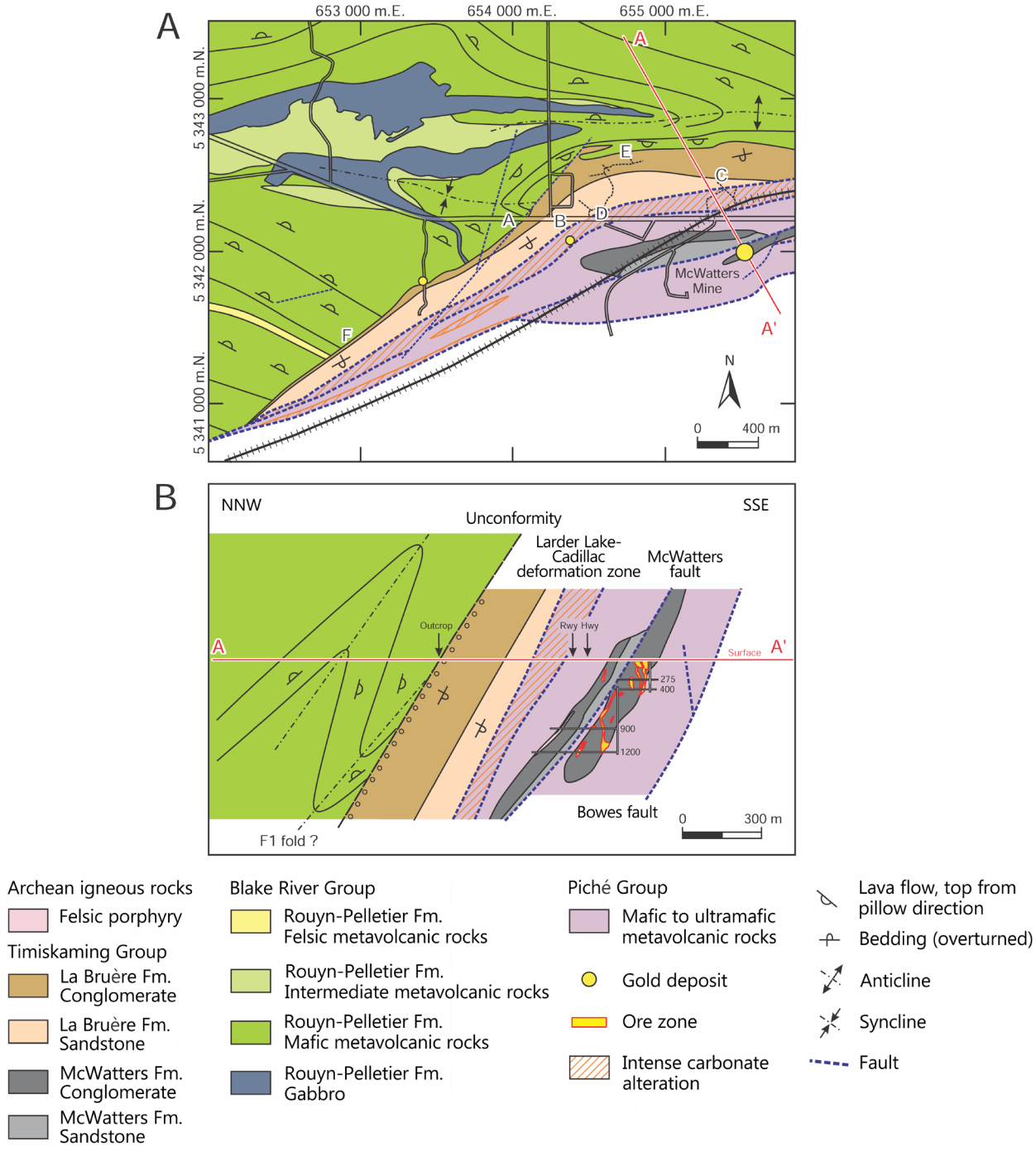

Figure 21. A) Geological map of the McWatters area showing the distribution of major lithological units (*from* Poulsen 2017a). Day 3 Stop 1 is indicated by "E" (other letters indicate optional substops at this location). The location of cross section A–A′, shown in Figure 21B, is indicated by a red line and letters. **B)** Cross section A–A′ through the Timiskaming unconformity in the McWatters area (*from* Poulsen 2017a). Abbreviation: FM: formation. All UTM co-ordinates provided using NAD83 in Zone 17.

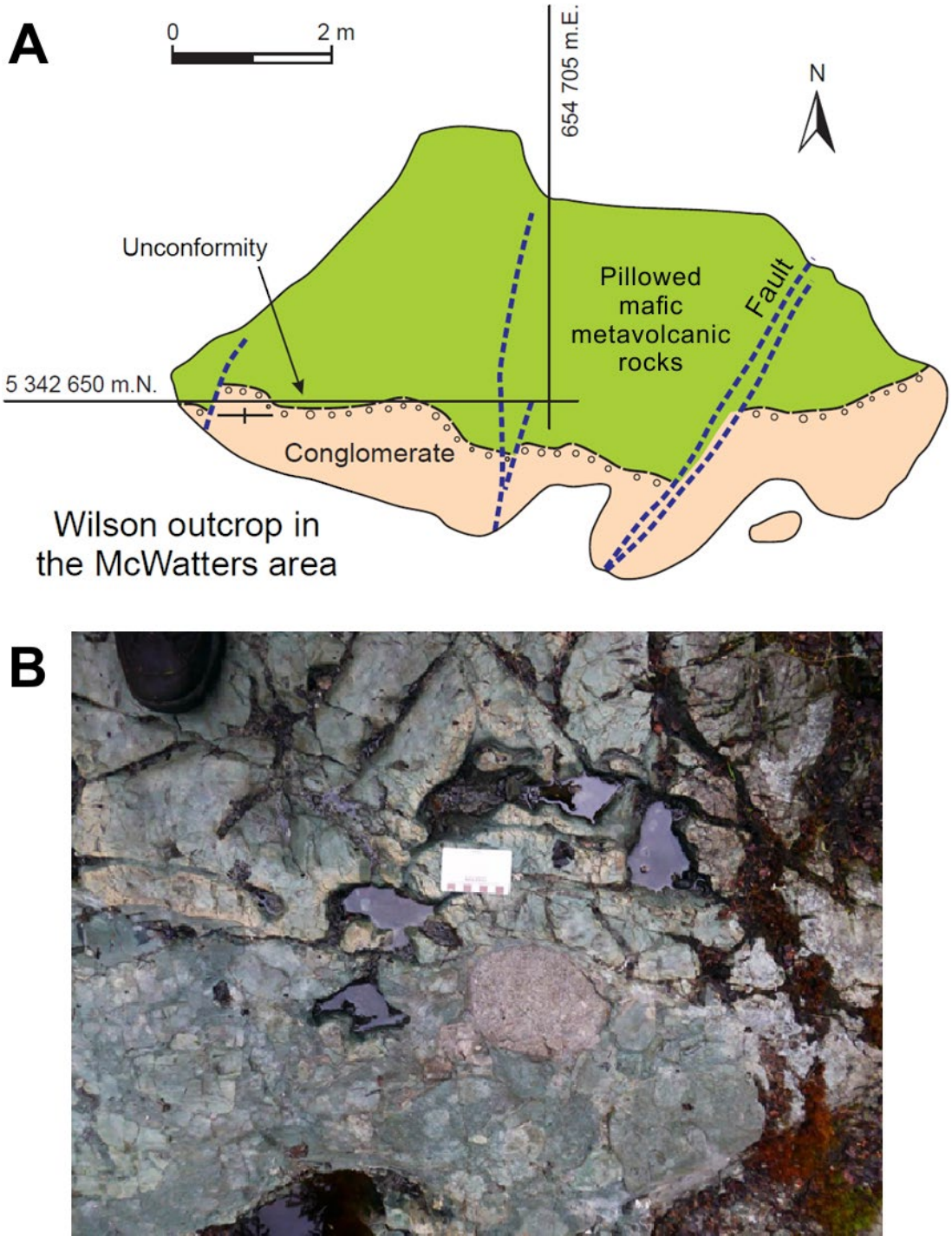

Figure 22. A) Map of the Wilson unconformity outcrop at Day 3 Stop 1 (*from* Poulsen 2017a). **B)** Image of the unconformity between Blake River Group andesite (top of photo) and Timiskaming Group conglomerate (similar field of view as Figure 14F in Poulsen 2017a). All UTM co-ordinates provided using NAD83 in Zone 17.

Stop 2. Timiskaming Group conglomerate south of the Larder Lake–Cadillac deformation zone (roadcut along Route des Pionniers)

UTM 650395E 5339050N

Potential hazards:

- Steep and/or slippery slopes; loose rocks
- Busy road with high-speed traffic; stay off road shoulder and remain away from parked vehicles if possible; high-visibility vests required
- Vertical outcrops with loose debris; rockfall hazard, hard hats must be worn

Highly strained Timiskaming Group conglomerate south of the Lac Bouzan segment of the Larder Lake–Cadillac deformation zone (Photo 13). Here, the Timiskaming conglomeratic rocks are thought to have been deposited on underlying greywacke-mudstone of the Pontiac Group (Wilson 1956, 1962). This is consistent with the development of an unconformity between 2680 and 2675 Ma as constrained by detrital zircon geochronology on both units (Davis 2002; Frieman et al. 2017). At this outcrop, the conglomerate is strongly deformed with clasts flattened and elongated.

Photo 13. Photo showing high-strain Timiskaming Group conglomerate with flattened and stretched clasts (Day 3 Stop 2).

Stop 3. Deformed pillowed basalt and quartz-tourmaline veins north of the Larder Lake–Cadillac deformation zone (Rang Ducharme)

UTM 648753E 5340424N

Potential hazards:

- Steep and/or slippery slopes; loose rocks
- Crossing road with high-speed traffic; high-visibility vests required

This Stop, just to the north of the Larder Lake–Cadillac deformation zone, exposes Blake River Group basalt with a pronounced stretching lineation best defined by elongated varioles (Photo 14). The outcrop also hosts quartz-tourmaline veins that are locally associated with gold mineralization along the Larder Lake–Cadillac deformation zone (Robert 1991).

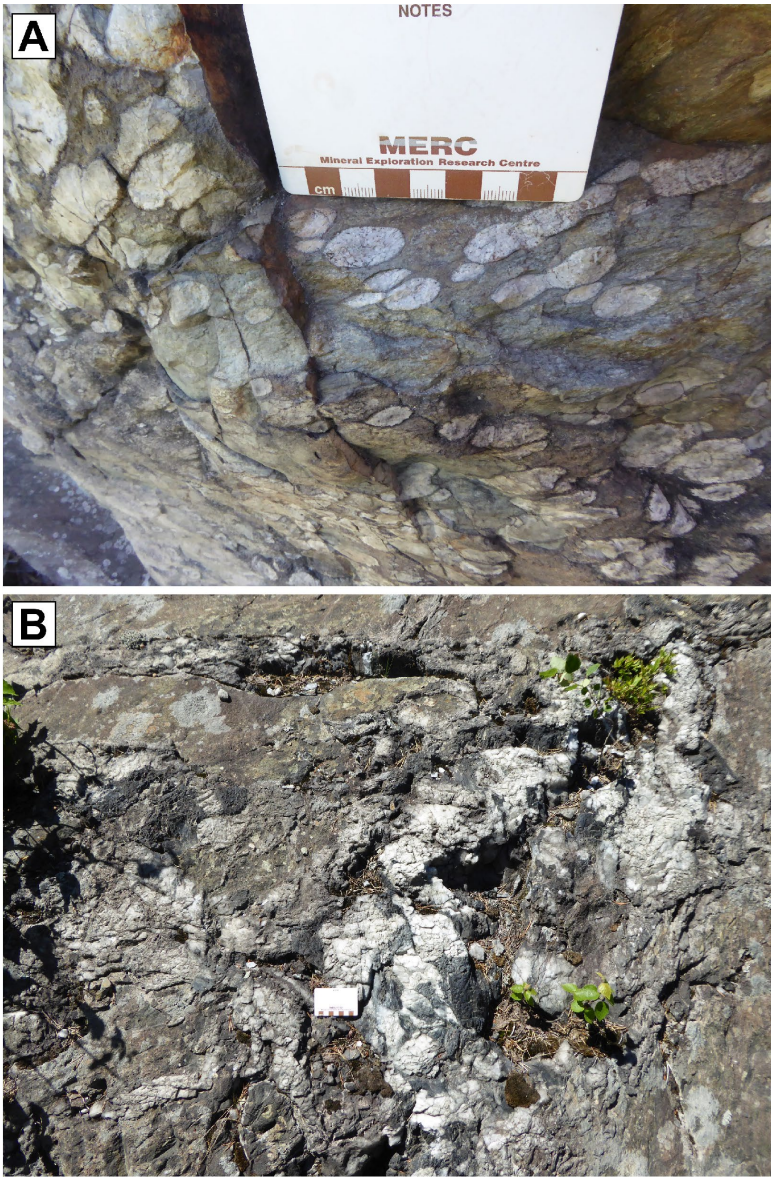

Photo 14. Photographs showing the outcrop visited on Day 3 Stop 3. **A)** Deformed variolitic basalt of the Blake River Group on the north side of the Larder Lake–Cadillac deformation zone. **B)** Tourmaline-quartz vein crosscutting the Blake River Group basalt.

Stop 4. Deformed contact between Blake River Group pillowed basalt and Timiskaming Group conglomerate near Astoria trench (Avenue Granada–Astoria trench area)

UTM 645950E 5340020N

Potential hazards:

- Steep and/or slippery slopes; loose rocks
- Be alert for the presence of bears

The first stop at the Astoria trench area exposes Blake River Group basalts in fault contact with Timiskaming conglomerates (Figures 23 and 24). The Astoria deposit was one of the first gold prospects to be discovered along the Larder Lake–Cadillac deformation zone, likely because gold ore was exposed on a prominent hill where 2 intersecting Proterozoic dikes, relatively resistant to glacial erosion, are exposed. The dikes provide a degree of geologic complication in that they not only disrupt and displace the surrounding Archean rocks (*see* Figure 24), but also impart a contact metamorphic aureole of calc-silicate hornfels along their margins. Furthermore, as indicated at this stop (location "A" on Figure 24), the rocks in the Astoria sector as a whole are strongly deformed.

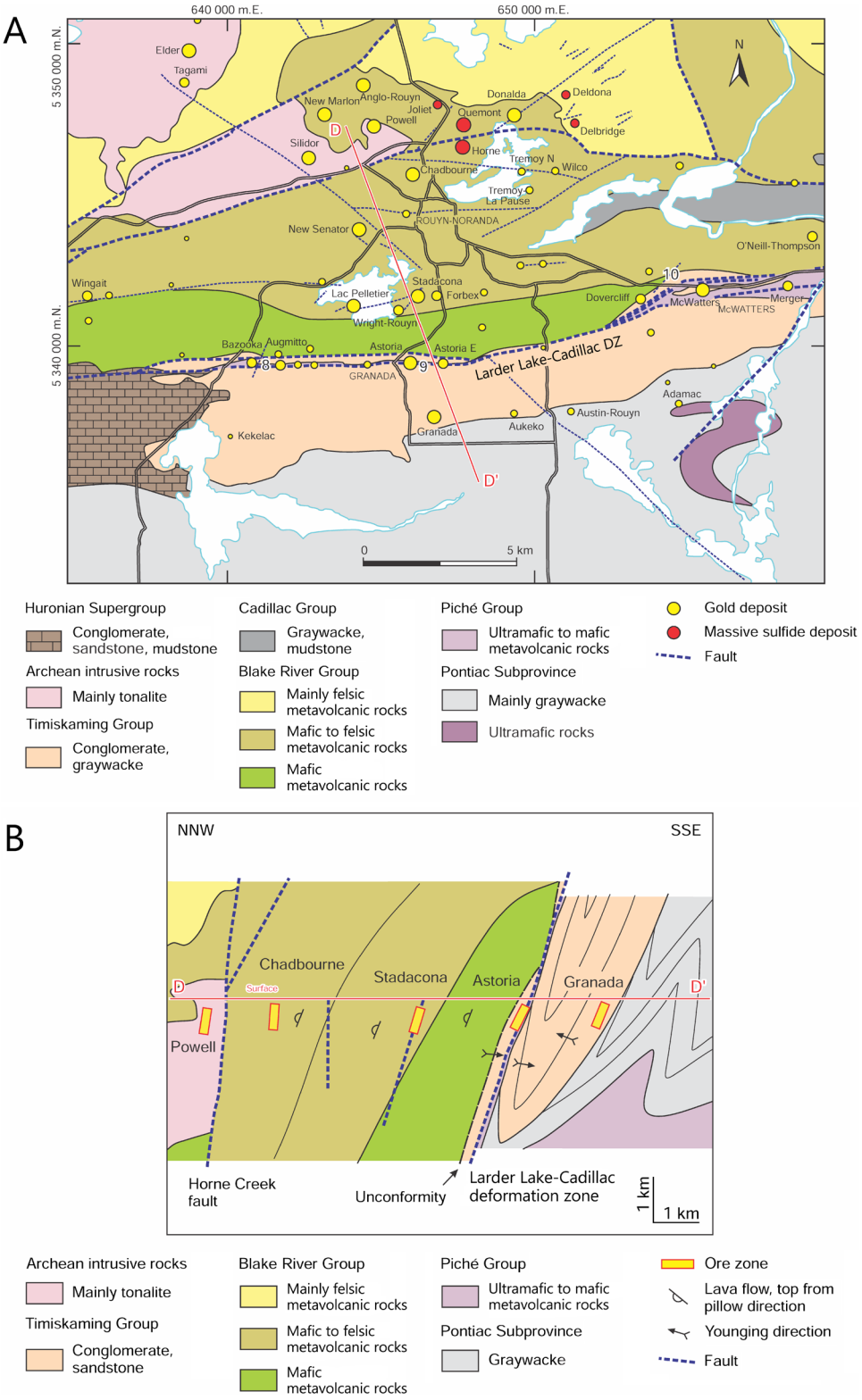

Figure 23. A) Geological map of the southern part of the Rouyn-Noranda District and location of the Astoria deposit (Day 3 Stop 4). The location of cross section D–D′, shown in Figure 23B, is indicated by a red line and letters. Abbreviation: DZ, deformation zone. All UTM co-ordinates provided using NAD83 in Zone 17. **B)** Cross section D–D′ (location shown in Figure 21A) through the southern Rouyn-Noranda District and in the vicinity of the Astoria deposit (*from* Poulsen 2017a).

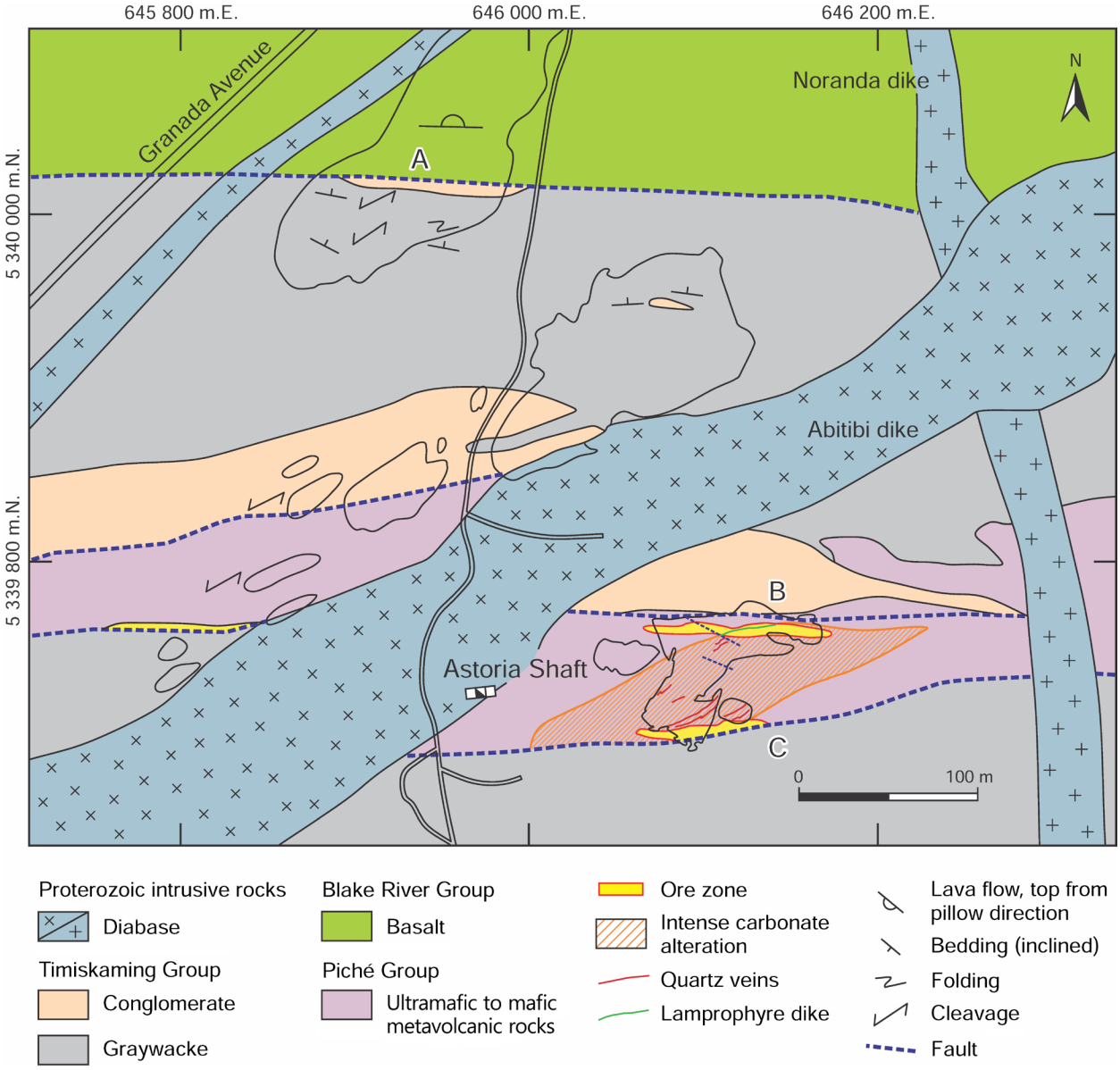

Figure 24. Geological map of the Astoria trench area (*from* Poulsen 2017a). Day 3 Stop 4 corresponds to the letter "A" on the figure (letters B and C are at the Astoria trench, *see* Day 3 Stop 5). All UTM co-ordinates provided using NAD83 in Zone 17.

Stop 5. Larder Lake–Cadillac deformation zone at Astoria: contact between carbonatized komatiite and Timiskaming metasedimentary rocks (Avenue Granada–Astoria trench)

UTM 646118E 5339785N

Potential hazards:

- Steep and/or slippery slopes; loose rocks
- Be careful to avoid areas of the trench that are under water
- Be alert to the presence of bears

The Astoria trench exposes the Larder Lake–Cadillac deformation zone near the old abandoned Astoria mine (Photo 15; Figure 25). The Piché Structural Complex is ~60 m wide (plan view) and composed of predominantly ultramafic rocks. The stripped outcrop shows the northern and southern contact between the Piché Structural Complex and Timiskaming Group sedimentary rocks. The Timiskaming Group metasedimentary rocks on the north side of the Piché Structural Complex belongs to the Labruère Formation and those on the south side of the Piché Structural Complex to the Granada Formation. Observable rock types across the deformation zone include, from north to south, intermediate to mafic conglomerate with a high proportion of porphyry clasts; ultramafic schist showing varying degrees of carbonate ± potassic alteration; and metasedimentary rocks consisting of argillite, conglomeratic sandstone, and granule to pebble conglomerate (*see* Figure 25). The rocks are strongly deformed with a principal schistosity defined by phyllosilicates, which is best developed in the ultramafic schists. The principal schistosity and the oldest observed at the stripping (S_1), is parallel to bedding in the metasedimentary rocks and overall oriented approximately to the east and dipping steeply to the north. An approximately down-dip stretching lineation associated with the principal schistosity is best observed in the southern metasedimentary rocks. A narrow (~40 cm) sandy bed or intermediate to mafic sill within the northern conglomerate exhibits 2 crenulation cleavages that are difficult to interpret, but likely represent S_2 and S_3 foliations. This area is spatially associated with a subhorizontal lineation. Several kinematic indicators are present on the stripping, most of which are compatible with a dextral movement, e.g., sigmoidal porphyry clasts in the northern conglomerate and locally, well-developed shear bands in the ultramafic schist oriented at approximately 280° where the principal schistosity is east trending. Locally, the principal schistosity appears to undergo back-rotation between individual shear bands, a relationship also reflected on the scale of the stripping with a few wider high strain zones that are parallel to the shear bands in the ultramafic schist. Mineralization occurs as free gold with minor sulfides (arsenopyrite + pyrite) associated with quartz-tourmaline veining and stockwork hosted by ultramafic schist with pervasive carbonate ± fuchsite alteration. This type of mineralization is commonly known as "green carbonate ore" at the Kerr Addison Mine located on Larder Lake–Cadillac deformation zone near Larder Lake, Ontario. Gold is also observed with arsenopyrite ± pyrite ± pyrrhotite ± loellingite associated with grey quartz-tourmaline ± biotite veins hosted in the Timiskaming metasedimentary rocks on the southern contact with the Piché Structural Complex. Most of the 1 t (~30 000 oz) gold production between 1986 and 1995 came from underground mining along the southern contact of the Piché Structural Complex down-plunge and beyond the western margin of the Proterozoic diabase dike.

Photo 15. Aerial view of the Astoria trench (Day 3 Stop 5) with the upper and lower contacts of the Piché Group indicated by a dotted yellow line. The approximate extent of the geological map provided in Figure 25 is indicated by thin white dotted line.

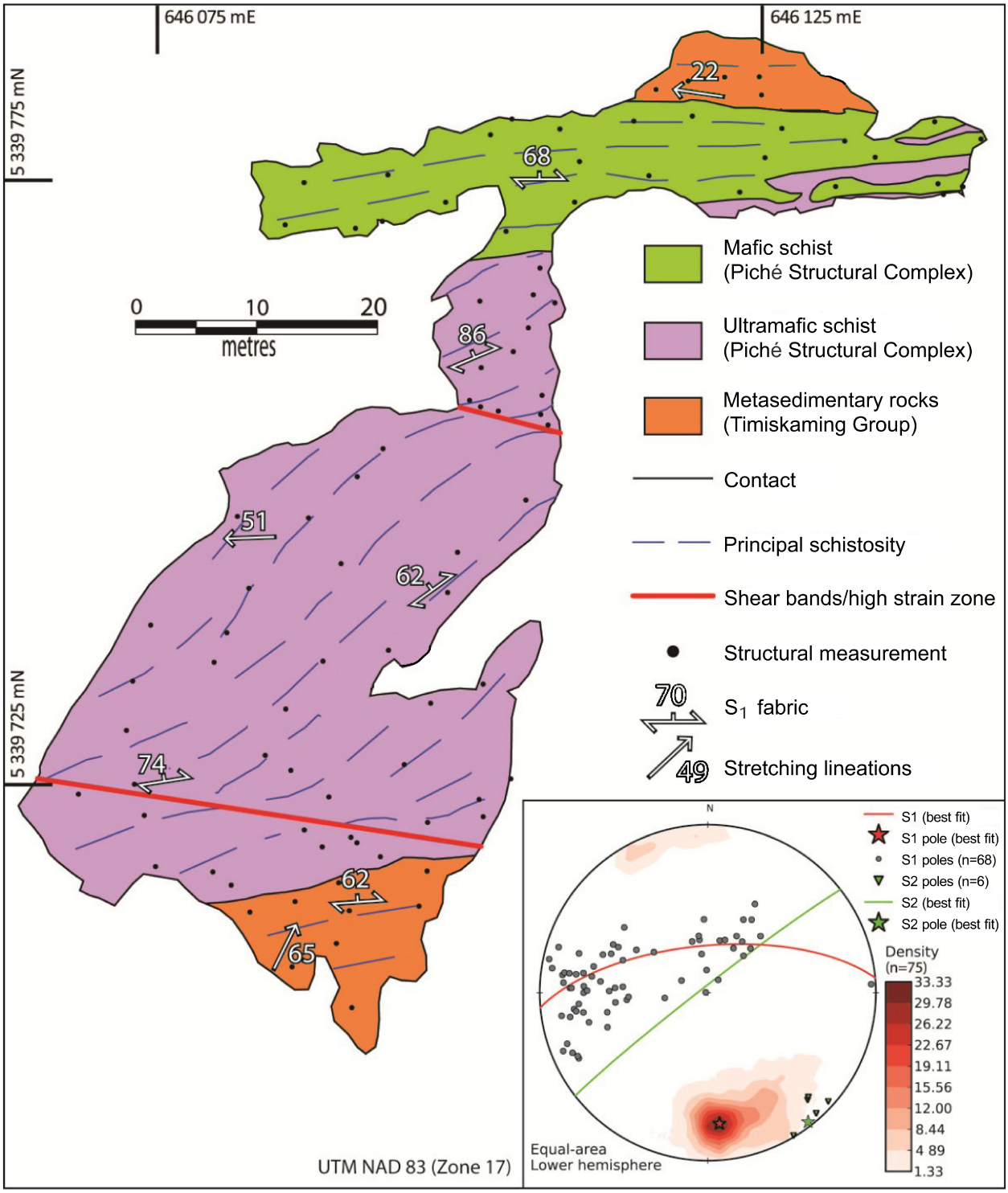

Figure 25. Geological map of the Astoria trench (Day 3 Stop 5), as marked on Photo 15, highlighting the footwall and hanging-wall contacts between carbonatized ultramafic rocks and Timiskaming Group metasedimentary rocks (*modified from* Bedeaux 2018, p.336).

Stop 6. Larder Lake–Cadillac deformation zone at Augmitto trenches 2 and 4: Piché Structural Complex komatiites, altered (albitized) mafic dike swarm, carbonate alteration, chromium-iron mica, tourmaline, folded Larder Lake–Cadillac deformation zone on the north side and calcite-chlorite-rich shear zone on the south side of the Piché Structural Complex (Rang Hull–Yorbeau–Augmitto trench)

UTM 641500E 5339770N

Potential hazards:

- Steep and/or slippery slopes; loose rocks
- Vertical outcrops with loose debris; rockfall hazard, hard hats must be worn

The best description for this stop is provided by Poulsen (2017a, p.164-165) (with minor modifications within square brackets):

> The hanging-wall sedimentary rocks are well-exposed near the headframe [and thought] as a whole to face southward based on graded bedding [(location "A" in Figure 26) before arriving at the Augmitto trenches 2 and 4 (location "B" in Figure 26)]. The rocks are moderately carbonate altered, and meter-wide sericite-carbonate bedding parallel shear zones containing gray quartz veins are common. These veins and related alteration are overprinted by the Z-shaped folds.
>
> Both contacts of the Piché Group [Figures 26 and 27] are arguably faults. The Piché Group is composed mainly of ultramafic komatiite that is variably carbonate altered and foliated. Spinifex texture is locally preserved (Trench 4) where deformation and alteration are weak. Distinctive calcite-chlorite-quartz alteration results in a banded rock, which also contains an Mn-bearing phase (possibly the pyroxene namansilite). This banded, Ca- and Mn-enriched, metasomatic rock is found along the southern, footwall of the Piché Group and, along with a local graphitic phyllonite, defines the Larder Lake-Cadillac Break as a shear zone in this sector.
>
> Albitite dikes [Figure 27] are typically [boudinaged with] the long axes aligned on an azimuth of 070°–080°. The dikes form a swarm which can be traced obliquely across the volcanic rocks of the Piché Group. At surface, the albitite dikes are distinguished by their red-brown oxidation in contrast to the orange-weathering ultramafic rocks but in drill core they appear to be distinctively pink to beige and are difficult to scratch. The mineral assemblage is albite-ankerite-quartz-pyrite-arsenopyrite and several channel samples indicate grades of 0.5 to 1 g/t Au. Whole-rock and trace element geochemical data suggest that the albitite dikes are derived from a mafic to intermediate igneous protolith, in places distinguished only by a higher than normal content of P_2O_5. Addition of both Na_2O and CO_2 is required to explain their current compositions.
>
> Although gold is locally found in Timiskaming sedimentary rocks in the immediate foot- or hanging-wall at Augmitto, ore is mostly composed of ankerite-magnesite assemblage carbonate rocks, particularly in the southern, structurally lower, part of the Piché Group. The highest gold grades tend to occur where green mica (fuchsite) is part of the assemblage. Arsenopyrite and dravite tend to mark the gold-bearing zone and visible gold is common in the deposit. In detail, visible gold is commonly associated with arrays of centimeter- to millimeter-thick buckled gray quartz veins and veinlets which tend to form irregular stockwork zones.

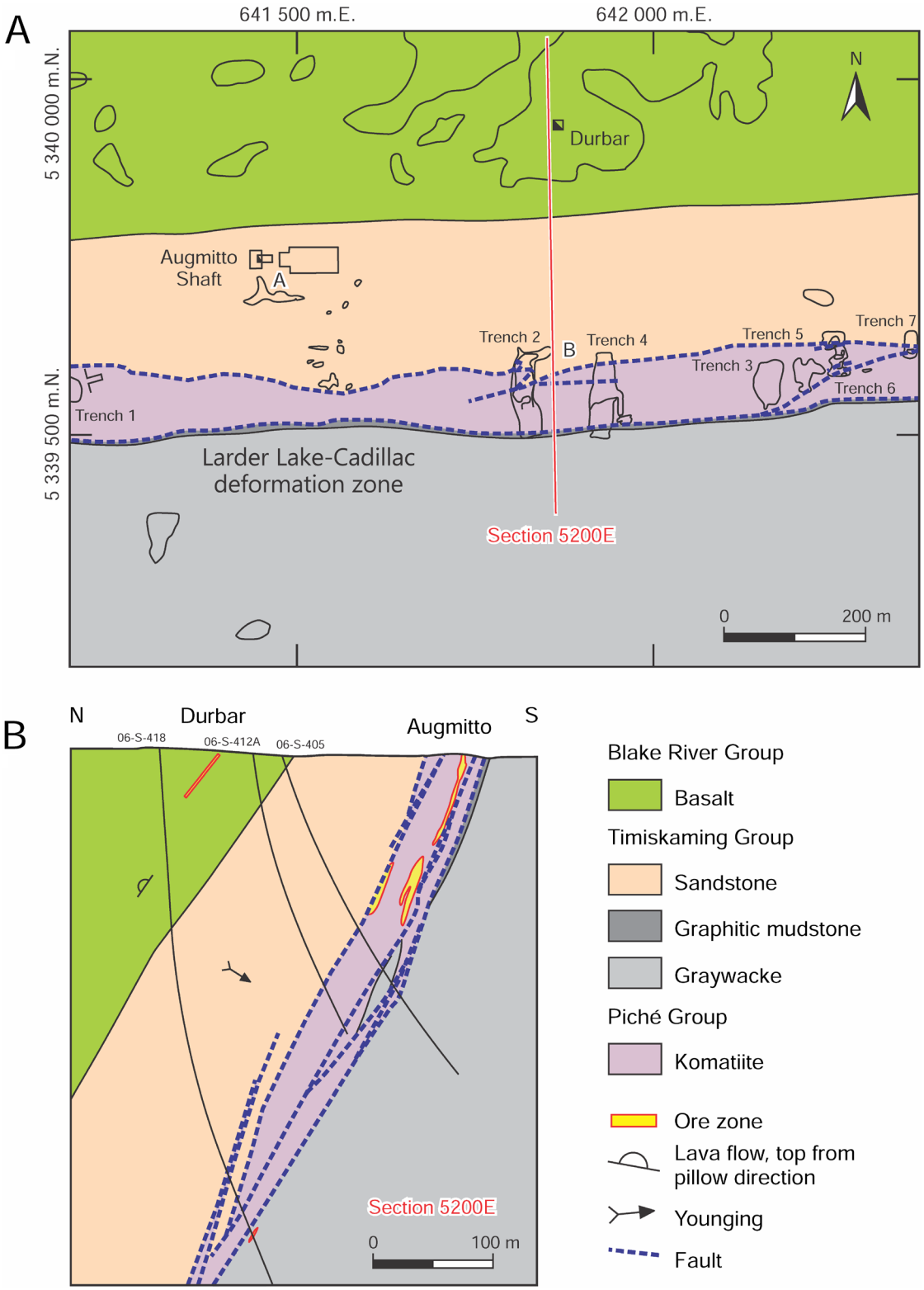

Figure 26. **A)** Geological map of the Augmitto deposit, Rouyn-Noranda (Day 3 Stop 6) (*from* Poulsen 2017a). The surface geology shows the distribution of rock types. The headframe area and trenches 2 and 4, identified by the letters "A" and "B", respectively, are described in the text for Stop 6. All UTM co-ordinates provided using NAD83 in Zone 17. **B)** Cross section through the Augmitto–Durbar deposits (*from* Poulsen 2017a).

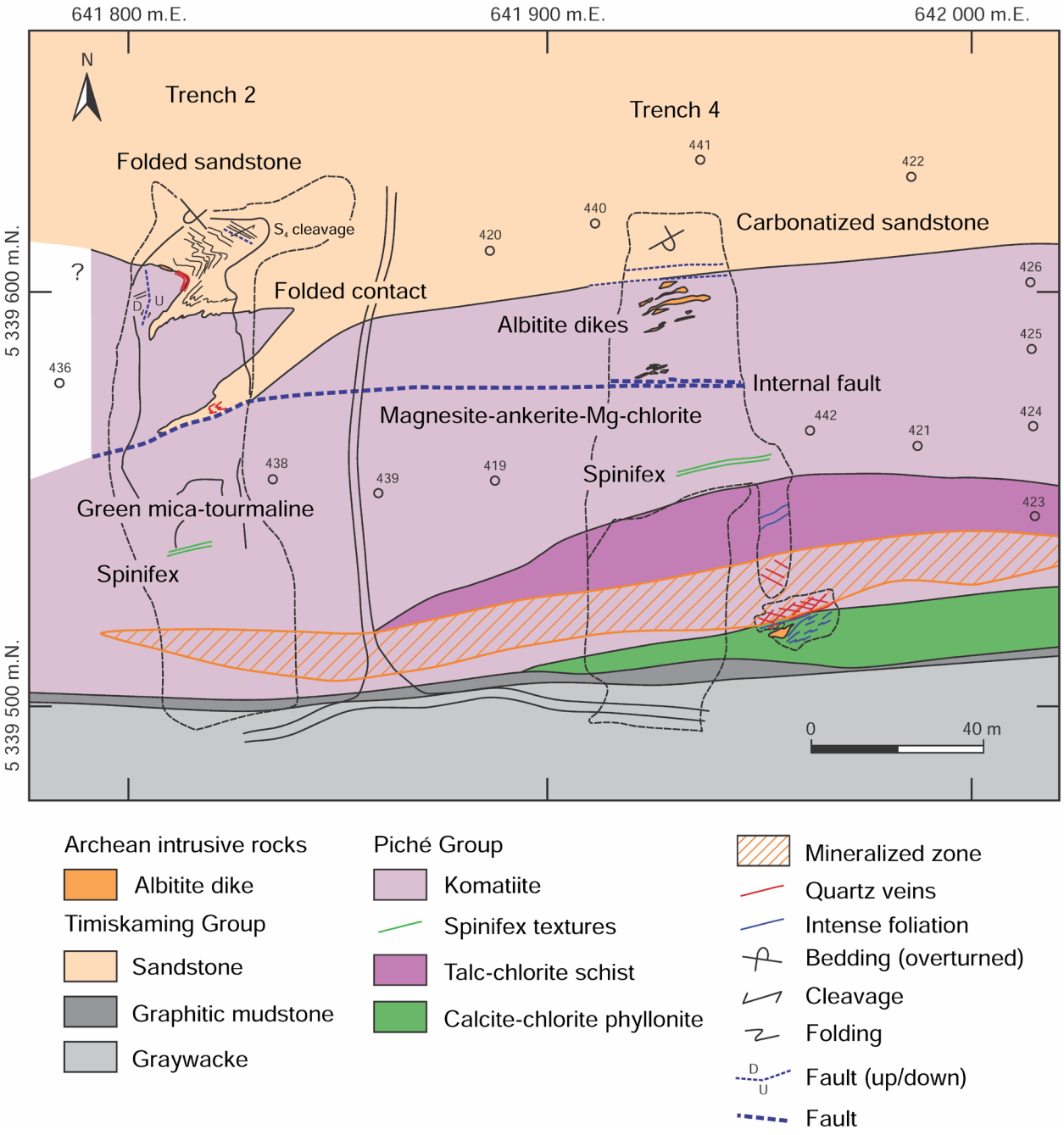

Figure 27. Detailed geological map of the Augmitto trenches 2 and 4 (outlined with small dashed lines) (Day 3 Stop 6) (*from* Poulsen 2017a). Collars of nearby diamond-drill holes (open circles) are numbered. All UTM co-ordinates provided using NAD83 in Zone 17. Abbreviation: Mg, magnesium.

Stop 7. Gold-mineralized core from the Augmitto–Astoria segment along the Larder Lake–Cadillac deformation zone (Rang Hull–Yorbeau Resources)

UTM 641509E 5339752N

Potential hazard:

- Stay away from machinery
- Please avoid lifting the core boxes or shifting the stands on which they rest. Improper lifting techniques and falling core boxes can cause serious injury.

At the time of writing this field guide, it is uncertain what core we will be inspecting but we plan to examine core of 2 mineralized sections from the Augmitto–Astoria segment.

DAY 4. ROUYN-NORANDA AREA, BLAKE RIVER GROUP: BASE METAL DAY

The day trip departs from the Quality Inn in Rouyn-Noranda and all the stop locations are shown on Figure 5. Logistics would be driving east-southeast along Highway 117 to Stop 1 and then returning on the same route to Stop 2 (*see* Figure 5). Stop 3 is located north of Stop 2 via rue Saguenay and then turning right onto rue Gibson, the last street leaving Rouyn-Noranda and before the Horne Smelter (*see* Figure 5). Continuing north on Highway 117, Stops 4 to 7 are accessed by turning left onto chemin Bradley and then immediately right onto chemin Powell (*see* Figure 5). Retrace route back to Highway 117, and continue north on Highway 117 to Stops 8 and 9 (*see* Figure 5). Continue north on Highway 117 to chemin Jolicoeur to access Stops 11, 12 and 13 (*see* Figure 5).

Stop 1. Parc Lapointe basalt flows (and iron-carbonate alteration)

UTM 648162E 5343078N

Potential hazards:

- Steep and/or slippery slopes; loose rocks

The Rouyn-Noranda District is famous for its VMS deposits and excellent exposures of well-preserved volcanic rocks that are weakly metamorphosed and little deformed. Parc Lapointe (Figure 28) provides an example of the exceptional preservation of primary features of Archean metabasaltic pillowed and massive coherent flows. Dimroth et al. (1982) invoked a lava plain setting to explain the nature and architecture of such widespread tholeiitic lava flows, which are located near the stratigraphic base of the Lower part of the Blake River Group. Well demonstrated here are pillow lavas, some with lava levels that formed by lava drainage during waning eruption, medium-grained lava tubes and massive coherent lavas with fluidal amoeboid breccia flow tops and hyaloclastite (localities A and B). At locality D (*see* Figure 28), the massive lavas are carbonate altered adjacent to a north-northeast-trending structure that locally contains auriferous quartz-arsenopyrite veins.

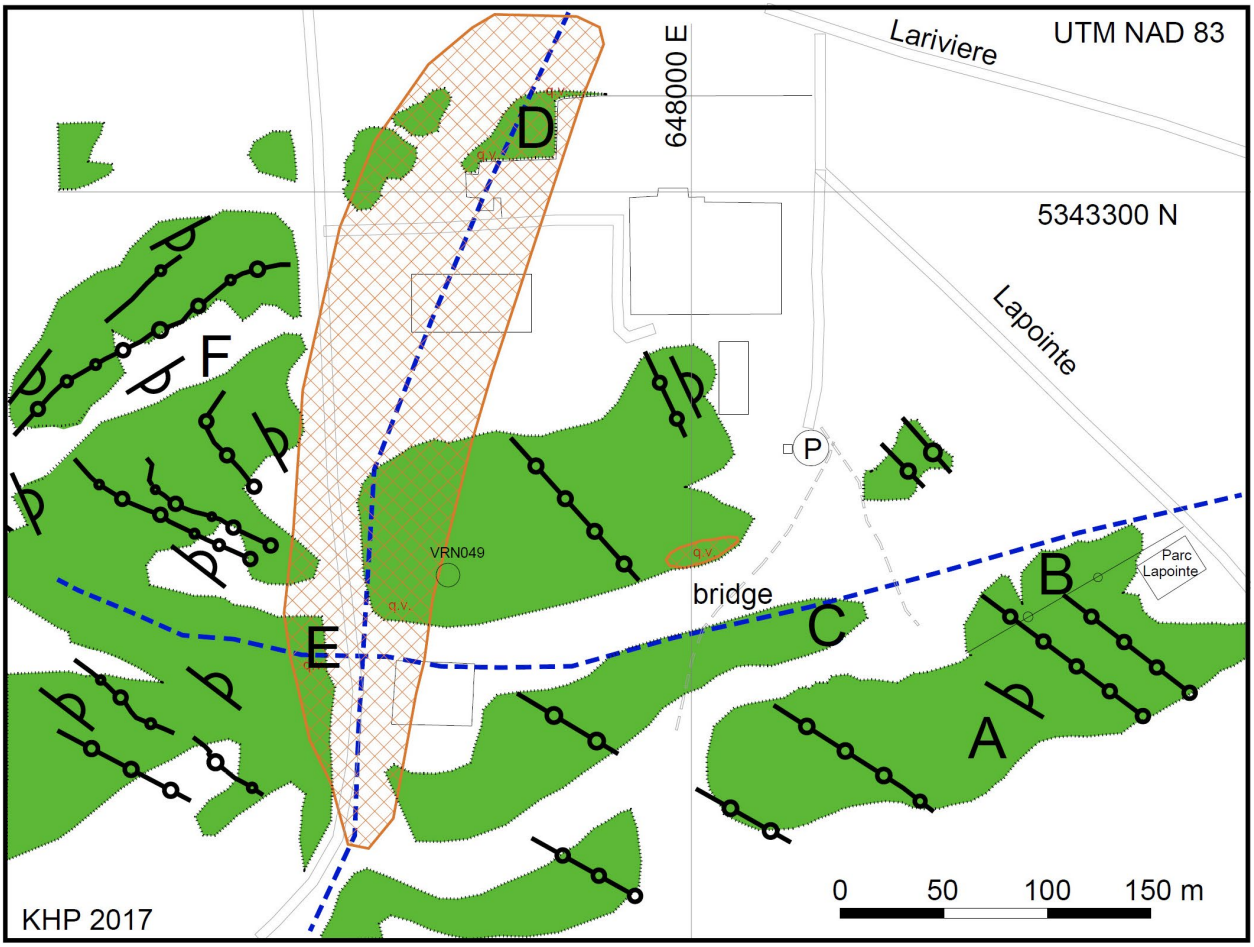

Figure 28. Geological map of basaltic lava (shown in green) at Parc Lapointe showing the locations of Day 4 Stop 1 localities A and D (*from* Poulsen 2017b). Flow contacts are indicated by lines with small circles; pillow lavas are shown by a half-circle on line symbol. Localities C, E and F are pillow lavas that are not visited.

Stop 2. Chadbourne breccia (small exposures in Park Chadbourne) (optional)

UTM 645520E 5345250N

Potential hazards:

- Park is in a residential area, monitor traffic
- Don't hammer outcrops

The rehabilitated site of the former Chadbourne gold deposit provides an excellent viewpoint of the city of Rouyn-Noranda (*see* Figure 5). The Chadbourne deposit is a gold-bearing breccia pipe that was discovered through trenching conducted by the Thompson–Chadbourne Syndicate in 1923 (Walker and Cregheur 1982; Gibson, Walker and Coad 1984; Couture 1996). However, as a result of the discovery of the Horne deposit, work at Chadbourne stopped in 1924 (Roberts 1956; Walker 1981). Following intermittent periods of surface and underground exploration during 1932–1969, gold mineralization to a depth of 320 m was confirmed. Following a period of lower gold price, production at Chadbourne commenced in 1979 (Walker 1981; Walker and Cregheur 1982) and the deposit produced 1.7 Mt of ore grading 3.24 g/t Au and 1.2 g/t Ag until closure in 1986 (Falco Pacific Resource Group, news release, December 19, 2013).

The Chadbourne breccia pipe crosscuts steeply dipping andesitic and rhyolitic flows of the Lower part of the Blake River Group south of the Andesite fault (Walker 1981; Walker and Cregheur 1982). The breccia is elliptical in plan with a northerly extent of 300 m and an easterly extent of 120 m. The breccia plunges 80° to the southeast and continues to a depth of 750 m below surface. Contacts between the wall rocks and Chadbourne breccia are transitional and *in situ* brecciation of adjacent wall rocks has been recognized (Walker 1981; Walker and Cregheur 1982). A description of the breccia from Walker (1981) and Walker and Cregheur (1982) follows. The breccia contains 90% andesite clasts, with lesser clasts of rhyolite and volcaniclastic rocks that are more abundant in the southern part of the breccia. The subangular, angular to tabular clasts range from 0.1 to 1.5 m in size, although clasts up to 15 m in size have been recognized. The clasts are affected by intense hydrothermal alteration and contain up to 30% pyrite. The matrix is a fine rock flour with up to 30% quartz, ankerite and dolomite cement. Economic concentration of gold occurs within a funnel-shaped ore zone that has a diameter of 120 m at surface and tapers to a diameter of 25 m at 240 m below surface. The highest gold concentrations are localized to cylindrical ore shoots the orientation of which is parallel to the plunge of the breccia pipe. Free gold is present as microscopic inclusions in pyrite and in quartz veinlets cutting andesite clasts (Walker 1981; Walker and Cregheur 1982). The age of the Chadbourne breccia is uncertain, but it does have similarities to the Joliet (Day 4 Stop 8) and the St. Jude breccias of the Upper part of the Blake River Group.

Stop 3. Horne West zone

UTM 646450E 5346250N

Potential hazards:

- Slippery slopes; loose rocks
- Business area, watch for local traffic

The Horne West outcrop represents the only exposed section of the Lower part of the Blake River Group stratigraphy outside of the smelter complex (*see* Figure 5); Barrett, MacLean and Cattalani 1991; Daigneault and Pearson 2006; Monecke et al. 2008; Laurin 2010; Monecke and Gibson 2013). It is located approximately 1 km west of the Horne deposit. Kerr and Gibson (1993) proposed that the volcanic succession at Horne West, which forms part of the West 3919 member of the Horne Rhyolite Formation, is located in the footwall of the giant Horne deposit (53.7 Mt, 2.22% Cu, 0.06 g/t Au, 13 g/t Ag) and is probably positioned several hundreds of metres stratigraphically below the Horne Upper and Lower H orebodies. A sample from a coherent, sericite-altered rhyolite flow from the base of the succession yielded an age of 2702±0.9 Ma (McNicol et al. 2014).

The volcanic succession at Horne West faces to the north, strikes approximately east-southeast, and dips steeply to the north (Figures 29 and 30). The Andesite fault is located immediately south of the outcrop area. Unfortunately, much of the lower portion of the volcanic succession shown in Figures 29 and 30 has been covered by recent construction, so the focus will be on the upper part which includes an aphyric, massive to flow banded and columnar jointed rhyolite cryptodome-dome overlain by monolithic rhyolite volcaniclastic units, the uppermost containing clasts of massive sulfide. The following description is *modified from* Monecke, Gibson and Goutier (2017, p.220, 222) (minor modifications within square brackets; figure and photo numbers are for this publication).

> The coherent rhyolite [cryptodome] is aphyric and aphanitic and weathers from white-buff to yellow-white and green, depending on alteration style. The rhyolite shows distinct flow [banding (Photo 16B] and is characterized by abundant mafic xenoliths. The xenoliths range from 1-2 cm to over 1.5 m in size and are gray to green [(Photo 16C)]. The contacts between the xenoliths and the enclosing rhyolite are sharp, but range from straight to scalloped. The large number of xenoliths may be a product of mafic-felsic magma mingling (Oseguera 2014). Columnar jointing represents a conspicuous feature of the coherent rhyolite unit. Joints representing the sides of the columns are regularly spaced and have orientations perpendicular to the rhyolite contact. Distinct polygonal jointing patterns can be observed in many locations within the rhyolite unit [(Photo 16D)].
>
> The upper contact of the coherent rhyolite unit to the enclosing volcaniclastic facies is sharp and strained, as evident by a pronounced foliation in volcaniclastic rocks within decimeters of the contact. Although the relationships in outcrop do not provide conclusive evidence for the emplacement mechanism... [the occurrence of] two large clasts of the xenoliths-bearing rhyolite [in an overlying volcaniclastic facies] provides evidence that the rhyolite at least locally emerged at the ancient sea floor. The rhyolite may have breached the sea floor during emplacement, or alternatively, became exposed during synvolcanic faulting.
>
> Three distinct volcaniclastic facies occur in the northernmost portion of the Horne West outcrop area [(Photos 16A and 16E)]. The lowermost unit in outcrop is a sulfide-clast-bearing lithic tuff-lapilli tuff [(*see* Photo 16A)]. This facies consists of up to 1 m thick, laterally continuous beds that range from massive to normally graded. The rhyolite clasts contained in this facies are aphyric. Pyrite-dominated sulfide clasts form a minor component of the facies and are typically concentrated at the base of individual beds. Erosional surfaces between beds of the sulfide-clast-bearing lithic tuff-lapilli tuff facies are common. This includes basal scours and channels. The channel axes of the basal scours have a steep plunge, not unlike the chlorite-wisp–bearing lithic lapilli tuff-breccia facies. This observation [is consistent with the interpretation] that the volcanic succession at Horne West formed within a discrete fault-bounded topographic low, allowing channeling of mass flows as proposed by Kerr and Mason

(1990). A synvolcanic fault that may have acted as a basin-bounding structure has been recognized in the western portion of the Horne West outcrop area.

Mass-flow deposition of the sulfide-clast-bearing lithic tuff-lapilli tuff facies was followed by deposition of a fine lithic tuff facies [(Photo 16E)]. Individual beds in this facies are typically planar and laterally continuous, but the presence of local scour surfaces indicates that deposition of this facies was accompanied by erosion of the substrate material. The fine lithic tuff facies contains several clasts of aphyric rhyolite that may represent ballistic fragments... or clasts derived from a nearby topographic high [(Photo 16E)]. Bedding sags below these clasts indicate that the fine lithic tuff was wet and cohesive at the time these clasts were deposited [(*see* Photo 16E)].

The fine lithic tuff facies is overlain by several up to 5-m-thick beds of a sulfide-clast-bearing quartz-phyric-rhyolite breccia [of the Mineralized zone (*see* Figures 29 and 30; *see* Photos 16A and 16F)]. Beds of the sulfide-clast-bearing quartz-phyric-rhyolite breccia have a reversely graded base and a normal graded interior. The breccia facies contains abundant rhyolite clasts, many of which are distinctly quartz-phyric. The coarse portions of the breccia beds are framework supported and contain cobble- to boulder-sized rhyolite fragments. In addition, large pyrite-dominated sulfide clasts are concentrated in the lower portion of individual beds [(*see* Photo 16F)]. Most of the sulfide clasts are recessive and strongly weathered, but their presence can be identified by extensive pitting in surface outcrop. Some of the pits exceed 50 cm in diameter, suggesting that the mass-flow depositing the sulfide-clast-bearing quartz-phyric-rhyolite breccia carried massive sulfide fragments of unusual size, arguing against long-distance transport. The matrix of the coarse breccia is locally silicified, sericitized and contains up to 25% fine-grained pyrite. The textural relationships are consistent with subseafloor infiltration and replacement of the breccia, indicating deposition of the breccia within and active hydrothermal vent area.

The three volcaniclastic facies outcropping at the northern end of the Horne West outcrop area have been affected by hydrothermal alteration [(*see* Figures 29 and 30; *see* Photo 16)]. Disseminated pyrite occurs at concentrations up to 5%. The metamorphic overprint of the hydrothermally altered rocks resulted in the formation of abundant Mn-rich garnet that can be most easily recognized with a hand lens in the fine lithic tuff facies. The presence of Mn-rich garnet may indicate that hydrothermal alteration originally involved the formation of carbonate minerals. Historic drilling shows that the zone of intense hydrothermal alteration and disseminated sulfide minerals recognized at surface persists to a depth of over 400 m from surface. Many of the historic drill holes show significant gold grades.

Subseafloor replacement and infiltration of permeable volcanic rocks was a key process resulting in the formation of two gold-rich disseminated sulfide zones at Horne West. Although no massive sulfides are present in outcrop, seafloor massive sulfide accumulations must have been present, allowing incorporation of sulfide clasts into the mass-flow-emplaced volcaniclastic deposits. Horne West may have been located on the fringe of, or marginal to, a long-lived hydrothermal ore system forming stratigraphically stacked massive sulfide lenses. The characteristics of Horne West are not unlike those reported for the Horne 5 deposit (Sinclair 1971; Fisher 1974; Gibson et al. 2000).

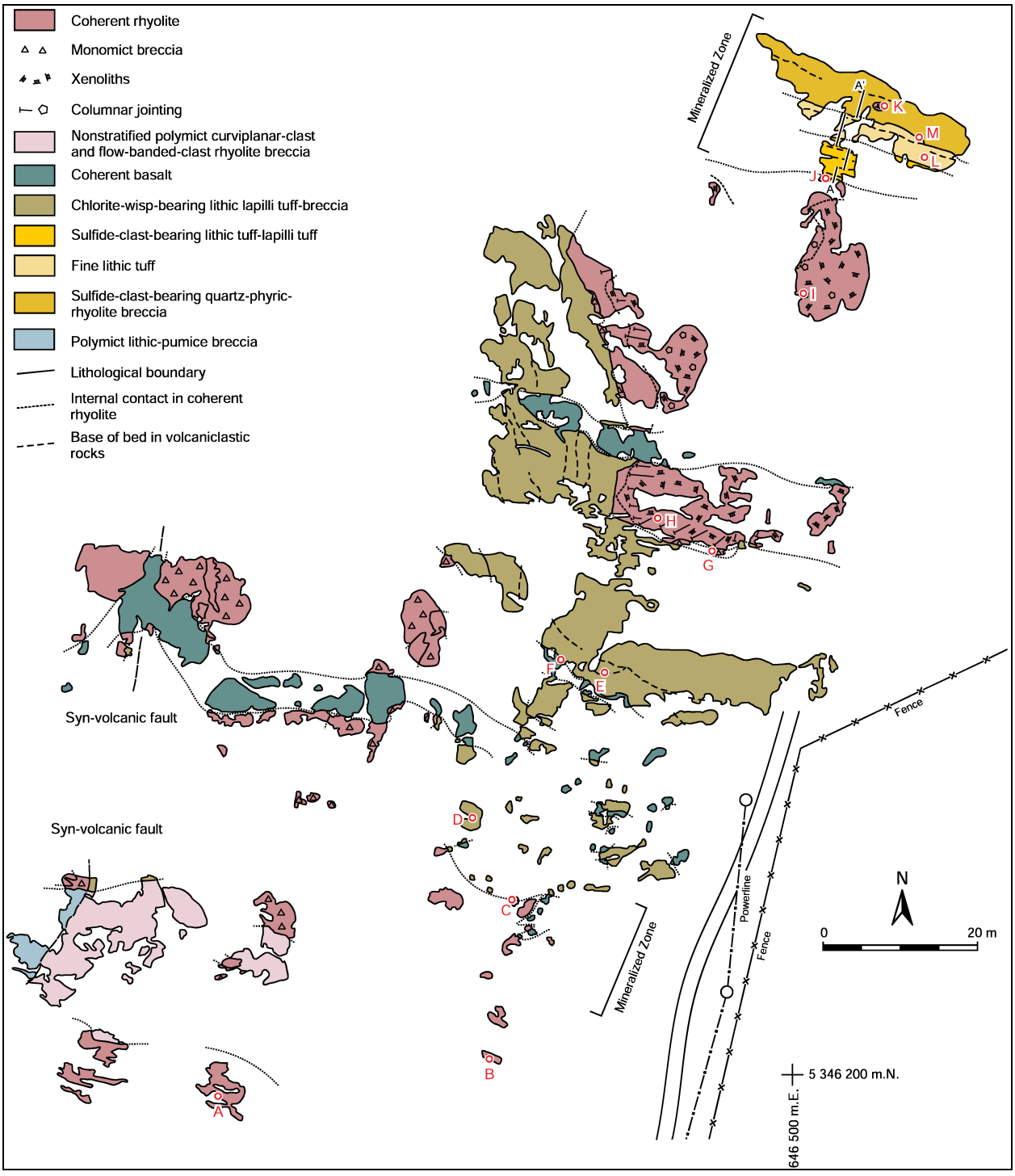

Figure 29. Geological map of the Horne West zone (Day 4 Stop 3) (*modified from* Monecke, Gibson and Goutier 2017). Details of lithofacies comprising the "mineralized zone" are shown in detail in Figure 30. All UTM co-ordinates provided using NAD83 in Zone 17.

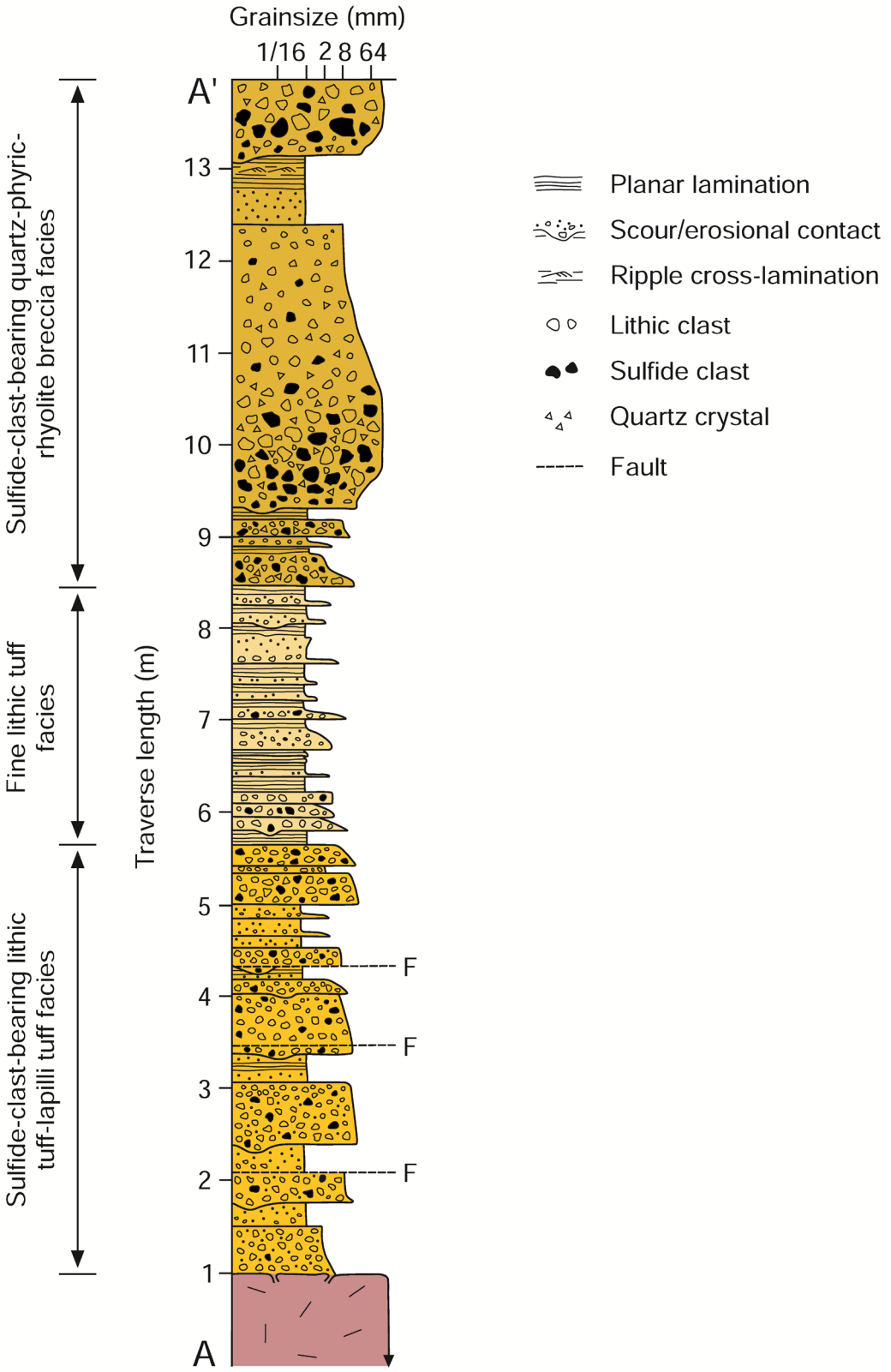

Figure 30. Stratigraphic section through lithofacies hosting the Horne West "mineralized zone" (section line A–A′) shown in Figure 29 (Day 4 Stop 3) (*from* Monecke, Gibson and Goutier 2017).

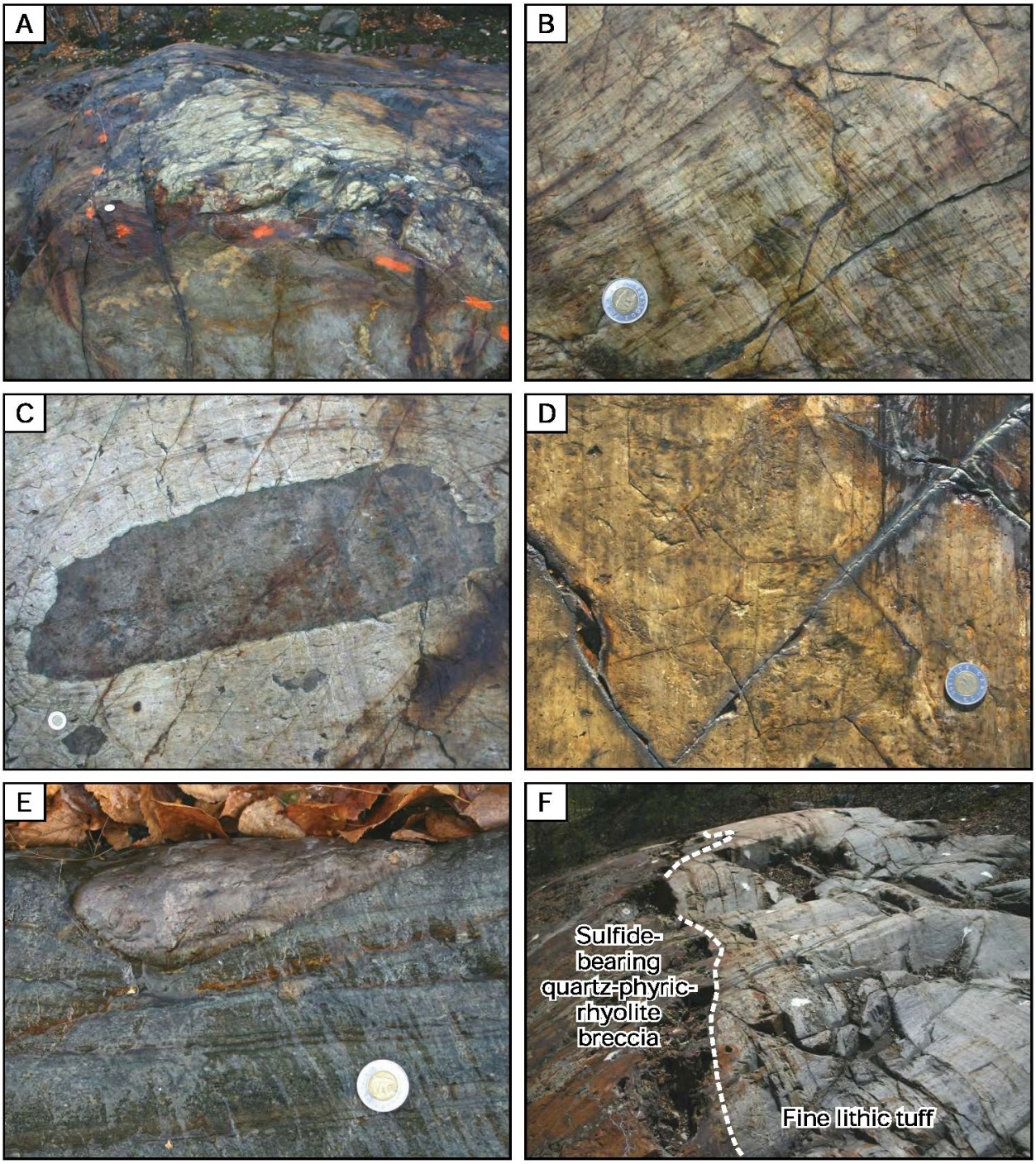

Photo 16. Photographs showing lithofacies and geological relationships at Horne West (Day 4 Stop 3) (*modified from* Monecke, Gibson and Goutier 2017). **A)** Contact between the rhyolite unit exposed in the upper portion of the Horne West outcrop and a surrounding chlorite wisp-bearing lithic lapilli tuff-breccia facies. **B)** Planar and laterally discontinuous flow banding in the coherent rhyolite cryptodome exposed in the upper portion of the Horne West outcrop. **C)** Large mafic xenolith within the rhyolite cryptodome exposed in the upper portion of the Horne West outcrop. Flow banding within the rhyolite envelops the xenolith. **D)** Small columnar joints with polygonal outlines in the rhyolite cryptodome exposed in the upper portion of the Horne West outcrop. **E)** Aphyric rhyolite fragment indenting the fine lithic tuff facies. Bedding sags beneath the fragment suggest that the volcaniclastic material was wet and cohesive at the time of fragment. deposition. **F)** Contact between the fine lithic tuff facies and the overlying sulfide-clast-bearing quartz-phyric rhyolite breccia (dashed line) of the mineralized zone shown in Figures 29 and 30. The large pits in the surface outcrop mark recessive and weathered sulfide clasts. Note for Photos 16A to 16F, coin, for scale, measures 28 mm.

Stops 4 and 5. Powell intrusive complex, Powell gold vein at Powell Hill

UTM 0644550E 5347363N

Potential hazards:

- Steep and slippery slopes when wet; loose rocks

This outcrop offers an overview of the main intrusive phases found within the Powell block and the associated mineralization and alteration features. The Powell intrusive complex is composed of shallow sill-like intrusions of quartz diorite, tonalite and trondhjemite and, similar to the Flavrian intrusive complex to the north, has been interpreted as the synvolcanic heat source that drove hydrothermal circulation and formation of the VMS deposits (*see* Figure 5; Goldie 1976; Cathles 1993; Galley 2003). The 2 main phases of the Powell intrusive complex, tonalite and quartz-diorite, are visible along the southern and western edges of the outcrop, respectively (Figure 31). The age of the older quartz-diorite phase is unknown, but age for the tonalite phase was determined to be 2701.0±0.8 Ma (Schofield et al. 2021). The quartz diorite and tonalite phases are fine grained, and aphyric, but the trondhjemite phase ranges from fine to medium grained and aphyric to weakly quartz phyric and spherulitic (Galley 2003). Miarolitic cavities filled by amphibole, quartz, chlorite and/or epidote are common in the tonalite and trondhjemite phases (Galley 2003) and are visible along the southern edge of the outcrop (Photos 17A and 17B). Contacts between the quartz-diorite and the tonalite are typically gradational over tens of metres, whereas the contacts between the felsic units are sharp to gradational over centimetres (Galley 2003).

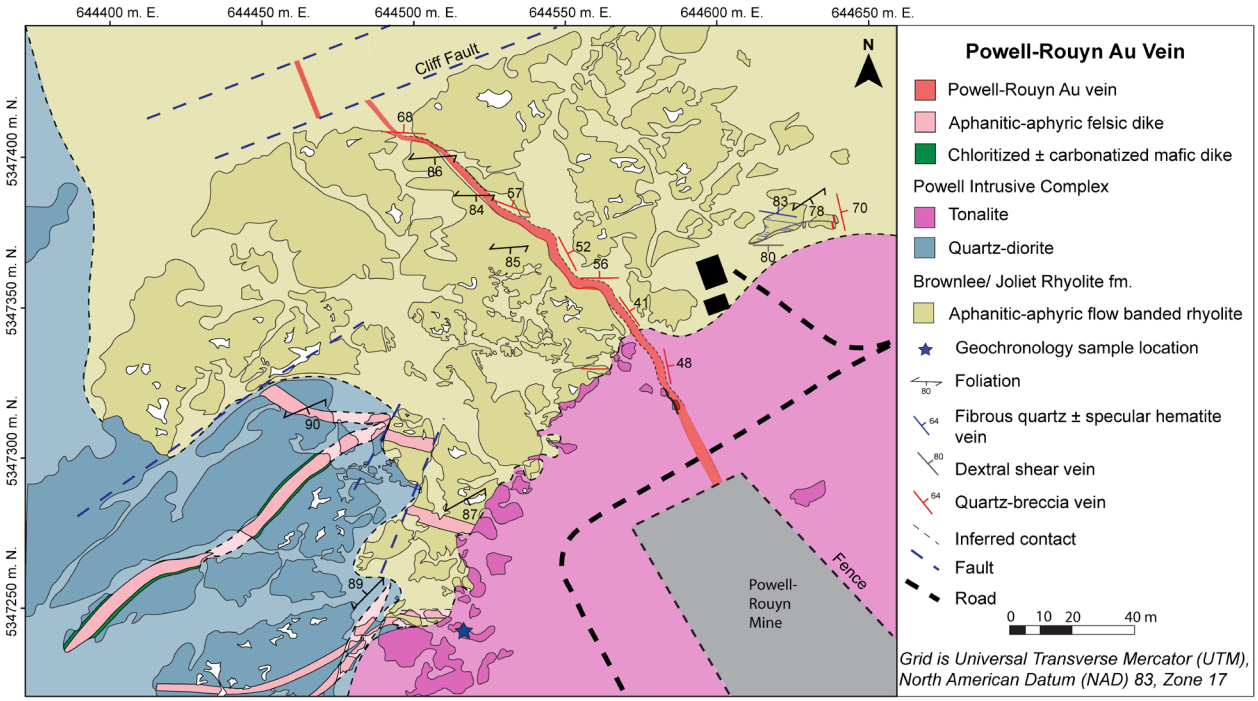

Figure 31. Geological map of the former Powell–Rouyn gold mine (Day 4 Stops 4 and 5) (*modified from* Schofield et al., in press). Note: differences in map unit colours indicate observed outcrops (darker) and interpreted geological units (lighter). All UTM co-ordinates provided using NAD83 in Zone 17.

Two types of dikes are also visible at this locality, including east-northeast-striking composite dikes with chloritized mafic margins and aphyric, spherulitic felsic cores (Photos 17C and 17D; *see* Figure 31) and north-northwest-striking chloritized and carbonatized mafic dikes. These dikes are often associated with 2 different types of veins that are found throughout the Powell block, copper-zinc-silver-rich quartz-sulfide and gold-quartz-carbonate veins, respectively.

The Powell–Rouyn gold-quartz-carbonate vein was discovered in 1922 by Tom Powell and this was the key event that triggered the Rouyn-Noranda gold rush in 1923. The deposit was in production during 1937–1956 and produced 2.7 Mt of ore at an average grade of 4.4 g/t Au, as gold-flux ore for the Noranda smelter (Carrier et al. 2000). The vein strikes 330° across the contact between the Powell tonalite and Brownlee rhyolite (Photos 17D and 17E; *see* Figure 31), and dips 65° to the northeast. It coincides with a carbonatized mafic dike, which also cuts the Powell tonalite. The vein is vuggy (Photo 17F) and is in part a breccia vein, which includes fragments of sericitized and carbonatized wall rock. It is folded and overprinted by the regional east-west-striking[†] cleavage.

This vein is one of numerous gold-bearing, quartz-carbonate vein deposits that occur within the Flavrian and Powell intrusions of the Rouyn-Noranda mining camp (Carrier et al. 2000). The majority of these veins strike north-northwest and dip moderately to the northeast, ranging in strike length from 200 to 1000 m with widths of approximately 2–3 m. The north-northwest strike of the veins appears to be controlled by mechanical anisotropies created by the mafic dikes, which occur within ~20° of the north-oriented bulk-shortening direction that led to the formation of the regional cleavage and folds and, thus, would be susceptible to dilation and slip (Robert and Poulsen 2001), likely with the assistance of elevated fluid pressures (Sibson 2001). This would suggest that the gold-quartz-carbonate veins in the Powell block formed at *circa* 2670–2660 Ma, as did many gold deposits in the southern Abitibi greenstone belt (Dubé and Mercier-Langevin 2020).

An east-west-striking brittle–ductile shear zone marked by a laminated fault-fill vein, S–C fabrics, horizontal slickenlines and oblique west-northwest-striking fibrous veins is located on the eastern edge of this outcrop (*see* Figure 31). A north-northwest-striking quartz-carbonate breccia vein that is parallel to the main Powell–Rouyn gold vein, is dextrally offset along this east-west-striking brittle–ductile shear zone. The east-west-striking veins are therefore interpreted as younger than the north-northwest striking veins, and are related to a northwest-oriented bulk shortening direction and dextral strike-slip movement along related east-west-striking faults (Schofield 2023).

[†]*Described as "east-west striking" because the dip of individual veins may change from vertical to steep north to steep south along their strike.*

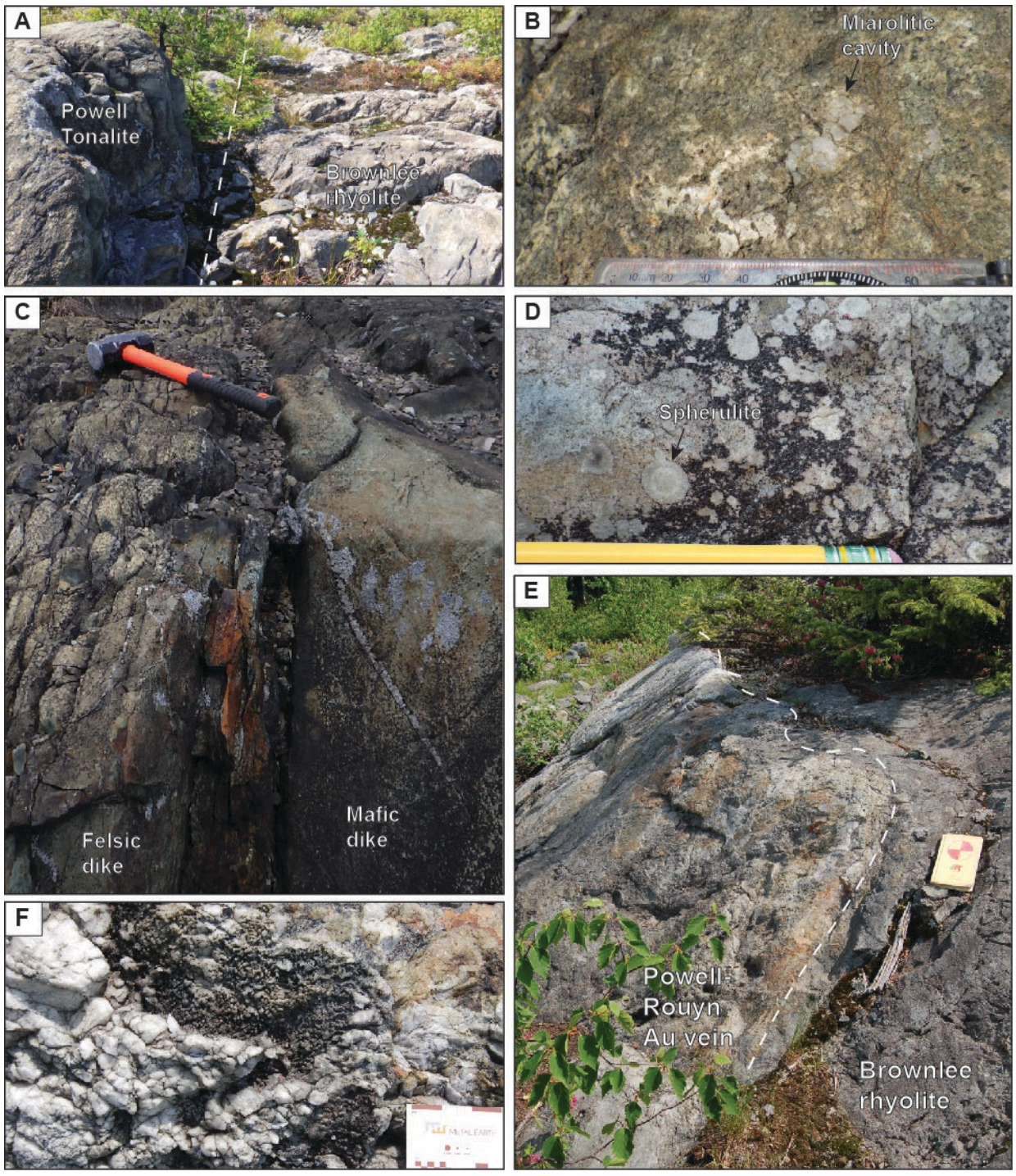

Photo 17. Field photographs of geologic relationships in the area of the former Powell–Rouyn gold mine (Day 4 Stops 4 and 5) (*from* Schofield 2023). **A)** Contact between the Powell tonalite and Brownlee rhyolite and location of geochronology sample (*see* Figure 31). **B)** Miarolitic cavities and equigranular texture of the Powell tonalite. **C)** Composite dike with chloritized mafic margins and a rhyolitic core. **D)** Spherulitic texture of rhyolite dike. **E)** Powell–Rouyn vein exposed along the edge of the outcrop showing the contact with the Brownlee rhyolite. **F)** Vuggy quartz of Powell–Rouyn vein.

Stop 6. Powell F-zone copper veins

UTM 645199E 5347752N

Potential hazards:

- Slippery slopes when wet; loose rocks on outcrops

After initial working of the Powell–Rouyn vein returned disappointing results, exploration activity turned to the copper potential of the claims during 1924–1931 (Wilson 1941). This exploration led to the discovery of the Powell and Anglo copper veins in the Powell block. At the time of discovery, besides metal content, no genetic distinction was made between the gold veins and the copper veins. Both vein systems were interpreted to have formed by magmatic hydrothermal fluids, originating from granite intrusions, which were channelled along fractures (Wilson 1941). However, early prospectors made an important observation, gold occurs along north-northwest-oriented structures and copper along east-northeast-oriented structures and, where the copper veins intersect rhyolite, massive sulfide deposits occur.

The ~1 m wide Powell F-zone vein is exposed at surface for a strike length of ~100 m, along the southern margin of an aphyric, spherulitic felsic dike (*see* Figure 5; Photo 18A). This east-northeast-striking dike crosscuts the north-northwest-striking volcanic strata at a high angle and marks a stratigraphic offset of approximately 500 m. A thick vent proximal association of quartz-phyric rhyolite comprises the northern edge of the outcrop, whereas the southern edge of the outcrop is characterized by massive to pillowed basalt flows. The contact of the felsic dike is sharp, irregular and flow banded (Schofield 2023). A polylithic breccia comprising clasts of aphyric rhyolite, quartz-phyric rhyolite and quench-fragmented, chloritized juvenile material within a silicified matrix is patchily distributed along both margins of the dike (Photo 18B) (Schofield 2023). In addition, this area is a zone of strong to intense alteration indicated by patches of massive iron-rich chlorite (Photo 18C), spotted sericite-chlorite and disseminated sulfide minerals that give the outcrop a rusty weathered appearance. The mineralogy and bulk chemistry of this alteration is similar to that associated with VMS deposits (e.g., Gibson, Watkinson and Comba 1983; Hannington et al. 2003; Franklin et al. 2005).

The Powell F-zone vein (Photos 18D and 18E) was sampled at surface, drilled by a series of holes in 1931; and, in 1951, an exploration drive was driven from the No. 2 shaft of the Powell–Rouyn mine toward the northeast along the 1550-foot level to test the economic potential of the Powell F-zone at depth (Schofield 2023). Lichtblau (1979) provided a non-compliant estimate of 24 460 tonnes of mineralization at a grade of 7.88% Cu, 118.3 g/t Ag and 0.24 g/t Au for the Powell F-zone occurrence.

The regional east-west-striking S_2 cleavage (S_1 at Astoria: Day3 Stop 5) overprints both the felsic dike and the vein. Furthermore, the vein pinches and swells along strike and is locally offset by east-west- and north-northwest-striking faults. Smaller (5–20 cm wide), oblique quartz-sulfide veins that branch off from the main vein are also offset by a brittle east-west-striking fault and the S_2 cleavage overprints the brittle fault and wraps around the competent segments of the offset vein (Photo 18F). This suggests that both the vein and dike were emplaced prior to the D_2 event. The Powell F-zone vein is interpreted to represent the deep plumbing system that may have fed VMS deposits higher in the stratigraphic pile (Schofield 2023).

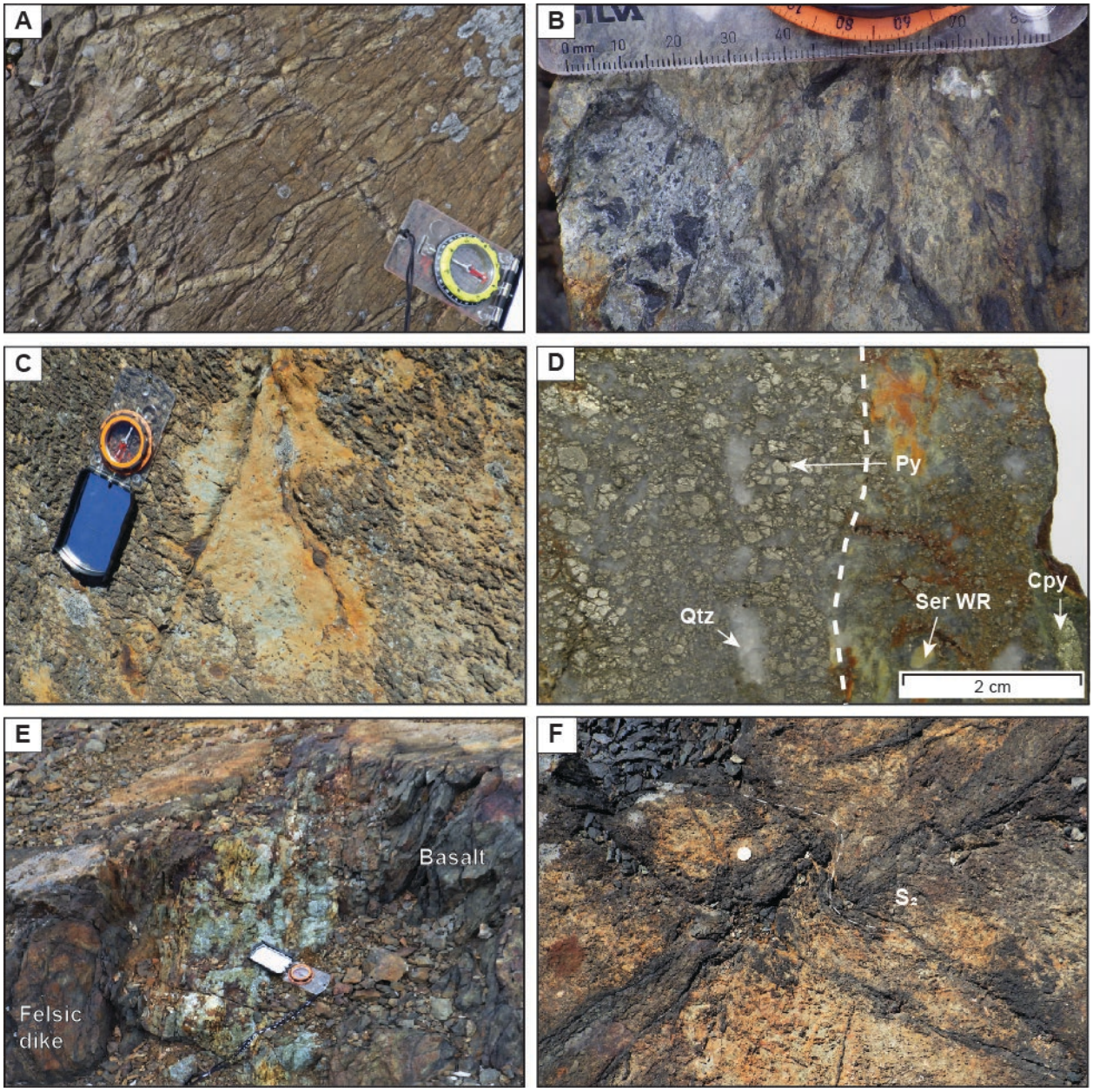

Photo 18. Field photographs of geologic relationships in the area of the Powell F-zone copper occurrence (Day 4 Stop 6) (*from* Schofield 2023). **A)** Columnar jointed aphyric-aphanitic felsic dike. **B)** Quench-fragmented juvenile fragments and silicified matrix of polylithic breccia along margin of felsic dike. **C)** Patch of intense iron-rich chlorite alteration and sulfides in basalt. **D)** Polished slab of Powell F-zone vein. **E)** Powell F-zone vein at contact between felsic dike and basalt. **F)** Oblique veins offset by brittle fault and overprinted by S_2 cleavage. Abbreviations: Cpy, chalcopyrite; Py, pyrite; Qtz, quartz; Ser WR, sericitized wall rock).

Stop 7. Joliet Rhyolite overview

UTM 645969E 5347640N

Potential hazards:

- Steep walk along access road
- Stay with group

This locality provides an excellent overview of a monogenic rhyolite shield that extends east from the Joliet Rhyolite approximately 6 km along the Horne Creek fault to the Delbridge rhyolite and VMS deposit (*see* Figure 5). This monogenic rhyolite shield is the largest in the Rouyn-Noranda District, and, along with the Powell intrusive complex, defines a magmatic centre within the NVC that contains not only the largest VMS deposits in the District, but deposits that are gold rich. The Horne Smelter occupies the site of the former Horne Mine, and the former Quemont mine site is located in the low ground north of the smelter complex.

Stop 8. Joliet Breccia

UTM 0646587E 5347815N

Potential hazards:

- Steep and slopes slippery when wet; loose rocks can make walking difficult
- 1 km walk to outcrop, bring water, sun screen
- Stay with group

This outcrop is composed of a spherulitic, quartz-feldspar porphyritic felsic dike, which is ~350 m wide with a strike length of ~1.5 km (Schofield 2023; Figures 5 and 32). This dike, along with 2 parallel dikes to the south, were named the Quemont feeder dikes by de Rosen-Spence (1976) because they were interpreted to feed the coherent rhyolite that forms the hanging wall to the Quemont VMS deposit. Similar to the Powell F-zone dike, the northernmost Quemont feeder dike marks a major stratigraphic offset and is associated with a copper occurrence (Joliet Breccia) (Schofield 2023). The contact margins of the dike are sharp, irregular, and typically not foliated. The age of this dike is uncertain, but it has been interpreted to have been emplaced during the same magmatic event as the 2 parallel dikes to the south, one of which yielded a U/Pb zircon age of 2702±0.8 Ma (McNicoll et al. 2014; Schofield et al. 2021).

The Joliet Breccia is a 250 m by 150 m breccia body (*see* Figure 32), composed of angular, poorly sorted, lithic clasts derived from the immediate host rocks in a hydrothermal cement. The cement consists of prismatic comb-textured quartz (3–5 mm long) ± acicular iron-chlorite rosettes ± sulfides (Photos 19A and 19B). Based on the relative abundance of felsic and mafic clasts, the Joliet Breccia is divisible into 3 west-southwest-striking domains: felsic, transitional and mafic (Photos 19C, 19D and 19E). Clasts within all domains are poorly size-sorted and have distinctly angular, rectangular to tabular shapes with curviplanar margins. They are commonly oriented with their long axis parallel to the internal contacts between domains. Internal domain contacts and the contact between the breccia and the host rocks are gradational and the breccia noticeably lacks sedimentary features such as bedding. The outer limit of the Joliet Breccia is defined by an asymmetrically developed, 6 m wide zone of altered conjugate fractures containing localized areas of *in situ* breccia. The contact between the *in situ* brecciated Quemont feeder dike and the felsic dominated domain of the Joliet Breccia is gradational and defined by the first appearance of breccia with quartz infilled open void space >10% by area (*see* Photo 19A). The tonalite contact with the breccia is sharp, and is not chilled (Photo 19F) (Schofield 2023). In addition, at the thin section scale, quartz phenocrysts within the tonalite at the contact are broken, indicating brecciation took place after the tonalite was emplaced. A new U/Pb TIMS zircon age of 2698.0±0.9 Ma (2σ) for a tonalite

block within the breccia constrains the maximum age of brecciation (Schofield et al. 2021). This would place the Joliet Breccia as broadly coeval with the Upper part of the Blake River Group stratigraphy and its defining characteristics discussed above suggest a subsurface magmatic-hydrothermal origin (Schofield et al. 2021).

In addition, the lateral zoning of alteration types, compositional gains and losses, and metal tenor associated with the Joliet Breccia occurrence are similar to the Powell F-zone and VMS footwall alteration zones within the District. As such, these breccias and veins are interpreted as part of a broad continuum of subsurface, cross-stratal magmatic-hydrothermal mineralization to seafloor, stratiform, VMS mineralization, a spectrum akin to the porphyry-epithermal continuum of modern subaerial volcanic arcs (Schofield et al. 2021).

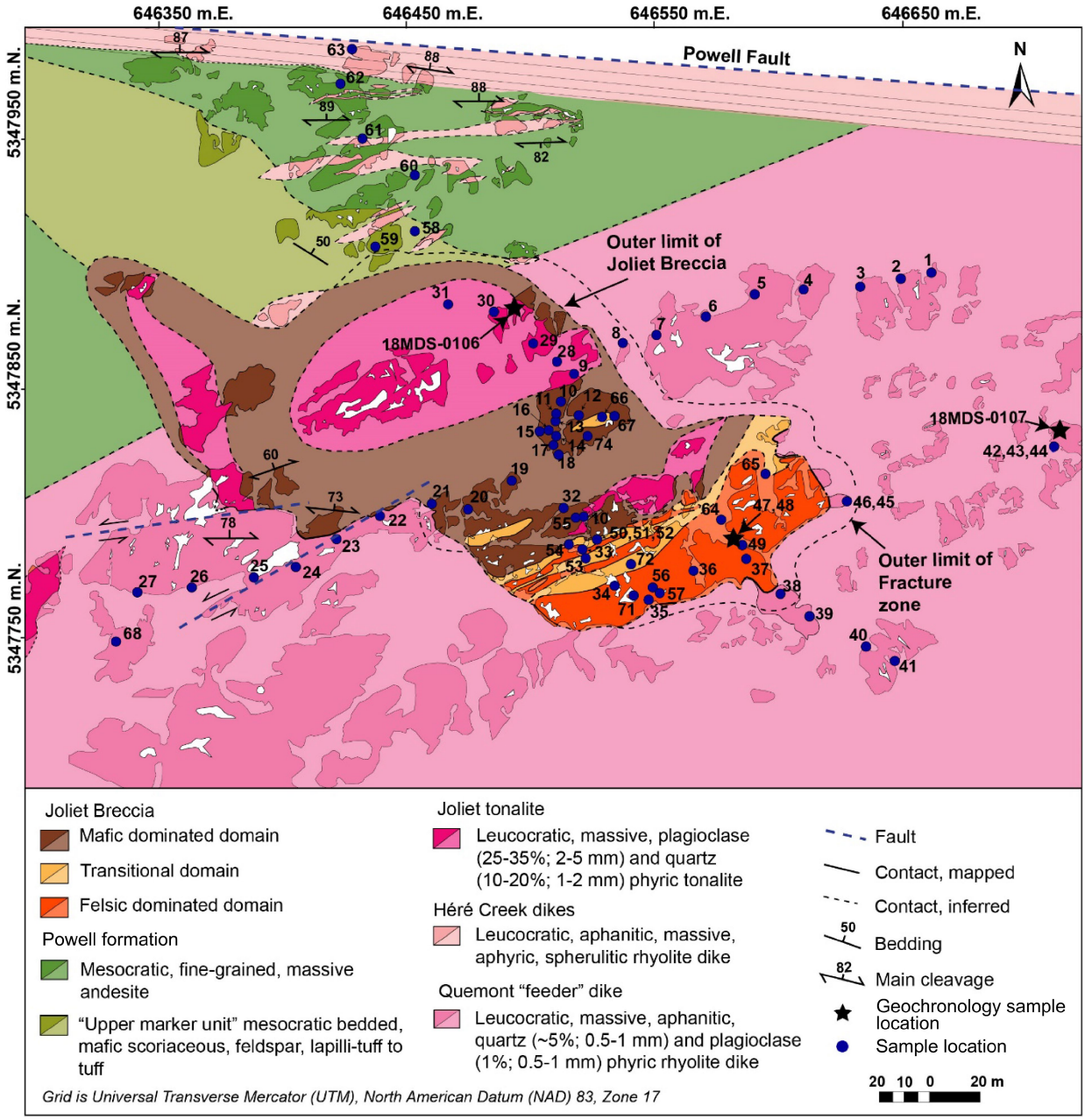

Figure 32. Geological map of the Joliet Breccia (Day 4 Stop 8) (*from* Schofield 2023, p.60). All UTM co-ordinates provided using NAD83 in Zone 17.

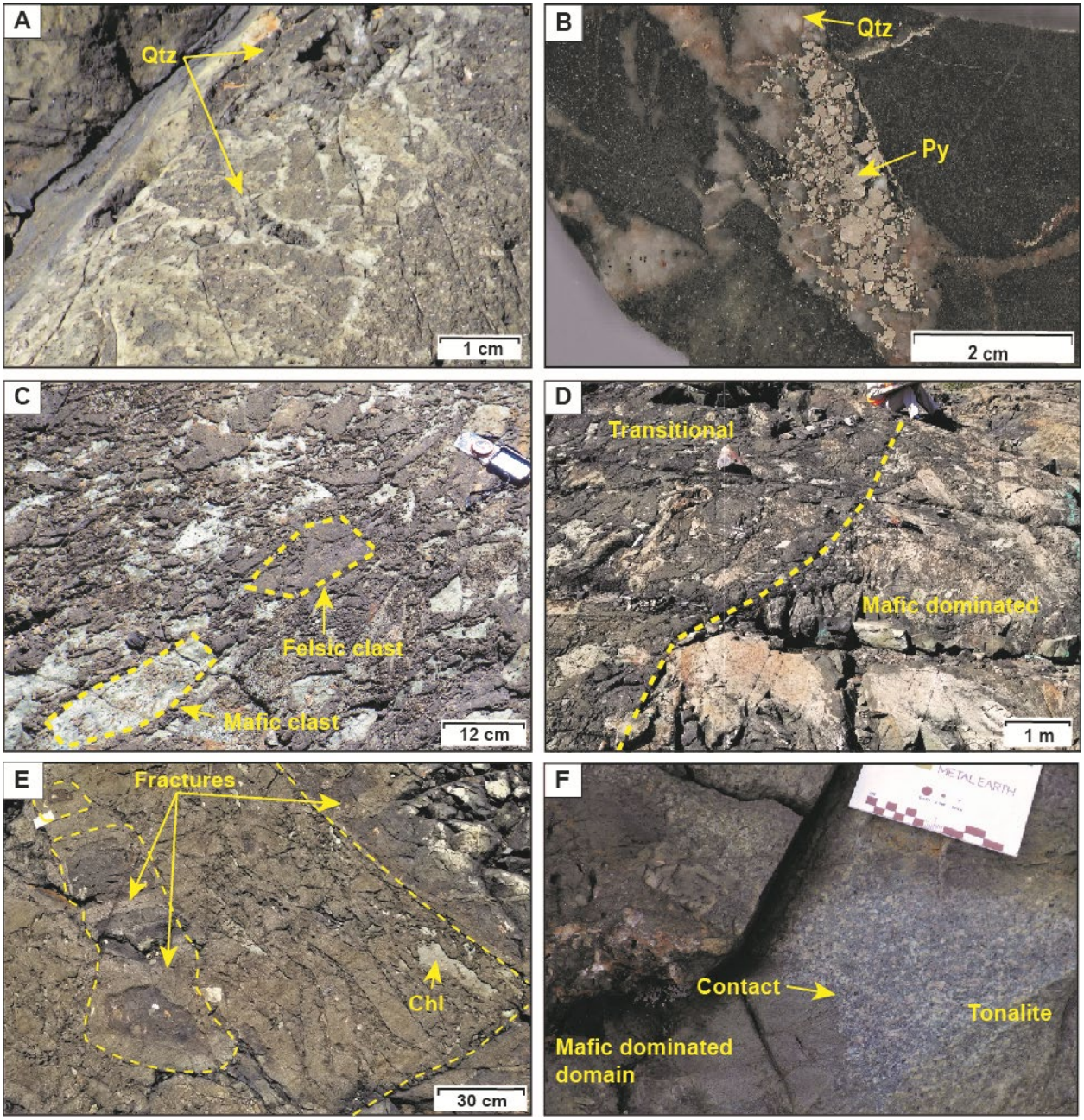

Photo 19. Field photographs of geologic relationships in the area of the Joliet Breccia (Day 4 Stop 8) (*from* Schofield 2023). **A)** *In situ* brecciated Quemont feeder dike with hydrothermal cement of vuggy quartz. **B)** Polished slab showing hydrothermal cement comprised of pyrite and quartz. **C)** Transitional domain. **D)** Contact between transitional domain and mafic-dominated domain. **E)** Felsic-dominated domain. **F)** Sharp brecciated contact between tonalite and mafic-dominated domain. Abbreviations: Chl, chlorite; py, pyrite; Qtz, quartz.

Stop 9. Joliet Rhyolite lobe hyaloclastite flow and Quemont Breccia

UTM 646978E 5347491N (Joliet Rhyolite)
UTM 647085E 5347465N (Quemont Breccia)

Potential hazards:

- Steep and slopes slippery when wet; loose rocks
- Busy road with high speed traffic; cross road only with group only, follow leaders
- High-visibility vests required

The Joliet Rhyolite on the west side of Highway 101 is lobe hyaloclastite rhyolite flow comprising massive, flow banded rhyolite lobes surrounded by monolithic rhyolite breccia and hyaloclastite. It represents the uppermost facies of massive Joliet Rhyolite observed at Stop 7, located 1 km to the west.

The Quemont deposit is the second largest VMS deposit in the Rouyn-Noranda camp. Discovered in 1945, the mine produced 13.82 Mt of ore grading 1.32% Cu, 2.44% Zn, 5.49 g/t Au and 30.9 g/t Ag (Gibson and Galley 2007). The Quemont deposit is hosted by felsic metavolcanic rocks with volcaniclastic units forming a significant proportion of the overall stratigraphy. A sample of massive quartz-feldspar porphyritic rhyolite, either from the Quemont Rhyolite or south Quemont Feeder Dike yielded an age of 2702±0.8 Ma, essentially identical to the age of the Horne footwall succession at West zone (McNicol et al. 2014). The lithostratigraphic position of the Quemont Breccia relative to the Quemont VMS deposit is uncertain, but mine data (Weeks 1963) suggest that the massive sulfides at Quemont were hosted by rhyolite breccia at or near the contact with a quartz porphyritic coherent rhyolite; the former and latter perhaps being the Quemont Breccia and Quemont Rhyolite.

The Quemont Breccia has been studied by Morris (1959), Dimroth et al. (1975), de Rosen-Spence (1976), Dimroth and Rocheleau (1979) and Lichtblau (1989). The following description (quoted and summarized) is from Lichtblau (1989, p.17-29), whose study built upon the results of the earlier studies.

> The Quemont Breccia is composed of two distinct breccia facies that overlies a massive coherent facies of the Joliet Rhyolite; a sharp contact suggests the latter could be a flow or sill. The breccia is overlain by the coherent quartz-feldspar porphyritic Quemont Rhyolite and intruded by the Quemont Feeder Dikes and Powell Rhyolite dikes (de Rosen-Spence 1976). The Quemont Breccia has a limited strike extent of 450m between the Quemont dikes, attains a maximum thickness of 240 m, and along with the overlying Quemont Rhyolite are folded into a westerly plunging anticline, the axis of which strikes N80 W. Subsequent cross folding on approximately a north axis has produced a domal effect on the original anticline. The south flank of the structural dome has been truncated by the Horne Creek fault.
>
> Quemont Breccia has been divided into two conformable facies, a lower Breccia I and an upper Breccia II; the former has been subdivided into two cycles. Breccia I is 120 m thick and comprises lapilli and blocks of plagioclase microphyric rhyolite and andesite in a matrix of plagioclase microphyric rhyolite, basalt, andesite and aphyric rhyolite. Rhyolite lapilli and blocks are massive to moderately vesiculated (chlorite-filled), are commonly flow banded, and they strongly resemble underlying Joliet Rhyolite. Quemont Breccia I displays an upward coarsening from the base, then gradually upward fining (Cycle 1). A discontinuous aphyric rhyolite flow and breccia separates Cycle 1 from Cycle 2. Cycle 2 displays an upward coarsening base and upward fining top. Quemont Breccia I was interpreted by Morris (1959) as a pyroclastic deposit, formed by nuée ardente-like eruptions. de Rosen-Spence (1976) interpreted Breccia I to be a pyroclastic deposit related to the opening of the Quemont Feeder dike prior to the extrusion of Quemont Rhyolite Flow. Dimroth [et al.] (1975) interpreted Breccia I to be a pyroclastic fall-back breccia and Dimroth and Rocheleau (1979), suggested that the breccia was a subaqueous analog of a subaerial co-ignimbrite lag-fall deposit.

Lichtblau (1989) interpreted the eruptive centre for Quemont Breccia I to be at the site of the middle Quemont Feeder dike as the largest breccia fragments occur in close proximity to the dike contacts. He interpreted Quemont Breccia I to have formed by subaqueous phreatic eruptions at the site of the present

middle Quemont Feeder Dike and the deposit to be a product of collapsing eruption columns that rimmed the vent with coarse debris left behind, as a lag deposit, by pyroclastic flows. The presence of a thin, localized Joliet Rhyolite type flow within the breccias attests to the continued presence of rhyolitic magma in the vent.

Lichtblau (1989) described Breccia II as a chaotic, unsorted tuff-breccia, composed of plagioclase microphyric rhyolite (as the underlying Breccia I) and quartz phyric rhyolite fragments, the latter identical to overlying Quemont Rhyolite. Lichtblau (1989) interpreted Breccia II to be, at least in part, a flow foot breccia to the Quemont Rhyolite. The recognition of wispy fluidal quartz-porphyritic rhyolite clasts and crystals in the matrix by the authors suggest that it may be a peperite developed at the base of the Quemont flow as it was emplaced onto unconsolidated Quemont Breccia I.

Stop 10. Delbridge Rhyolite complex and volcanogenic massive sulfide deposit (optional)

UTM 651068E 5347847N

Potential hazards:

- Slippery slopes when wet; loose rocks
- May have to walk-in along access road, stay with group
- Watch for local traffic

The Delbridge Rhyolite complex is host to the small but gold-enriched Delbridge (0.37 Mt@ 0.61% Cu, 9.66% Zn, 2.8 g/t Au, 110 g/t Ag) and D'Eldona (0.08 Mt @ 0.2% Cu, 7.7% Zn, 5.3 g/t, 62.4 g/t Ag) VMS deposits (*see* Figure 5) (Gibson and Galley 2007).

The Delbridge Rhyolite complex comprises 8 flows and domes intruded by a central aphyric rhyolite intrusion that is the feeder for the youngest flow (Boldy 1968; Barrett, Cattalani and MacLean 1993). Strata of the 900 m thick, 1.5 km complex face and dip steeply to the east and lie within an anticline. A pronounced 080° trending axial planar cleavage transects the units. The Horne Creek and Donalda faults define the southern and northern extents of the complex. The flows and domes are characterized by massive, flow banded, *in situ* brecciated and transported monolithic breccia facies that are aphyric to variably quartz and feldspar porphyritic; variation in the percent and size of phenocrysts subdivide the complex into individual flows. Massive and pillowed basalt lavas conformably overlie the complex.

Four, thin intervals of thinly bedded to laminated intercalated mafic and felsic tuff occur within the Delbridge rhyolitic complex. The tuff, at this stop locality, is the lowermost tuff interval and defines the Delbridge–D'Eldona ore interval. The tuff is a fine-grained, thin bedded to laminated volcaniclastic unit that conformably overlies poorly stratified rhyolite breccia that contains irregular lobes of coherent and flow-banded rhyolite that are up to several metres in diameter. The breccia consists of hyaloclastite that is compositionally similar to the rhyolite lobes and may have originated from the disintegration of lobes during subaqueous emplacement. The facies relationships observed are consistent with those described for the distal portion of rhyolitic lobe-hyaloclastite flows elsewhere in the Noranda camp (Gibson 1990). The rhyolite breccia and flow below the tuff are sericite and carbonate altered and contain finely disseminated pyrite. Iron-carbonate alteration is widespread in the Delbridge–D'Eldona area and most pronounced in the stratigraphic footwall of this fine-grained volcaniclastic interval. Iron-carbonate alteration occurs in stockwork veinlets and as cement in coarse rhyolite breccia. The alteration is interpreted to be synvolcanic in timing, although the pronounced tectonic fabric and proximity to the Horne Creek fault, which is also associated with iron-carbonate alteration, makes a synvolcanic timing ambiguous.

Stop 11. Dufresnoy Gabbro

UTM 644540E 5352729N

Potential hazards:

- Steep and slippery slopes when wet; loose rocks
- Watch for local traffic; high-visibility vests required

Located at the former Millenbach mine site, this stop provides a panoramic view of the Rouyn-Noranda Main camp (*see* Figure 5). The fine- to medium-grained Dufresnoy Gabbro is several hundred metres thick, strikes north-northwest and dips at 45–50° to the east-northeast; it is one of several gabbro dikes than transect the main Rouyn-Noranda camp. A sample collected from a coarse, pegmatitic phase of the Dufresnoy gabbro at this site yielded a U/Pb crystallization age of 2697.9±0.8 Ma (McNicoll et al. 2014). This age indicates an Upper part of the Blake River Group timing for emplacement.

Stop 12. Bluff outcrop, Main Contact Tuff

UTM 643196E 5352587N

Potential hazards:

- Slippery slopes when wet; loose rocks
- Local traffic; follow trail and stay with group

The Bluff outcrop shows the Main Contact Tuff, which occurs between the Millenbach Andesite formation and the overlying Amulet Andesite formation (*see* Figure 5). The laminated tuffaceous deposit (Main Contact Tuff) is draped over large pillows (lava tubes). The brown colouration of the outcrop reflects fine biotite produced by contact metamorphism during emplacement of the Lac Dufault pluton (De Rosen-Spence 1976). The Main Contact Tuff is composed of chemical sedimentary, exhalative material (chert) intermixed with tuffaceous deposits showing local preservation of feldspar crystals and former glass, now chloritized shards (Kalogeropoulos and Scott 1989; Monecke, Gibson and Goutier 2017). The composition of the Main Contact Tuff varies from 53.0 to 78.1% SiO_2 (Kalogeropoulos and Scott 1989; G. Riverin, personal communication, 2010).

The thinly bedded to laminated tuffaceous Main Contact Tuff contains 5% pyrite, with trace sphalerite and chalcopyrite. The presence of sulfide minerals, as well as elevated base metal grades (900 ppm Cu and 700 ppm Zn), indicate hydrothermal input during tuff sedimentation at this stratigraphic interval. The variation in copper versus zinc grade can be used to vector toward mound-style massive sulfide accumulations that formed at the ancient seafloor at the time the laminated tuffaceous deposit was accumulated (Gibson and Galley 2007). The Bluff outcrop is located approximately 70 m up-dip from the small Bluff massive sulfide orebody and 450 m up-dip from the large Lower Amulet A orebody.

Stop 13. Amulet Upper A area (Upper A and Lower A deposits)

UTM 643318E 5352219N

Potential hazards:

- Steep and slippery slopes when wet; loose rocks
- Local traffic; high-visibility vests required; stay with group

The Amulet Lower and Upper A orebodies are 2 stacked massive sulfide lenses that are underlain by an extensive, discordant, well-defined alteration zone that plunges 60°–70° to the west (Figure 33). The Amulet Upper A orebody was discovered in 1927 and the Amulet Lower A orebody, located 500 m below, was found in 1938 during testing for copper stringers in the alteration zone below the Amulet Upper A orebody (*see* Figures 5 and 33). The Lower and Upper A deposits occur within the same discordant alteration zone (*see* Figure 33).

The Amulet Upper A orebody is located within basaltic lavas of the Amulet Andesite formation (*see* Figure 33), at a stratigraphic position that is marked by the occurrence of a thin pyritic andesitic tuff referred to as the Upper A Tuff. The tuff is exposed in the trench located between the glory hole of the Amulet Upper A ore lens and the Corbet Mine Road (Photo 20B). The pyritic Upper A Tuff is areally restricted to basalt massive and pillowed flows proximal to the Amulet Upper A ore lens (Santaguida, Gibson and Watkinson 1999).

The Amulet Upper A deposit offers an excellent view of the eastern part of the Rouyn-Noranda camp. The low depression to the east, which is partly occupied by Lake Dufault, marks the extent of the Lac Dufault pluton. The Glencore smelter at the location of the former Horne mine in Rouyn-Noranda can be seen to the south.

The outcrops to the west of the fenced area are located in the alteration zone of the Amulet Upper A deposit (Hall 1982; Santaguida, Gibson and Watkinson 1999), as expressed by “dalmatianite” in mafic lavas of the Amulet Andesite formation (Photos 20C and 20D). Pillowed margins are locally recognized despite the high abundance of cordierite porphyroblasts that impart a prominent “dalmatianite” spotting in outcrop (*see* Photos 20C and 20D). The cordierite porphyroblasts formed as a result of the contact metamorphism of hydrothermally altered (sericitic) lava flows during emplacement of the Lac Dufault pluton (de Rosen-Spence 1976). The occurrence of anthophyllite needles suggests that the outcrops along the fence are located close to the transition from a primary sericite alteration zone to the inner chlorite alteration core. Abundant anthophyllite, marking the former chlorite alteration zone, occurs within the fenced area closer to the glory hole. During greenschist regional metamorphism, the cordierite porphyroblasts have retrograded into a fine-grained assemblage of chlorite, sericite and biotite.

Along the hill side, a small felsic dike crosscuts lava flows of the Amulet Andesite formation in the footwall of the Amulet Upper A deposit. The dike exhibits well-developed columnar jointing with the joints oriented perpendicular to the intrusive contacts (Photo 20E); it does not contain “dalmatianite” so it was emplaced after VMS formation (Santaguida, Gibson and Watkinson 1999). Across the Corbet Mine Road, a small outcrop of pillowed and massive lavas of the Amulet Andesite formation displays patchy, epidote-quartz alteration (Photo 20F). The presence of feldspar phenocrysts in the pillowed flows suggests that the outcrop area is located outside the zone of intense hydrothermal chlorite and sericite alteration associated with the formation of the Amulet Upper A deposit. Only weak “dalmatianite” spotting is present.

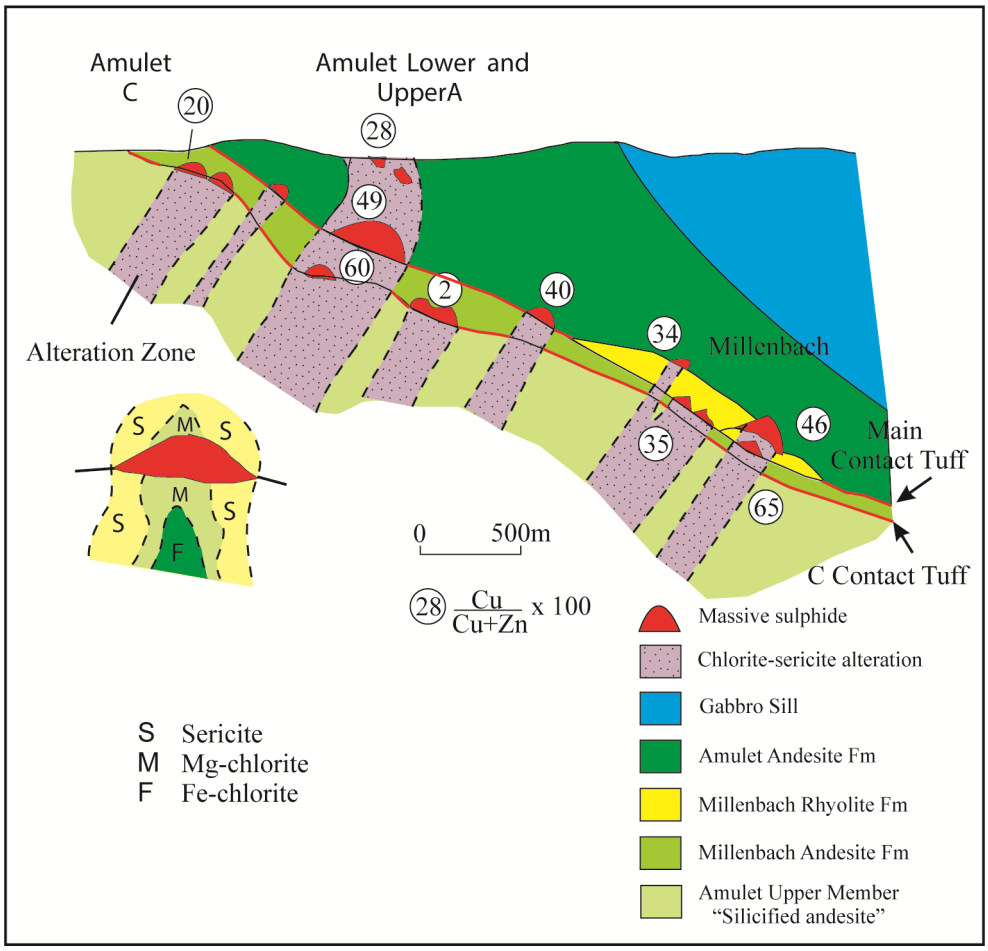

Figure 33. Geological cross section through the Amulet and Millenbach VMS deposits showing the geology, alteration and metal zonation (Gibson and Galley 2007) (Day 4 Stop 13). The sericite (S), Mg-chlorite (M) and Fe-chlorite (F) alteration zones when contact metamorphosed are represented by cordierite-biotite (dalmatianite), chlorite-anthophyllite and chlorite-gedrite mineral associations, respectively.

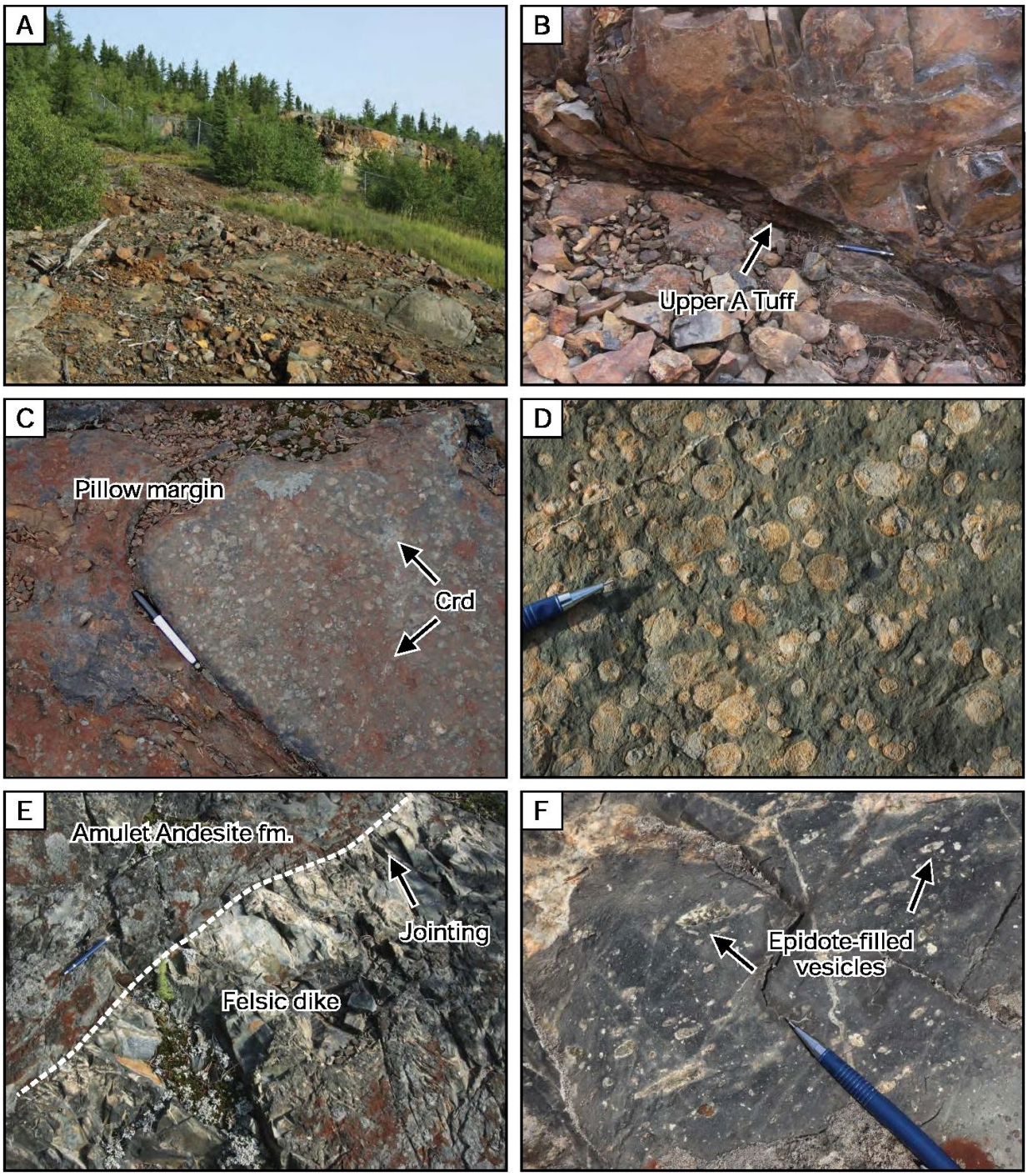

Photo 20. Field photographs of geological relationships at the former Amulet Upper A mine site (*from* Monecke, Gibson and Goutier 2017) (Day 4 Stop 13). **A**) View of the Amulet Upper A deposit "glory hole". Lavas in the foreground belong to the Amulet Andesite formation. **B**) Upper A Tuff, which marks the stratigraphic interval containing the Amulet Upper A massive sulfide lens. The Upper A Tuff occurs within mafic lavas of the Amulet Andesite formation. Note pen for scale. **C**) Dalmatianite in quartz amygdaloidal pillowed lava of the Amulet Andesite formation. Note pen for scale. **D**) Dalmatianite in mafic lava of the Amulet Andesite formation. Clearly visible are retrogressive cordierite porphyroblasts. The groundmass contains abundant retrograde chlorite. Note pen for scale. **E**) Aphyric, aphanitic felsic dike crosscutting mafic lava of the Amulet Andesite formation. The felsic dike displays columnar jointing oriented perpendicular to the contact. Note pen for scale. **F**) Epidote-quartz alteration patches and filled amygdules of mafic lavas of the Amulet Andesite formation. The preservation of feldspar phenocrysts in the mafic lava suggests that the outcrop is located outside the zone of intense VMS hydrothermal alteration. Note pen for scale.

Stop 14. Lac Dufault Intrusion – near Old Waite (optional)

UTM 642149E 5355550N

Potential hazards:

- Steep and slippery slopes when wet; loose rocks
- Watch for local road, short up-hill rock through bush to outcrop

The Lac Dufault Intrusion consists of western and eastern intrusions. The tonalitic eastern intrusion contains a roof pendant of volcanic rocks that is hosts the Mine Gallen (West MacDonald) VMS deposit (*see* Figure 5); it is not associated with a contact metamorphic aureole and is interpreted to be synvolcanic (Gibson and Galley 2007). The western body is a potassium feldspar–bearing granitoid body that crystallized at approximately 2690 Ma (Mortensen 1993) and imparted a contact metamorphic aureole to the immediately surrounding Blake River Group metavolcanic rocks and is responsible for the development of biotite, cordierite (dalmatianite) and orthoamphiboles that characterize VMS sericite and chlorite alteration zones within the contact aureole.

End of Rouyn-Noranda area road logs.

Acknowledgments

The authors acknowledge that many of the stop descriptions contained in the guidebook are modified from previous field guides. For Rouyn-Noranda, these include Gibson (1980, Falconbridge Copper Ltd., internal guidebook) and Gibson, Walker and Coad (1984) that were also used by Betrand (1990), Watkinson (1991), and Santaguida, Gibson and Watkinson (1999), Péloquin, Verpaelst and Goutier (1996), Goutier et al. (2009, 2011), and Monecke, Gibson and Goutier (2017). IAMGOLD acknowledges the efforts of Brian Tomczuk (Project Geologist, Côté Gold Exploration) in the preparation of many of the figures and photos in the Côté Gold field stops section of this guidebook. We thank Monica Gaiswinkler Easton, Geoscience Editor, and Sonia Préfontaine, Geoscientist, Ontario Geological Survey, for thorough editorial reviews of this guidebook.

We also acknowledge the permission to use many of the figures contained within this guidebook from the Society of Economic Geologists (Economic Geology, Reviews in Economic Geology v.19), Geological Survey of Canada, Ontario Geological Survey, IAMGOLD Corporation and Schofield (2023); and from TPG (work-in-progress). The Mineral Exploration Research Centre at the Harquail School of Earth Sciences, Laurentian University, the Mineral Deposits Division of the Geological Association of Canada, and Dawn Zhou, CSIT Group of Companies are thanked for providing financial support for students to attend the field trip.

We thank IAMGOLD Corporation for their support and for providing stops on their Côté Gold property and deposit, and to Falco Resources Ltd., Yorbeau Resources Inc., and Mortimer Magnan jasper project that provided access to properties visited on the Swayze and Rouyn-Noranda segments. Discussions with numerous colleagues and graduate students who have contributed to our understanding of the geology and metallogeny of the Rouyn-Noranda and Swayze areas are greatly appreciated. This is MERC–Metal Earth publication number MERC-ME 2023-11.

References

Ayer, J.A., Ketchum, J.W.F. and Trowell, N.F. 2002. New geochronological and neodymium isotopic results from the Abitibi greenstone belt, with emphasis on the timing and the tectonic implications of Neoarchean sedimentation and volcanism; *in* Summary of Field Work and Other Activities, 2002, Ontario Geological Survey, Open File Report 6100, p.5-1 to 5-16.

Ayer, J.A., Thurston, P.C., Bateman, R., Dubé, B., Gibson, H.L., Hamilton, M.A., Hathway, B., Hocker, S.M., Houlé, M.G., Hudak, G., Ispolatov, V.O., Lafrance, B., Lesher, C.M., MacDonald, P.J., Péloquin, A.S., Piercey, S.J., Reed, L.E. and Thompson, P.H. 2005. Overview of results from the Greenstone Architecture Project: Discover Abitibi Initiative; Ontario Geological Survey, Open File Report 6154, 146p.

Barrett, T.J., Cattalani, S. and MacLean, W.H. 1993. Volcanic lithogeochemistry and alteration of the Delbridge massive sulfide deposit, Noranda, Quebec; Journal of Geochemical Exploration, v.48, p.135-173.

Barrett, T.J., MacLean, W.H. and Cattalani, S. 1991. Massive sulphide deposits of the Noranda area, Quebec. I. The Horne mine; Canadian Journal of Earth Sciences, v.28, p.465-488.

Barrett, T.J., MacLean, W.H., Cattalani, S., Hoy, L. and Riverin, G. 1991. Massive sulfide deposits of the Noranda area, Quebec. III. The Ansil mine; Canadian Journal of Earth Sciences, v.28, p.1699-1730.

Barrie. C.T., Ludden, J.N. and Green, T.H. 1993. Geochemistry of volcanic rocks associated with Cu-Zn and Ni-Cu deposits in the Abitibi Subprovince; Economic Geology, v.88, p.1341-1358.

Beaty, D.W. and Taylor, H.P. 1982. Some petrologic and oxygen isotopic relationships in the Amulet Mine, Noranda, Quebec, and their bearing on the origin of Archean massive sulfide deposits; Economic Geology, v.77, p.95-10.

Bedeaux, P. 2018. Évolution structurale, modélisation des paléocontraintes et implications sur les minéralisations aurifères orogéniques le long de failles majeures: Application à la Faille de Cadillac, Abitibi, Canada; unpublished PhD thesis, l'Université du Québec à Chicoutimi, Chicoutimi, Québec, 409p.

Bedeaux, P., Pilote, P., Daigneault, R. and Rafini, S. 2017. Synthesis of the structural evolution and associated gold mineralization of the Cadillac Fault, Abitibi, Canada; Ore Geology Reviews, v.82, p.49-69.

Benn, K. 2006. Tectonic delamination of the lower crust during Late Archean collision of the Abitibi-Opatica and Pontiac terranes, Superior Province, Canada; *in* Archean Geodynamics and Environments, American Geophysical Union, Geophysical Monograph Series 164, p.267-282. doi.org/10.1029/164GM17

Berger, B.R. 2012. Interpretation of geochemistry in the south of Gogama area; *in* Summary of Field Work and Other Activities, 2012, Ontario Geological Survey, Open File Report 6280, p.3-1 to 3-14.

Betrand, P. 1990. Central Mine Sequence stratigraphy field trip; *in* The northwestern Quebec Polymetallic Belt: A Summary of 60 Years of Mining Exploration—Excursion Guidebook: Rouyn-Noranda, The Canadian Institute of Mining and Metallurgy, p.27-35.

Biagioni, C., George, L.L., Cook, N.J., Mackovicky, E., Moëlo, Y., Pasero, M., Sejkora, J., Stanley, C.J., Welch, M.D. and Bosi, F. 2020. The tetrahedrite group: Nomenclature and classification; American Mineralogist, v.105, p.109-122.

Bleeker, W. 2012. Targeted Geoscience Initiative 4. Lode gold deposits in ancient deformed and metamorphosed terranes: The role of extension in the formation of Timiskaming basins and large gold deposits, Abitibi greenstone belt—A discussion; *in* Summary of Field Work and Other Activities, 2012, Ontario Geological Survey, Open File Report 6280, p.47-1 to 47-12.

——— 2015. Synorogenic gold mineralization in granite-greenstone terranes: The deep connection between extension, major faults, synorogenic clastic basins, magmatism, thrust inversion, and long-term preservation; Geological Survey of Canada, Open File 7852, p.25-47.

Boldy, J. 1968. Geological observations on the Delbridge massive sulphide deposit; Canadian Mining and Metallurgical Bulletin, v.61, p.1045-1054.

——— 1979. Exploration discoveries, Noranda district, Quebec (case histories of a mining camp); Geological Survey of Canada, Economic Geology Report 31, p.593-603.

Burt, P.D., Chance, P.N. and Burns, J.G. 2011. Technical report on a resource estimate on the Jerome mine property, Osway Township, Porcupine Mining Division, Ontario, prepared for Augen Gold Corp.; Augen Gold Corp., NI 43-101 Technical Report, filed August 29, 2011 with SEDAR®, see SEDAR Home Page, 92p.

Cameron, E.M. 1993. Precambrian gold: Perspectives from the top and bottom of shear zones; The Canadian Mineralogist, v.31, p.917–944.

Campbell, I.H., Franklin, J.M., Gorton, M.P., Hart, T.R. and Scott, S.D. 1981. The role of subvolcanic sills in the generation of massive sulfide deposits; Economic Geology, v.76, p.2248-2253.

Carrier, A., Jébrak, M., Angelier, J. and Holyland, P. 2000. The Silidor deposit, Rouyn-Noranda District, Abitibi belt: Geology, structural evolution, and paleostress modelling of an Au quartz vein-type deposit in an Archean trondhjemite; Economic Geology, v.95, p.1049-1065.

Cathles, L.M. 1993. Oxygen isotope alteration in the Noranda mining district, Abitibi greenstone belt, Quebec; Economic Geology, v.88, p.1483-1511.

Corcoran, P.L. and Mueller, W.U. 2007. Time-transgressive Archean unconformities underlying molasse basin-fill successions of dissected oceanic arcs, Superior Province, Canada; Journal of Geology, v.115, p.655-674.

Coté, R. 1975. Carte structurale, partie des Cantons de Rouyn et de Beauchastel, Comté Témiscamingue, Québec; Ministère des Richesses naturelles du Québec, DP-300, scale 1:12 000.

Couture, J.F. 1996. Géologie du gisement Chadbourne; Ministère des Ressources naturelles du Québec, report MB 96-06, p.67-68.

Cox, J.J., Ciuculescu, T., Teben, S., Bugnon, M-F., Smith, A.R., Coulson, A.L., Shah, B., Davachi, M.M., O'Hara, P.M., Turenne, R.J., Daniel, S.E. and Nada, D. 2022. Technical Report on the Côté Gold project, Ontario, Canada, prepared for IAMGOLD Corporation by SLR Consulting (Canada) Ltd., IAMGOLD Corporation and Wood Canada Limited; NI 43-101 Technical Report, filed August 12, 2022 with SEDAR®, see SEDAR Home Page, 425p.

Daigneault, R., Mueller, W.U. and Chown, E.H. 2002. Oblique Archean subduction: accretion and exhumation of an oceanic arc during dextral transpression, Southern Volcanic Zone, Abitibi greenstone belt, Canada; Precambrian Research v.115, p.261-290.

Daigneault, R. and Pearson, V. 2006. Physical volcanology of the Blake River calderas complex: A new interpretation of an old structure; *in* The komatiite-komatiitic basalt-basalt association in oceanic plateaus and calderas, Geological Association of Canada–Mineralogical Association of Canada, Joint Annual Meeting, Montreal 2006, Field Trip Guidebook A3, p.62-72.

David, J., Vaillancourt, D., Bandyayera, D., Simard, M., Goutier, J., Pilote, P., Dion, C. and Barbe, P. 2010. Datations U-Pb effectuées dans les sous-provinces d'Ashuanipi, de la Grande, d'Opinaca et d'Abitibi en 2008-2009; Ministère des Ressources naturelles et de la Faune Québec, report RP 2010-11, 37p.

Davis, D.W. 2002. U-Pb geochronology of Archean metasedimentary rocks in the Pontiac and Abitibi subprovinces, Québec, constraints on timing, provenance and regional tectonics; Precambrian Research, v.115, p.97-117.

——— 2021. Geochronology of rocks from northwest Ontario 2015–16 Part 2: LA-ICP-MS geochronology; revised May 31, 2021; internal report for the Ontario Geological Survey, Toronto, Ontario, Jack Satterly Geochronology Laboratory, University of Toronto, 83p.

de Rosen-Spence, A.[F.] 1969. Genèse des roches à cordierite-anthophyllite des gisements cupro-zincifères de la région de Rouyn-Noranda, Québec, Canada; Canadian Journal of Earth Sciences, v.6, p.1339–1345.

——— 1976. Stratigraphy, development and petrogenesis of the central Noranda volcanic pile, Noranda, Quebec; unpublished PhD thesis, University of Toronto, Toronto, Ontario, 298p.

Dimroth, E., Gélinas, L., Rocheleau, M., Provost, G. and Tassé, N. 1975. Field trip and field conference on the volcanology and sedimentology of Rouyn-Noranda area, August 4–7, 1975, Rouyn, Québec; Bureau du géologue résident, Rouyn-Noranda, Ministère des Richesses naturelles du Québec, 76p.

Dimroth, E., Imreh, L., Goulet, N. and Rocheleau, M. 1983. Evolution of the south-central segment of the Archean Abitibi Belt, Quebec. Part II: Tectonic evolution and geomechanical model; Canadian Journal of Earth Sciences, v.20, p.1355-1373.

Dimroth, E., Imreh, L., Rocheleau, M. and Goulet, N. 1982. Evolution of the south-central part of the Archean Abitibi Belt, Québec. Part I: Stratigraphy and paleogeographic model; Canadian Journal of Earth Sciences, v.19, p.1729-1758.

Dimroth, E. and Rocheleau, M. 1979. Volcanology and sedimentology of the Rouyn-Noranda area, Quebec; Geological Association of Canada–Mineralogical Association of Canada, Joint Annual Meeting, Quebec ’79, Guidebook A-1, 183p.

Dubé, B. and Mercier-Langevin, P. 2020. Gold deposits of the Archean Abitibi greenstone belt, Canada; *in* Geology of the World’s Major Gold Deposits and Provinces, Society of Economic Geologists, Special Publication 23, p.669-708.

Fisher, D.F. 1970. The origin of the Number Five zone, Horne Mine, Noranda, Quebec; unpublished MSc thesis, University of Western Ontario, London, Ontario, 114p.

——— 1974. A volcanic origin for the No. 5 zone of the Horne Mine, Noranda, Quebec; Economic Geology, v.69, p.1352-1353.

Franklin, J.M., Gibson, H.L., Jonasson, I.R. and Galley, A.G. 2005. Volcanogenic massive sulfide deposits; Society of Economic Geologists, Economic Geology 100th Anniversary Volume, p.523-560.

Franklin, J.M., Lydon, J.W. and Sangster, D.F. 1981. Volcanic-associated massive sulfide deposits; Society of Economic Geologists, Economic Geology 75th Anniversary Volume, p.485-627.

Frieman, B.M., Kuiper, Y.D., Kelly, N.M., Monecke, T. and Kylander-Clark, A. 2017. Constraints on the geodynamic evolution of the southern Superior Province: U-Pb LA-ICP-MS analysis of detrital zircon in successor basins of the Archean Abitibi and Pontiac subprovinces of Ontario and Quebec, Canada; Precambrian Research, v.292, p.398-416.

Galley, A.G. 2003. Composite synvolcanic intrusions associated with Precambrian VMS-related hydrothermal systems; Mineralium Deposita, v.38, p.443-473.

Galley, A.G. and van Breemen, O. 2002. Timing of synvolcanic magmatism in relation to base-metal mineralization, Rouyn-Noranda, Abitibi volcanic belt, Québec; Geological Survey of Canada, Current Research 2002-F8, p.1-9.

Gauthier, N., Rocheleau, M., Kelly, D. and Gagnon, Y. 1990. Controls on the distribution of gold mineralization within the Cadillac tectonic zone, Rouyn-Beauchastel segment, Abitibi Belt, Quebec; *in* The Northwestern Quebec Polymetallic Belt: A Summary of 60 Years of Mining Exploration, Canadian Institute of Mining and Metallurgy, Special Volume 43, p.185-198.

Gélinas, L., Trudel, P. and Hubert, C. 1984. Chemostratigraphic division of the Blake River Group, Rouyn-Noranda area, Abitibi, Quebec; Canadian Journal of Earth Sciences, v.21, p.220-231.

Gemmell, T.P. 2015. Geology and mineral potential of Chester Township, southern Swayze greenstone belt; *in* Summary of Field Work and Other Activities, 2015, Ontario Geological Survey, Open File Report 6313, p.8-1 to 8-14.

Gemmell, T.P. and MacDonald, P.J. 2016. Geology and mineral potential of Yeo and southern Potier townships, southern Swayze area, Abitibi greenstone belt; *in* Summary of Field Work and Other Activities, 2016, Ontario Geological Survey, Open File Report 6323, p.7-1 to 7-13.

Gemmell, T .P. and MacDonald, P.J. 2017. Precambrian geology of the Yeo and Chester townships area, Chester intrusive complex, southern Abitibi greenstone belt; Ontario Geological Survey, Preliminary Map P.3817, scale 1:20 000.

Gibson, H.L. 1980. Volcanic stratigraphy and VMS deposits of the Central Noranda Camp; unpublished internal document, Falconbridge Copper Ltd., Field Guide, 12p.

Gibson, H.L. 1990. The mine sequence of the central Noranda volcanic complex: Geology, alteration, massive sulfide deposits and volcanological reconstruction; unpublished PhD thesis, Carleton University, Ottawa, Ontario, 715p.

——— 2005. Volcanic-hosted ore deposits; Chapter 12 *in* Volcanoes and the Environment, Cambridge University Press, p.333-386.

Gibson, H.L., Allen, R.L., Riverin, G. and Lane, T.E. 2007. The VMS model: Advances and application to exploration targeting; *in* Ore deposits and Exploration Technology, Proceedings of Exploration 07: Fifth Decennial International Conference on Mineral Exploration, Decennial Mineral Exploration Conferences, Toronto, Ontario, p.713-730.

Gibson, H.L. and Galley, A.G. 2007. Volcanogenic massive sulphide deposits of the Archean Noranda District, Quebec; *in* Mineral Deposits of Canada: A Synthesis of Major Deposit Types, District Metallogeny, the Evolution of Geological Provinces and Exploration Methods, Geological Association of Canada, Mineral Deposits Division, Special Publication No.5, p.533-552.

Gibson, H.L. and Kerr, D.J. 1993. Giant volcanic associated massive sulfide deposits: With an emphasis on Archean deposits; *in* Giant ore deposits, Society of Economic Geologists, Special Publication No.2, p.319-348.

Gibson, H.L., Kerr, D.J. and Cattalani, S. 2000. The Horne mine: Geology, history, influence on genetic models, and a comparison to the Kidd Creek Mine; Exploration and Mining Geology, v.9, p.91-111.

Gibson, H.L., Morton, R.L. and Hudak, G.J. 1999. Submarine volcanic processes, deposits, and environments favorable for the location of volcanic-associated massive sulfide deposits; *in* Volcanic-Associated Massive Sulfide Deposits: Processes and examples in modern and ancient settings, Society of Economic Geologists, Reviews in Economic Geology, v.8, p.13-51.

Gibson, H.L., Walker, S.D. and Coad, P.R. 1984. Surface geology and volcanogenic base metal massive sulphide deposits and gold deposits of Noranda and Timmins; Geological Association of Canada–Mineralogical Association of Canada, Joint Annual Meeting, London ’84, Field Trip 14 Guidebook, 124p.

Gibson, H.L. and Watkinson, D.H. 1990. Volcanogenic massive sulphide deposits of the Noranda Cauldron and shield volcano, Quebec; *in* The Northwest Quebec Polymetallic Belt: A Summary of 60 Years of Mining Exploration, Canadian Institute of Mining and Metallurgy, Special Volume 43, p.119-132.

Gibson, H.L., Watkinson, D.H. and Comba, C.D.A. 1983. Silicification: Hydrothermal alteration in an Archean geothermal system within the Amulet rhyolite formation, Noranda, Quebec; Economic Geology, v.78, p.954-971.

Gilmour, P. 1965. The origin of massive sulfide mineralization in the Noranda district, northwestern Quebec; Proceedings of the Geological Association of Canada, v.16, p.63-81.

Goldie, R.J. 1976. The Flavrian and Powell plutons, Noranda area, Québec: A geological investigation of the Flavrian and Powell plutons and their relationships to other rocks and structures of the Noranda area; unpublished PhD thesis, Queen's University, Kingston, Ontario, 381p.

Goldie, R.J., Kotila, B. and Seward, D. 1979. The Don Rouyn mine: An Archean porphyry copper deposit near Noranda, Quebec; Economic Geology, v.74, p.1680-1684.

Goulet, N. 1978. Stratigraphy and structural relationships across the Cadillac-Larder Lake Fault, Rouyn-Beauchastel area, Quebec; unpublished PhD thesis, Queen's University, Kingston, Ontario, 141p.

Goutier, J. 1997. Géologie de la région de Destor, Québec; Ministère des ressources naturelles du Québec, Rapport Géologique RG 96-13, 37p.

Goutier, J., McNicoll, V., Dion, C., Ross, P.S. and Mercier-Langevin, P. 2009. Portrait des grandes unités du Groupe de Blake River et leur relation avec les sulfures massifs volcanogènes; Ministère des Ressources naturelles et de la Faune, Québec, Congrès 2009 Abitibi, Rouyn-Noranda, Excursions, p.9-28.

Goutier, J., Ross, P.S., McNicoll, V., Dion, C., Mercier-Langevin, P., Thurston, P., Dubé, B. and Gibson, H. 2011. Geology, stratigraphy and geochronology of the Blake River Group and relationships with VMS deposits; Geological Survey of Canada, Open File 6869, p.10-21.

Gunning, H.C. 1937. Cadillac area, Quebec; Geological Survey of Canada, Memoir 206, 80p.

Gunning, H.C. and Ambrose, J.W. 1940. Malartic area, Quebec; Geological Survey of Canada, Memoir 222, 142p.

Hall, B.V. 1982. Geochemistry of the alteration pipe at the Amulet Upper A deposit, Noranda, Quebec; Canadian Journal of Earth Sciences, v.19, p.2060-2084.

Hannington, M.D., Santaguida, F., Kjarsgaard, I.M. and Cathles, L.M. 2003. Regional-scale hydrothermal alteration in the central Blake River Group, western Abitibi Subprovince, Canada: Implications for VMS prospectivity; Mineralium Deposita, v.38, p.393-422.

Hart, T.R., Gibson, H.L. and Lesher, C.M. 2004. Trace element geochemistry and petrogenesis of felsic volcanic rocks associated with volcanogenic massive Cu-Zn-Pb sulfide deposits; Economic Geology, v.99, p.1003-1013.

Hastie, E.C.G. 2017. Gold metallogeny of the southern Swayze area, Abitibi greenstone belt: A field trip guidebook; Ontario Geological Survey, Open File Report 6334, 19p.

Hastie, E.C.G., Kontak, D.J. and Lafrance, B. 2020. Gold remobilization: Insights from gold deposits in the Archean Swayze greenstone belt, Abitibi Subprovince, Canada; Economic Geology, v.115, p.241-277.

Hastie, E.C.G., Kontak, D.J., Lafrance, B., Petrus, J.A., Sharpe, R. and Fayek, M. 2023. Evaluating geochemical discriminants in Archean gold deposits: A Superior Province perspective with an emphasis on the Abitibi greenstone belt; Economic Geology, v.118, p.123-155.

Haugaard, R., White, S., Jørgensen, T.R.C., Frieman, B., Meek, D., Zhou, X., Mathieu, L. and Ayer, J. 2022. Sedimentary processes, provenance, and tectonic control on fluvial sandstone geochemistry during Superior craton stabilization; *in* Laurentia: Turning Points in the Evolution of a Continent, Geological Society of America, Memoir 220, p.25-42.

Heather, K.B. 2001. The geological evolution of the Archean Swayze greenstone belt, Superior Province, Canada; unpublished PhD thesis, Keele University, Keele, England, 370p.

Holubec, J. 1972. Lithostratigraphy, structure and deep crustal relations of Archean rocks of the Canadian Shield, Rouyn-Noranda area, Quebec; Krystalinikum, v.9, p.63-89.

Hubert, C. 1990. Geologic framework, evolution and structural setting of gold and base metal deposits of the Abitibi greenstone belt, Canada; *in* Gold and Base-Metal Mineralization in the Abitibi Subprovince, Canada, with Emphasis on the Quebec Segment, short course notes, University of Western Australia, Geology Department (Key Centre) and University Extension, Publication No.24, p.53-62.

Hubert, C., Trudel, P. and Gélinas, L. 1984. Archean wrench fault tectonics and structural evolution of the Blake River Group, Abitibi Belt, Quebec; Canadian Journal of Earth Sciences, v.21, p.1024-1032.

Huston, D.L., Champion, D.C. and Cassidy, K.F. 2014. Tectonic controls on the endowment of Neoarchean cratons in volcanic-hosted massive sulfide deposits: Evidence from lead and neodymium isotopes; Economic Geology, v.109, p.11-26.

Hutchinson, R.W. 1965. Genesis of Canadian massive sulphides reconsidered by comparison to Cyprus deposits; The Canadian Mining Metallurgical Bulletin, v.58, p.972-986.

Ispolatov, V., Lafrance, B., Dubé, B., Creaser, R. and Hamilton, M. 2008. Geologic and structural setting of gold mineralization in the Kirkland Lake-Larder Lake gold belt, Ontario; Economic Geology, v.103, p.1309-1340.

Jackson, S.L., Cruden, A.R., White, D. and Milkereit, B. 1995. A seismic-reflection-based regional cross section of the southern Abitibi greenstone belt; Canadian Journal of Earth Sciences, v.32, p.135-148.

Jaireth, S. and Huston, D. 2010. Metal endowment of cratons, terranes and districts: Insights from a quantitative analysis of regions with giant and super-giant deposits; Ore Geology Reviews, v.38, p.288-303.

Jébrak, M., Harnois, L., Carrier, A. and Lafrance, J. 1997. The Don Rouyn-Cu-Au porphyry system; *in* Atypical Gold Deposits in the Abitibi Belt, Geological Association of Canada, Ottawa '97, Field Trip Guidebook B5, p.72-78.

Jørgensen, T.R.C., Gibson, H.L., Roots, E.A., Vayavur, R., Hill, G.J., Snyder, D.B. and Naghizadeh, M. 2022. The implications of crustal architecture and transcrustal upflow zones on the metal endowment of a world-class mineral district; Nature, Scientific Reports, v.12, article 14710. doi.org/10.1038/s41598-022-18836-y

Kalogeropoulos, S.I. and Scott, S.D. 1989. Mineralogy and geochemistry of an Archean tuffaceous exhalite: The Main Contact Tuff, Millenbach mine area, Noranda, Québec; Canadian Journal of Earth Sciences, v.26, p.88-105.

Kamo, S.L. 2018. Part A: Report on U-Pb ID-TIMS geochronology for the Ontario Geological Survey: Bedrock mapping projects, Ontario, Year 3: 2017–2018; internal report prepared for the Ontario Geological Survey, Jack Satterly Geochronology Laboratory, University of Toronto, Toronto, Ontario, 44p.

Katz, L.R., Kontak, D.J., Dubé, B. and McNicoll, V. 2017. The geology, petrology, and geochronology of the Archean Côté Gold large-tonnage, low-grade intrusion-related Au(-Cu) deposit, Swayze greenstone belt, Ontario, Canada; Canadian Journal of Earth Sciences, v.54, p.173-202.

Katz, L.R., Kontak, D.J., Dubé, B., McNicoll, V., Creaser, R. and Petrus, J.A. 2021. An Archean porphyry-type gold deposit: The Côté Gold Au(-Cu) deposit, Swayze greenstone belt, Superior Province, Ontario, Canada; Economic Geology, v.116, p.47-89.

Kennedy, L.P. 1985. The geology and geochemistry of the Archean Flavrian Pluton, Noranda, Quebec; unpublished PhD thesis, The University of Western Ontario, London, Ontario, 491p.

Kerr, D.J. and Gibson, H.L. 1993. A comparison of the Horne volcanogenic massive sulfide deposit and intracauldron deposits of the Mine sequence, Noranda, Quebec; Economic Geology, v.88, p.1419-1422.

Kerr, D.J. and Mason, R. 1990. A re-appraisal of the geology and ore deposits of the Horne mine complex at Rouyn-Noranda, Quebec; *in* The Northwest Quebec Polymetallic Belt: A Summary of 60 Years of Mining Exploration, Canadian Institute of Mining and Metallurgy, Special Volume 43, p.153-165.

Kerrich, R. and Wyman, D. 1990. Geodynamic setting of mesothermal gold deposits: An association with accretionary tectonic regimes; Geology, v.18, p.882-885.

Knuckey, M.J., Comba, C.D.A. and Riverin, G. 1982. Structure, metal zoning and alteration at the Millenbach deposit, Noranda, Quebec; *in* Precambrian Sulphide Deposits, Geological Association of Canada, Special Paper 25, p.255-295.

Knuckey, M.J. and Watkins, J.J. 1982. The geology of the Corbet massive sulphide deposit Noranda district, Québec, Canada; *in* Precambrian Sulphide Deposits, Geological Association of Canada, Special Paper 25, p.297-317.

Kontak, D.J., Creaser, R.A. and Hamilton, M.A. 2013. Section 2: Geological and geochemical studies of the Côté Lake Au(-Cu) deposit area, Chester Township, northern Ontario; report *in* Results from Shining Tree, Chester Township and Matachewan gold projects and the northern Cobalt Embayment polymetallic vein project, Ontario Geological Survey, Miscellaneous Release—Data 294.

Kotila, B.W. 1975. An Archean porphyry copper deposit: The Don Rouyn mine, Noranda, Québec; unpublished BSc thesis, Queen's University, Kingston, Ontario, 21p.

Krushnisky, A., Mercier-Langevin, P., Ross, P.S., Goutier, J., Pilote, C. and Bernier, C. 2020. Geology and gold enrichment at the Horne 5 Archean volcanogenic massive sulphide deposit, Abitibi greenstone belt, Québec: A synthesis; *in* Targeted Geoscience Initiative 5: Contributions to the Understanding of Canadian Gold Systems, Geological Survey of Canada, Open File 8712, p.31-44.

Laurin, J. 2010. Geology, gold mineralization and alteration of the Horne West property, Rouyn-Noranda; unpublished MSc thesis, University of Ottawa, Ottawa, Ontario, 161p.

Lesher, C.M., Gibson, H.L. and Campbell, I.H. 1986. Composition-volume changes during hydrothermal alteration of andesite at Buttercup Hill, Noranda District, Québec; Geochimica et Cosmochimica Acta, v.50, p.2693-2705.

Lichtblau, A.F. 1989. Stratigraphy and facies at the south margin of the Archean Noranda caldera; unpublished MSc thesis, Université du Québec à Chicoutimi, Chicoutimi, Quebec, 136p.

Lichtblau, A.F. 1979. Property acquisition proposal, Powell-Rouyn Gold Mines; unpublished internal report, Falconbridge Copper, 17p.

Lichtblau, A.P. [*sic* A.F.] and Dimroth, E. 1980. Stratigraphy and facies at the south margin of the Archean Noranda Caldera, Noranda, Quebec; *in* Current Research, Part A, Geological Survey of Canada, Paper 80-1A, p.69-76.

Lickus, R.J. 1965. Geology and geochemistry of the ore deposits at the Vauze mine, Noranda district, Quebec; unpublished PhD thesis, McGill University, Montreal, Quebec, 135p.

Ludden, J.N., Gélinas, L. and Trudel, P. 1982. Archean metavolcanic rocks from the Rouyn-Noranda District, Abitibi greenstone belt, Quebec: Mobility of trace elements and petrogenetic constraints; Canadian Journal of Earth Sciences, v.19, p.2276-2287.

Lydon, J.W. 1988. Ore deposit models: Volcanogenic massive sulfide deposits. Part 1: A descriptive model; Geoscience Canada, v.11, p.195-202.

MacDonald, P.J., Bisaillon, J.M. and Gemmell, T.P. 2018. Precambrian geology of the Osway and Huffman townships area, Opeepeesway basin, southern Abitibi greenstone belt; Ontario Geological Survey, Preliminary Map.3819, scale 1:20 000.

MacDonald, P.J., Hastie, E.C.G. and Davis, D.W. 2017. Preliminary geology of Osway and Huffman townships and parts of Eric, Fingal and Arbutus townships, southern Swayze area, Abitibi greenstone belt; *in* Summary of Field Work and Other Activities, 2017, Ontario Geological Survey, Open File Report 6333, p.7-1 to 7-13.

McNicoll, V., Goutier, J., Dubé, B., Mercier-Langevin, P., Ross, P.S., Dion, C., Monecke, T., Legault, M., Percival, J. and Gibson, H. 2014. U-Pb geochronology of the Blake River Group, Abitibi greenstone belt, Quebec, and implications for base metal exploration; Economic Geology, v.109, p.27-59.

Mercier-Langevin, P., Gibson, H.L., Hannington, M.D., Goutier, J., Monecke, T., Dubé, B. and Houlé, M.G. 2014. A special issue on Archean magmatism, volcanism, and ore deposits: Part 2. Volcanogenic massive sulfide deposits preface; Economic Geology, v.109, p.1-9.

Mercier-Langevin, P., Hannington, M., Dubé, B. and Bécu, V. 2011. The gold content of volcanogenic massive sulfide deposits; Mineralium Deposita, v.46, p.509-539.

Mole, D.R., Freeman, B.M., Thurston, P.C., Marsh, J.H., Jørgensen, T.R.C., Stern, R.A., Martin, L.A.J., Lu, Y.J. and Gibson, H.L. 2022. Crustal architecture of the south-east Superior Craton and controls on mineral systems; Ore Geology Reviews, v.148, p.1-34.

Monecke, T. and Gibson, H.L. 2013. Surface geology of the giant Horne volcanic-hosted massive sulphide deposit, Rouyn-Noranda, Quebec; Geological Survey of Canada, Open File 7412.

Monecke, T., Gibson, H., Dubé, B., Laurin, J., Hannington, M.D. and Martin, L. 2008. Geology and volcanic setting of the Horne deposit, Rouyn-Noranda, Québec: Initial results of a new research project; Geological Survey of Canada, Current Research 2008-9, 16p.

Monecke, T., Gibson, H.L. and Goutier, J. 2017. Volcanogenic massive sulfide deposits of the Noranda camp; Chapter 6 *in* Archean Base and Precious Metal Deposits, Southern Abitibi Greenstone Belt, Canada, Society of Economic Geologists, Reviews in Economic Geology, v.19, p.169-223.

Monecke, T., Mercier-Langevin, P., Dubé, B. and Frieman, B.M. 2017. Geology of the Abitibi greenstone belt; Chapter 1 *in* Archean Base and Precious Metal Deposits, Southern Abitibi Greenstone Belt, Canada: Society of Economic Geologists, Reviews in Economic Geology, v.19, p.7-50.

Moore, L.N., Daigneault, R., Aird, H.M., Banerjee, N.R. and Mueller, W.U. 2016. Reconstruction and evolution of Archean intracaldera facies: The Rouyn-Pelletier Caldera Complex of the Blake River Group, Abitibi greenstone belt, Canada; Canadian Journal of Earth Sciences, v.53, p.355-377.

Moore, L.N., Mueller, W.U. and Daigneault, R. 2012. In situ hyaloclastitic fragmentation of subaqueous ponded lavas, New Senator caldera, Abitibi greenstone belt, Quebec, Canada; Precambrian Research, v.215, p.44-59.

Morris, H.R. 1959. Anglo-Rouyn, Powell-Rouyn and Joliet-Québec Mines; Bureau du géologue résident, Rouyn-Noranda, Ministère des Richesses naturelles du Québec, various unpublished maps and reports.

Mortensen, J.K. 1987. Preliminary U-Pb zircon ages for volcanic and plutonic rocks of the Noranda-Lac Abitibi area, Abitibi Subprovince, Quebec; *in* Current Research, Part A, Geological Survey of Canada, Paper 87-1A, p.581-590.

——— 1993. U–Pb geochronology of the eastern Abitibi Subprovince. Part 2: Noranda–Kirkland Lake area; Canadian Journal of Earth Sciences, v.30, p.29-41.

Mortensen, J.K. and Card, K.D. 1993. U–Pb age constraints for the magmatic and tectonic evolution of the Pontiac Subprovince, Quebec; Canadian Journal of Earth Sciences, v.30, p.1970-1980. https://doi.org/10.1139/e93-173

Mueller, W. 2006. A new interpretation of the Blake River Group, Abitibi greenstone belt: The importance of volcanological facies mapping and the discovery of a megacaldera; Geological Association of Canada, Ashfall, Newsletter of the Volcanology and Igneous Petrology Division, v.62, p.10-13.

Mueller, W.U., Friedman, R., Daigneault, R., Moore, L. and Mortensen, J. 2012. Timing and characteristics of the Archean subaqueous Blake River megacaldera complex, Abitibi greenstone belt, Canada; Precambrian Research, v.214-215, p.1-27.

Mueller, W., Donaldson, J.A. and Doucet, P. 1994. Volcanism and tectonoplutonic influences on sedimentation in the Archean Kirkland Lake basin, Abitibi greenstone belt, Canada; Precambrian Research, v.68, p.201-230.

Mueller, W.U., Stix, J., Corcoran, P.L. and Daigneault, R. 2009. Subaqueous calderas in the Archean Abitibi greenstone belt: An overview and new ideas; Ore Geology Reviews, v.35, p.4-46.

North American Commission on Stratigraphic Nomenclature 2005. North American Stratigraphic Code; AAPG Bulletin, v.89, p.1547-1591.

——— 2021. North American Stratigraphic Code; Stratigraphy, v.18, p.153-204.

Ontario Geological Survey 2011. 1:250 000 scale bedrock geology of Ontario; Ontario Geological Survey, Miscellaneous Release—Data 126 – Revision 1.

——— 2019. Geochronology inventory of Ontario—2019; Ontario Geological Survey, Geochronology Inventory of Ontario, database.

Oseguera, O. 2014. The significance of magma mingling and mixing during the formation of the host-rock successions of Archean massive sulfide deposits in the Noranda camp, Abitibi Subprovince, Quebec; unpublished MSc thesis, Colorado School of Mines, Golden, Colorado, 105p.

Pearson, V. 2005. The Blake River Group: An imbricated caldera complex; Québec Exploration 2005, Abstracts of oral presentations and posters, p.45.

Pearson, V. and Daigneault, R. 2009. An Archean megacaldera complex: The Blake River Group, Abitibi greenstone belt; Precambrian Research, v.168, p.66-82.

Pelletier, C. and Jébrak, M. 1994. Au-(Cu-Mo) porphyries in the Noranda area, Blake River Group, southern Abitibi greenstone belt, Quebec; abstract *in* Geological Association of Canada–Mineralogical Association of Canada–Canadian Geophysical Union, Joint Annual Meeting, Waterloo ’94, Program with Abstracts, v.19, p.A-19.

Péloquin, A.S. 2000. Reappraisal of the Blake River Group stratigraphy and its place in the Archean volcanic record; unpublished PhD thesis, University of Montreal, Montreal, Quebec, 189p.

——— 2005. Geology and base metal mineralization in Ben Nevis, Katrine and Clifford townships: Discover Abitibi Initiative; Ontario Geological Survey, Open File Report 6161, 86p.

Péloquin, A.S., Potvin, R., Paradis, S., Lafleche, M.R., Verpaelst, P. and Gibson, H.L. 1990. The Blake River Group, Rouyn-Noranda area, Quebec; *in* The Northwest Quebec Polymetallic Belt: A Summary of 60 Years of Mining Exploration, Canadian Institute of Mining and Metallurgy, Special Volume 43, p.107-118.

Péloquin, A.S., Verpaelst, P. and Goutier, J. 1996. Le volcanism du Group de Blake River; Ministère des Ressources naturelles du Québec, report MB 96-06, p.28-32.

Piette-Lauzière, N., Guillmette, C., Bouvier, A., Perrouty, S., Pilote, P., Gaillard, N., Lypaczewski, P., Linnen, R.L. and Olivo, G.R. 2019. The timing of prograde metamorphism in the Pontiac Subprovince, Superior craton: Implications for Archean geodynamics and gold mineralization; Precambrian Research, v.320, p.111-136.

Poulsen, K.H. 2010. Polymictic conglomerate as a guide to gold in Archean greenstone belts with reference to Hutti and Kolar, eastern Dharwar craton, India; *in* Gold Metallogeny, India and Beyond, Alpha Science International, Oxford, United Kingdom, p.83-94.

——— 2017a. The Larder Lake–Cadillac break and its gold districts; Chapter 5 *in* Archean Base and Precious Metal Deposits, Southern Abitibi Greenstone Belt, Canada, Society of Economic Geologists, Reviews in Economic Geology v.19, p.133-167.

——— 2017b. MERC Greenstone Gold and Base Metal Field Course; Mineral Exploration Research Centre, Harquail School of Earth Sciences, Laurentian University, Sudbury, Ontario, unpublished course notes.

Powell, W.G., Carmichael, D.M. and Hodgson, C.J. 1995. Conditions and timing of metamorphism in the southern Abitibi greenstone belt, Quebec; Canadian Journal of Earth Sciences, v.32, p.787-805.

Ramos, L.N., Aitken, A.R.A., Occhipinti, S.M. and Lindsay, M. 2021. Rift structures and magmatism focus VMS and gold mineralization in the Paleoproterozoic Bryah Rift Basin; Ore Geology Reviews, v.135, p.104-192.

Richard, M.G. 1998. Evolution of the Flavrian Pluton and its association with VHMS deposits and granitoid-hosted gold deposits of the Noranda cauldron, Rouyn-Noranda, Quebec, Canada; unpublished PhD thesis, University of Montreal, Montreal, Quebec, 218p.

Riverin, G., Bernard, D. and Boily, B. 1990. The Donalda gold deposit, Rouyn-Noranda, Québec; *in* The Northwestern Quebec Polymetallic Belt: A Summary of 60 Years of Mining Exploration, Canadian Institute of Mining and Metallurgy, Special Volume 43, p.199-209.

Riverin, G. and Hodgson. C.J. 1980. Wallrock alteration at the Millenbach Cu-Zn Mine, Noranda, Quebec; Economic Geology, v.75, p.424-444.

Robert, F. 1989. Structural setting and control of gold-quartz veins of the Val d'Or area, southern Abitibi Subprovince; *in* Gold and Base-Metal Mineralization in the Abitibi Subprovince, Canada, with Emphasis on the Quebec Segment, short course notes, University of Western Australia, Geology Department (Key Centre) and University Extension, Publication v.24, p.167-209.

——— 1990. An overview of gold deposits in the eastern Abitibi belt; *in* The Northwest Quebec Polymetallic Belt: A Summary of 60 Years of Mining Exploration, Canadian Institute of Mining and Metallurgy, Special Volume 43, p.93-105.

——— 1991, Gold metallogeny of greenstone belts: Considerations from the eastern Abitibi Subprovince, Canada; extended abstract *in* Brazil Gold '91: The Economics, Geology, Geochemistry, and Genesis of Gold Deposits, A.A. Balkema, Rotterdam, p.31-47.

Robert, F. and Poulsen, K.H. 2001. Vein formation and deformation in greenstone gold deposits; *in* Structural Controls on Ore Genesis, Society of Economic Geologists, Reviews in Economic Geology, v.14, p.111-155.

Roberts, L. 1956. Noranda; Clarke, Irwin, Toronto, 223p.

Roots, E., Hill, G.J., Frieman, B.M., Wannamaker, P.E., Maris, V., Calvert, A.J., Craven, J.A., Smith, R.S. and Snyder, D.B. 2022. Magmatic, hydrothermal and ore element transfer processes of the southeastern Archean Superior Province implied from electrical resistivity structure; Gondwana Research, v.105, p.84-95.

Roscoe, S.M. 1965. Geochemical and isotopic studies, Noranda and Matagami areas; Transactions of the Canadian Institute of Mining and Metallurgy and the Mining Society of Nova Scotia, v.68, p.279-286.

Sangster, D.F. 1972. Precambrian volcanogenic massive sulfide deposits in Canada: A review; Geological Survey of Canada, Paper 72-22, 44p.

Santaguida, F., Gibson, H.L. and Watkinson, D.H. 1999. Hydrothermal alteration mineral assemblages associated with volcanic-hosted massive sulphide mineralization in the Noranda area, Quebec; Geological Association of Canada–Mineralogical Association of Canada, Joint Annual Meeting, Sudbury '99, Field Trip B8 Guidebook, 57p.

Schofield, M.D. 2023. Metallogeny of the Powell block, Rouyn-Noranda mining district, Quebec; unpublished PhD thesis, Laurentian University, Sudbury, Ontario, 353p.

Schofield, M.[D.], Gibson, H.[L.], Lafrance, B., Poulsen, K.H., Marsh, J., Hamilton, M.A. and Jørgensen, T.R.C. 2021. Recognizing subsurface breccias in Archean terranes: Implications for district scale metallogeny; Precambrian Research, v.361, article 106264. doi.org/10.1016/j.precamres.2021.106264

Schofield, M.D., Lafrance, B., Gibson, H.L., Poulsen, H., Scheffwe, C., Quesnel, B., Beaudoin, G. and Hamilton, M.A., in press. Discriminating superimposed alteration associated with epigenetic base and precious metal vein systems in the Rouyn-Noranda mining district, Québec; Implications for exploration in ancient volcanic districts; Economic Geology.

Sharman, E.R., Taylor, B.E., Minarik, W.G., Dubé, B. and Wing, B.A. 2015. Sulfur isotope and trace element data from ore sulfides in the Noranda district (Abitibi, Canada): Implications for volcanogenic massive sulfide deposit genesis; Mineralium Deposita, v.50, p.591-606.

Sibson, R.H. 2001. Seismogenic framework for hydrothermal transport and ore deposition; *in* Structural Controls on Ore Genesis, Society of Economic Geologists, Reviews in Economic Geology, v.14, p.25-50.

Sinclair, W.D. 1971. A volcanic origin for the No. 5 zone of the Horne mine, Noranda, Quebec; Economic Geology, v.66, p.1225-1231.

Smith, J.C. 2016. An integrated structural and geochemical study of auriferous sheeted quartz veins within the 2740 Ma Côté Gold deposit, Swayze greenstone belt, Ontario; unpublished MSc thesis, Laurentian University, Sudbury, Ontario, 129p.

Smith, R.L. and Bailey, R.A. 1968. Resurgent cauldrons; Geological Society of America, Memoir 116, p.613-662.

Spence, C.D. 1967. The Noranda area; *in* Northwestern Quebec and Northern Ontario, Canadian Institute of Mining and Metallurgy, Centennial Field Excursion Guidebook, p.36-39.

Spence, C.D. and de Rosen-Spence, A.F. 1975. The place of sulfide mineralization in the volcanic sequence at Noranda, Quebec; Economic Geology, v.70, p.90-101.

Stern, R.A., Syme, E.C., Bailes, A.H. and Lucas, S.B. 1995. Paleoproterozoic (1.90-1.86 Ga) arc volcanism in the Flin Flon belt, Trans-Hudson Orogen, Canada; Contributions to Mineralogy and Petrology, v.119, p.117-141.

Sutton, J. 2020. Volcanic stratigraphy and hydrothermal alteration of the ca. 2701 Ma Duprat-Montbray formation: Implications for targeting new volcanogenic massive sulfide (VMS) deposits formed during the Lower Blake River episode, Rouyn-Noranda, Québec; unpublished MSc thesis, Laurentian University, Sudbury, Ontario, 142p.

Syme, E.C., Lucas, S.B., Bailes, A.H. and Stern, R.A. 1999. Contrasting arc and MORB-like assemblages in the Paleoproterozoic Flin Flon belt, Manitoba, and the role of intra-arc extension in localizing volcanic-hosted massive sulfide deposits; Canadian Journal of Earth Sciences, v.36, p.1767-1788.

Thurston, P.C., Ayer, J.A., Goutier, J. and Hamilton, M.A. 2008. Depositional gaps in Abitibi greenstone belt stratigraphy: A key to exploration for syngenetic mineralization; Economic Geology, v.103, p.1097-1134.

van Breemen, O., Heather, K.B. and Ayer, J.A. 2006. U-Pb geochronology of the Neoarchean Swayze sector of the southern Abitibi greenstone belt; Geological Survey of Canada, Current Research 2006-F1, 32p.

van Hees, E.H., Bousquet, P., Suma-Momoh, J., Daniels, C.M., Hinz, S.L.K., Boucher, C., Sword, P., Wang, L., Fudge, S.P., Millette, A. and Patterson, C. 2020. Report of Activities 2019, Resident Geologist Program, Timmins Regional Resident Geologist Report: Timmins and Sault Ste. Marie Districts; Ontario Geological Survey, Open File Report 6366, 160p.

Verpaelst, P., Péloquin, S., Adam, E., Barnes, A.E., Ludden, J., Dion, D.J., Hubert, C., Milkereit, B. and Labrie, M. 1995. Seismic reflection profiles across the “Mine Series” in the Noranda camp of the Abitibi belt, eastern Canada; Canadian Journal of Earth Sciences, v.32, p.167-176.

Vice, L.E.D. and MacDonald, P.J. 2019. Preliminary geology of Reeves and Sewell townships, northern Swayze area, Abitibi greenstone belt; *in* Summary of Field Work and Other Activities, 2019, Ontario Geological Survey, Open File Report 6360, p.8-1 to 8-10.

Walker, S.D. 1981. Geology of the auriferous Chadbourne breccia, Noranda, Quebec; unpublished MSc thesis, University of Western Ontario, London, Ontario, 97p.

Walker, S.D. and Cregheur, P. 1982. The Chadbourne mine, Noranda, Quebec: A gold-bearing breccia; *in* Geology of Canadian Gold Deposits, Canadian Institute of Mining and Metallurgy, Special Volume 24, p.58-66.

Watkinson, D.H. 1991. Mineral deposits of Noranda, Quebec and Cobalt, Ontario; Geological Survey of Canada, Open File 2159, 52p.

Weeks, R.M. 1963. The relative ages of the chalcopyrite and the rhyolite dykes in the rhyolite dyke zone orebodies at Quemont mine, Quebec; unpublished MSc thesis, Dalhousie University, Halifax, Nova Scotia, 143p.

Wilkinson, L., Cruden, A.R. and Krogh, T.E. 1999. Timing and kinematics of post-Timiskaming deformation within the Larder Lake–Cadillac deformation zone, southwest Abitibi greenstone belt, Ontario, Canada; Canadian Journal of Earth Sciences, v.36, p.627-647.

Williams, H. and McBirney, A.R. 1979. Volcanology; Freeman, Cooper and Company, San Francisco, California, 397p.

Wilson, M.E. 1941. District de Noranda, Québec; Geological Survey of Canada, Memoir 229, 162p.

——— 1948. McWatters Mine; extended abstract *in* Structural Geology of Canadian Ore Deposits: A Symposium, Canadian Institute of Mining and Metallurgy, Jubilee Volume, p.783-789.

——— 1956. Early Precambrian rocks of the Timiskaming region, Quebec and Ontario, Canada; Geological Society of America Bulletin, v.67, p.1397-1430.

——— 1962. Rouyn-Beauchastel map areas; Geological Survey of Canada, Memoir 315, 140p.

Zubowski, S. 2011. Characterization of hydrothermal fluids within synvolcanic faults of the ~2.7 Ga, Mine Sequence, Noranda district, Québec; unpublished MSc thesis, Laurentian University, Sudbury, Ontario, 168p.

Metric Conversion Table

Conversion from SI to Imperial			Conversion from Imperial to SI		
SI Unit	*Multiplied by*	*Gives*	*Imperial Unit*	*Multiplied by*	*Gives*
		LENGTH			
1 mm	0.039 37	inches	1 inch	**25.4**	mm
1 cm	0.393 70	inches	1 inch	**2.54**	cm
1 m	3.280 84	feet	1 foot	**0.304 8**	m
1 m	0.049 709	chains	1 chain	20.116 8	m
1 km	0.621 371	miles (statute)	1 mile (statute)	**1.609 344**	km
		AREA			
1 cm^2	0.155 0	square inches	1 square inch	**6.451 6**	cm^2
1 m^2	10.763 9	square feet	1 square foot	**0.092 903 04**	m^2
1 km^2	0.386 10	square miles	1 square mile	2.589 988	km^2
1 ha	2.471 054	acres	1 acre	0.404 685 6	ha
		VOLUME			
1 cm^3	0.061 023	cubic inches	1 cubic inch	**16.387 064**	cm^3
1 m^3	35.314 7	cubic feet	1 cubic foot	0.028 316 85	m^3
1 m^3	1.307 951	cubic yards	1 cubic yard	0.764 554 86	m^3
		CAPACITY			
1 L	1.759 755	pints	1 pint	0.568 261	L
1 L	0.879 877	quarts	1 quart	1.136 522	L
1 L	0.219 969	gallons	1 gallon	**4.546 090**	L
		MASS			
1 g	0.035 273 962	ounces (avdp)	1 ounce (avdp)	28.349 523	g
1 g	0.032 150 747	ounces (troy)	1 ounce (troy)	**31.103 476 8**	g
1 kg	2.204 622 6	pounds (avdp)	1 pound (avdp)	**0.453 592 37**	kg
1 kg	0.001 102 3	tons (short)	1 ton(short)	**907.184 74**	kg
1 t	1.102 311 3	tons (short)	1 ton (short)	**0.907 184 74**	t
1 kg	0.000 984 21	tons (long)	1 ton (long)	**1016.046 908 8**	kg
1 t	0.984 206 5	tons (long)	1 ton (long)	**1.016 046 9**	t
		CONCENTRATION			
1 g/t	0.029 166 6	ounce (troy) / ton (short)	1 ounce (troy) / ton (short)	34.285 714 2	g/t
1 g/t	0.583 333 33	pennyweights / ton (short)	1 pennyweight / ton (short)	1.714 285 7	g/t

OTHER USEFUL CONVERSION FACTORS

	Multiplied by	
1 ounce (troy) per ton (short)	31.103 477	grams per ton (short)
1 gram per ton (short)	0.032 151	ounces (troy) per ton (short)
1 ounce (troy) per ton (short)	20.0	pennyweights per ton (short)
1 pennyweight per ton (short)	0.05	ounces (troy) per ton (short)

*Note: Conversion factors in **bold** type are exact. The conversion factors have been taken from or have been derived from factors given in the* Metric Practice Guide for the Canadian Mining and Metallurgical Industries*, published by the Mining Association of Canada in co-operation with the Coal Association of Canada.*

ISSN 0826-9580 (print)
ISBN 978-1-4868-7225-1 (print)

ISSN 1916-6117 (online)
ISBN 978-1-4868-7226-8 (PDF)